# Quantification of time-dependent redox signalling in the Tpx1/Pap1 pathway in *Schizosaccharomyces pombe*

By

Diane Lind

BSc. (*Hons*) Genetics

Submitted in fulfilment of the academic requirements for the degree of Master of Science in the Discipline of Genetics, School of Life Sciences, College of Agriculture, Engineering and Science, University of KwaZulu-Natal, Pietermaritzburg, South Africa


As the candidate's supervisor I, have approved this dissertation for submission

**Supervisor**: Dr C. S. Pillay

Signature: _____

Date: _____

# Preface

The research contained in this dissertation was completed by the candidate while based in the discipline of Genetics, School of Life Sciences of the College of Agriculture, Engineering and Science, University of KwaZulu-Natal, Pietermaritzburg, South Africa under the supervision of Dr C. S. Pillay.

These studies represent original work by the candidate and have not otherwise been submitted in any form to another University. Where use has been made of the work by other authors it has been duly acknowledged in the text.

**Supervisor**: Dr C. S. Pillay

Signature: _____

Date: _____

# College of Agriculture, Engineering, and Science

# Declaration of Plagiarism

I, Diane Lind, declare that:

(i) the research reported in this dissertation, except where otherwise indicated or acknowledged, is my original work;

(ii) this dissertation has not been submitted in full or in part for any degree or examination to any other university;

(iii) this dissertation does not contain other persons' data, pictures, graphs or other information, unless specifically acknowledged as being sourced from other persons;

(iv) this dissertation does not contain other persons' writing, unless specifically acknowledged as being sourced from other researchers. Where other written sources have been quoted, then:

(a) their words have been re-written but the general information attributed to them has been referenced;

(b) where their exact words have been used, their writing has been placed inside quotation marks, and referenced;

(c) where I have used material for which publications followed, I have indicated in detail my role in the work;

(v) this dissertation is primarily a collection of material, prepared by myself, published as journal articles or presented as a poster and oral presentations at conferences. In some cases, additional material has been included;

(vi) this dissertation does not contain text, graphics or tables copied and pasted from the Internet, unless specifically acknowledged, and the source being detailed in the dissertation and in the References sections.

_____

Signature: Diane Lind

Date: _____

*Declaration Plagiarism 22/05/08 FHDR Approved*

# Abstract

Reactive oxygen species (ROS) can damage cellular components leading to cell death, but paradoxically, ROS also play essential roles in metabolism and signalling in eukaryotic cells. Dysregulation of this balance is associated with a range of host diseases and cells have consequently evolved sophisticated signalling networks to sense, detoxify and adapt to changes in ROS levels. Hydrogen peroxide, for example, is reduced by thiol-peroxidases which in turn, can trigger the oxidation of thiol-dependent redox transcription factors. However, the relationship between hydrogen peroxide stimuli and the level of redox transcription factor activation has largely been described in qualitative terms. Because quantitative measures of the redox signal have been lacking, we tested whether three signalling parameters viz. the signalling time, duration and amplitude could be used to quantify the hydrogen peroxide-dependent redox signal in the Tpx1/Pap1 pathway in *Schizosaccharomyces pombe*. We found significant differences in the signalling time and duration, but not signal amplitude as hydrogen peroxide concentrations were increased from 100 to 1000 µM in our assays. By way of comparison, we also found that the general oxidant, tert-butyl hydroperoxide at 200 µM, decreased signal time and duration in the Pap1 pathway when compared to an equivalent hydrogen peroxide concentration. This method was also used to compare the hydrogen peroxide signalling by OxyR in *Escherichia coli* and Yap1 in *Saccharomyces cerevisiae* showing that these measures could be used to characterize and compare redox signalling from different oxidants and in different species. Thus, quantification of time-dependent redox signalling revealed new insights into hydrogen peroxide signalling that could not be readily obtained by qualitative methods and, these measures are expected to facilitate a better understanding of the role of redox signalling in health and disease.

# Acknowledgements

I would like to express my thanks and appreciation to the following people:

To my supervisor Dr Ché Pillay for your guidance and support throughout this project. Thank you for always striving for excellence and challenging me to do the same. I have thoroughly enjoyed the time spent in your lab.

Dr Elizabeth Veal and Dr Zoë Underwood for teaching me how to western blot, without which this project would not have been possible. To Prof. Johann Rohwer, Dr Carl Christensen and Chris Barry for advice on computational modelling. A big thank you to Nolyn and Letrisha for introducing me to Lab B23 and for being patient enough to hear my thoughts over the years. To the newer lab members, Erin and Keli for the laughs, chats and interesting discussions. I would also like to thank Rob, Lauren and the Biochemistry department for technical advice on working with protein, I greatly appreciated the help. Finally, to the technical staff, Megan, Jess and Goodman for the use of equipment and help around the lab. The National Research Foundation for financial support for my studies and to Dr Pillay and Prof. Rohwer for awarding me a bursary to complete this degree.

To my dear friends, Erin Blom and Sophia Bam, we started this journey back in 2013 and you two have been there for me every step of the way. I truly value the encouragement and support you have offered me and for all the coffee and food breaks that accompanied our studies.

To my parents, Justin and Ingrid Lind, for the sacrifices you have made for my education, I can't thank you enough for everything you have done for me. My siblings, Julia and Bradley, for listening to the details of my project even when you didn't really want to. Pops and Nana for the prayers and encouragement and for being there from the beginning. To my One Life church family for your support and fun adventures that we've had along the way.

# List of Abbreviations

| | |
|---|---|
| Ahp | Alkyl hydroperoxide reductase |
| ALS | Amyotrophic lateral sclerosis |
| AP-1 | Activating protein -1 |
| APS | Ammonium persulfate |
| ASK1 | Apoptosis signal-regulating kinase |
| Atf1 | Transcription factor Atf1 |
| ATP | Adenosine Triphosphate |
| BCA | Bicinchoninic acid |
| BSA | Bovine serum albumin |
| cDNA | Complementary deoxyribonucleic acid |
| ChIP | Chromatin immunoprecipitation |
| CTAB | Hexadecyltrimethylammonium bromide |
| Ctt | Catalase |
| Cu Zn-SOD | Copper Zinc superoxide dismutase |
| Cys | Cysteine |
| DNA | Deoxyribonucleic acid |
| DNTP | 5, 5'-dithiobis (2-nitrobenzoic acid) |
| DTT | Dithiothreitol |
| ECL | Enhanced Chemiluminescence |
| EDTA | Ethylenediaminetetraacetic acid |
| EMM | Edinburgh Minimal Media |
| ER | Endoplasmic reticulum |
| ERK | Extracellular regulated kinases |
| ETC | Electron transport chain |
| GLR1 | Glutathione reductase |
| Gpx | Glutathione peroxidases |
| GSH | Glutathione |
| H2O2 | Hydrogen peroxide |
| HCl | Hydrochloric acid |
| HyPer | Hydrogen peroxide sensor |
| IAM | Iodoacetamide |

| | |
|---|---|
| IgG | Immunoglobulin G |
| KatG | Catalase peroxidase |
| LDL | Low density lipoproteins |
| MAPK | Mitogen-activated protein kinases |
| MgCl2 | Magnesium Chloride |
| mRNA | Messenger ribonucleic acid |
| NaCl | Sodium chloride |
| NADPH | ß-nicotinamide adenine dinucleotide phosphate |
| NO- | Nitric oxide |
| O2° | Superoxide |
| OD | Optical density |
| OH· | Hydroxyl radical |
| ONOO- | Peroxynitrate |
| OxyR | Hydrogen peroxide-inducible genes activator |
| PCR | Polymerase chain reaction |
| Prr1 | Pombe response regulator 1 |
| Prx | Peroxiredoxin |
| PVP | Polyvinylpyrrolidene |
| PySCeS | Python Simulator of Cellular Systems |
| ROS | Reactive oxygen species |
| SDS-PAGE | Sodium dodecyl sulfate-polyacrylamide gel electrophoresis |
| SOD | Superoxide dismutase |
| Sty1 | Mitogen-activated protein kinase sty1 |
| TAE | Tris-base, acetic acid and EDTA |
| tBOOH | Tert-butyl hydroperoxide |
| TBST | Tris Buffered Saline with Tween |
| TCA | Trichloroacetic acid |
| TE | Tris-EDTA buffer solution |
| TEMED | N,N,N', N'-tetramethylethylenediamine |
| Tpx1 | Thioredoxin peroxidase |
| Trr1 | Thioredoxin reductase |
| Trx1 | Thioredoxin |
| TSA1 | Thiol-specific antioxidant |

| | |
|---|---|
| Ura4 | orotidine 5'-phosphate decaroxylase |
| UV | Ultraviolet radiation |
| Yap1 | Yeast activating protein 1 |
| Ybp1 | Yeast binding protein 1 |
| YE5S | Yeast extract supplemented with 5 amino acids |

# Contents

# List of Tables



86

# List of Figures

# Chapter 1: Literature Review

## 1.1 Oxygen panacea or poison?

In the late 1700's, Karl Scheele and Joseph Priestley independently co-discovered oxygen when they observed that candles burnt brighter in the presence of heated mercuric oxide (Priestley, 1775; West, 2014). Oxygen was later shown to be essential for most living organisms and oxygen-based therapies soon arose with some practitioners claiming that oxygen could be used to cure all diseases (Figure 1.1) (Grainge, 2004; Kelly, 2014; West, 2014). However, only two years after its discovery, Antoine Lavoisier found high oxygen concentrations were poisonous to mice and from the 1800's right through to the 1920s several studies had reported that pro-longed oxygen exposure at high concentrations caused death in animals (Figure 1.1) (Knight, 1998). Despite this evidence, the clinical practice of oxygen therapy did not change and its toxic effects were ignored until 1967 when high oxygen concentrations correlated to pulmonary hyaline membrane formation (Figure 1.1) (Nash, 1967). Consequently, most clinicians now treat patients with oxygen concentrations of up to 40 % at low pressure to avoid the toxic effects associated with high oxygen concentrations (Heyboer *et al*, 2017; Gregory *et al*, 2018). To explore oxygen's apparently paradoxical role in life and disease, it is necessary to describe its mechanism of toxicity.

### 1.1.1 Molecular mechanisms of oxidative stress

The mechanism underlying oxygen toxicity is oxidizing radical formation which was originally reported by Fenton (1894) who showed that when iron combined with hydrogen peroxide, hydroxyl radicals were formed. This phenomenon was not accepted as biologically probable until McCord and Fridovich discovered superoxide dismutase which converts superoxide ions to hydrogen peroxide (Figure 1.1) (McCord and Fridovich, 1969; Knight, 1998). It was then realised that aerobic respiration generated oxygen molecules with unpaired electrons (free radicals) which could be dismutated into hydrogen peroxide and other reactive oxygen species (ROS) (Knight, 1998).

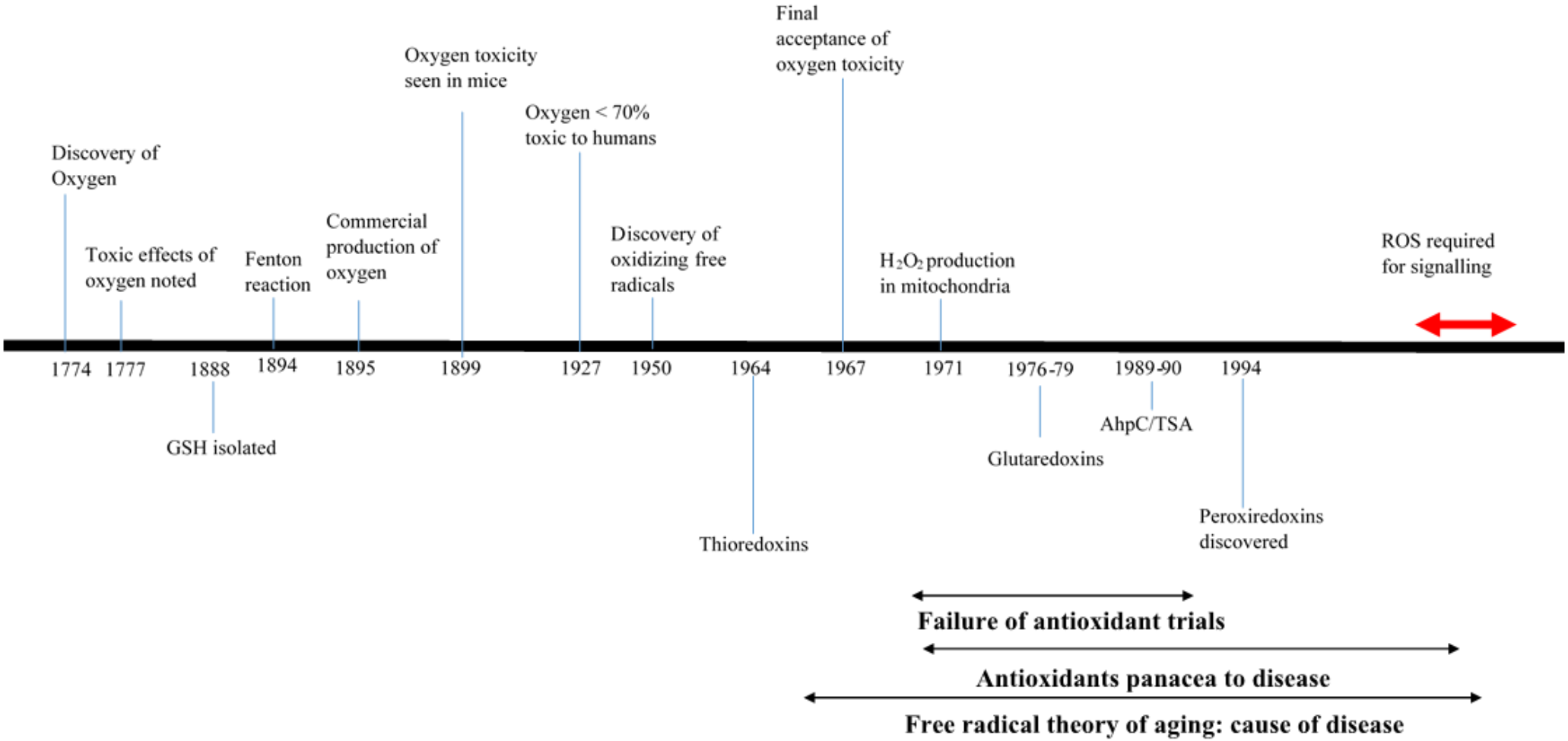


**Figure 1.1: Key discoveries of oxygen, reactive oxygen and antioxidants that shaped the field of redox biology over the last 200 years. (Details in text).**

Researchers soon began to uncover a number of diseases associated with elevated ROS (For further detail on ROS reader is referred to Halliwell and Gutteridge, 2015). For example, oxidation of low density lipoproteins (LDL) by ROS resulted in fat deposit build-up in arteries which is central to atherosclerosis and strokes (Chroni *et al*, 2011). Mutations in a major antioxidant enzyme, cytosolic superoxide dismutase (Cu, Zn-SOD), resulted in motor neuron oxidative damage leading to amyotrophic lateral sclerosis (ALS) (Liu *et al*, 2017). Increased ROS in the brain have also been linked with the development of Alzheimer's, Parkinson's and Huntington's diseases (Sultana *et al*, 2006) and several chemical, physical and inflammatory processes lead to free radical formation which results in DNA damage and ultimately tumorigenesis (Figure 1.2) (Reuter *et al*, 2010; Chikara *et al*, 2018).

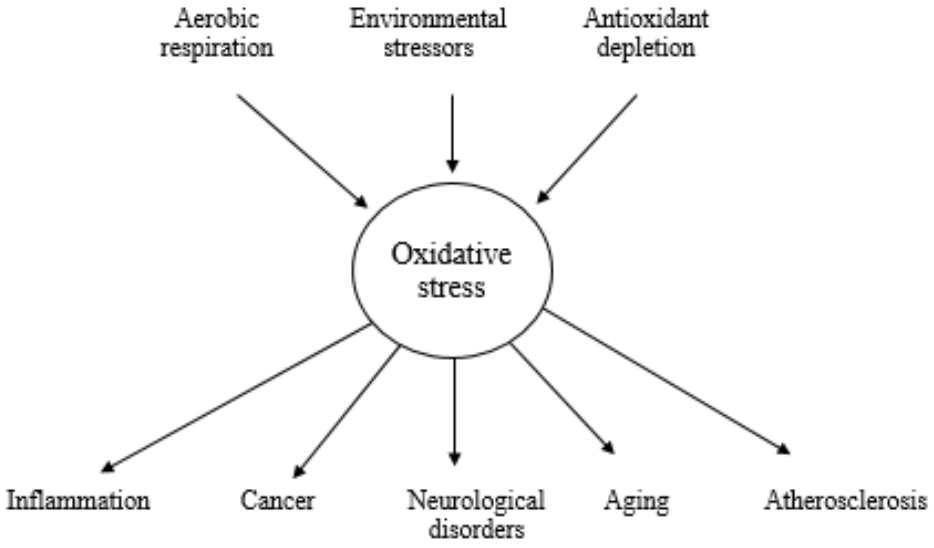


**Figure 1.2: The role of oxidative stress in disease.** In summary, aerobic respiration, certain environmental factors and the imbalance in antioxidant function lead to oxidative stress which contributes to disease. This figure was developed from (Steinhubl (2008)).

These and other results lent support to the Free Radical Theory of Disease which was first proposed in 1950 (Figure 1.1). It was reasoned that ROS removal could prevent or alleviate many diseases and at the turn of the 21$^{st}$ century, ROS were generally regarded as '*potent oxidants of lipids, proteins and nucleic acids that some researchers believed broke down cellular environments'* (Finkel, 2011). As more cellular antioxidant proteins were discovered, the Free Radical Theory of Disease was adjusted to include the concept of

oxidative stress which resulted from a purported imbalance between ROS generation and ROS degradation (Gough and Cotter, 2011).

The development of antioxidant therapies to 'rebalance' oxidative stress with additional antioxidants was a logical step for the field and therefore dietary supplementation with antioxidants such as vitamin C were tested in clinical studies (Figure 1.1) (Robinson *et al*, 2012; Sorriento *et al*, 2018). However, many of these clinical trials, particularly with vitamins, showed that these interventions had either no effect or were even detrimental to patients (Heart Protection Study, 2002; Pingitore *et al*, 2015; Henkel *et al*, 2018). For example, the use of vitamin E to treat cardiovascular disease resulted in an *increase* in oxidation of heart tissue while vitamin C supplementation to cancer patients showed no significant effect compared to control groups (Lee *et al*, 2015). Glutathione, a natural cellular antioxidant present at high concentrations, has been used in clinical trials to treat patients with atherosclerosis, but no significant changes were observed (Leopold, 2015; Meister, 1992).

Thus, like oxygen therapy, antioxidants were also believed to be a panacea to many complex diseases, but the failure of these trials showed that additional molecular mechanisms are involved in oxidative stress. Recent studies have begun to uncover the role of ROS, particularly hydrogen peroxide, in normal cellular function and redox signalling (Figure 1.1) (Chen *et al*, 2016; Circu *et al*, 2010). It is therefore apparent that our understanding of ROS and their role in health and disease remains obscure and hydrogen peroxide generation, antioxidant proteins and hydrogen peroxide signalling will be explored in more detail to resolve the conflicting roles of ROS in cellular function and disease.

## 1.2 Intracellular generation of hydrogen peroxide

Superoxide and hydrogen peroxide can react with a number biological molecules, but under limiting conditions, do not cause substantial harm to their immediate cellular environment (Halliwell and Gutteridge, 2015). However, hydrogen peroxide can diffuse from its site of production and can react with metals or metal-containing proteins leading to hydroxyl radical formation. It is this species that reacts rapidly and indiscriminately with most cellular constituents (Figure 1.3A) (Halliwell and Gutteridge, 2015).

Hydrogen peroxide is generated by four main enzymatic processes and is generally localized to the plasma membrane, mitochondria, peroxisomes and endoplasmic reticulum (Stone and Yang, 2006). First, NADPH oxidases transfer electrons from intracellular NADPH to extracellular molecular oxygen generating superoxide which is dismutated to hydrogen peroxide that can diffuse into cells through aquaporins (Figure 1.3B) (Stone and Yang, 2006; Sies, 2017). Second, the mitochondrial electron transport chain (ETC) also generates a substantial amount of superoxide due to electron leakage from the ETC or when excess oxygen is available (Sies *et al*, 2017). Superoxide is localized to its site of production and in itself does not cause major damage to cell components because of its rapid dismutation to hydrogen peroxide by superoxide dismutases (Halliwell and Gutteridge, 2015). Hydrogen peroxide can also be produced during protein folding in the ER when cysteine residues are oxidized (Figure 1.3B) (Sies *et al*, 2017; Winterbourn, 2018). Finally, during fatty acid oxidation in peroxisomes, electron transfer to molecular oxygen also results in hydrogen peroxide formation (Sies *et al*, 2017). Cells are equipped with defenses to metabolize hydrogen peroxide and these defense systems will be described next.

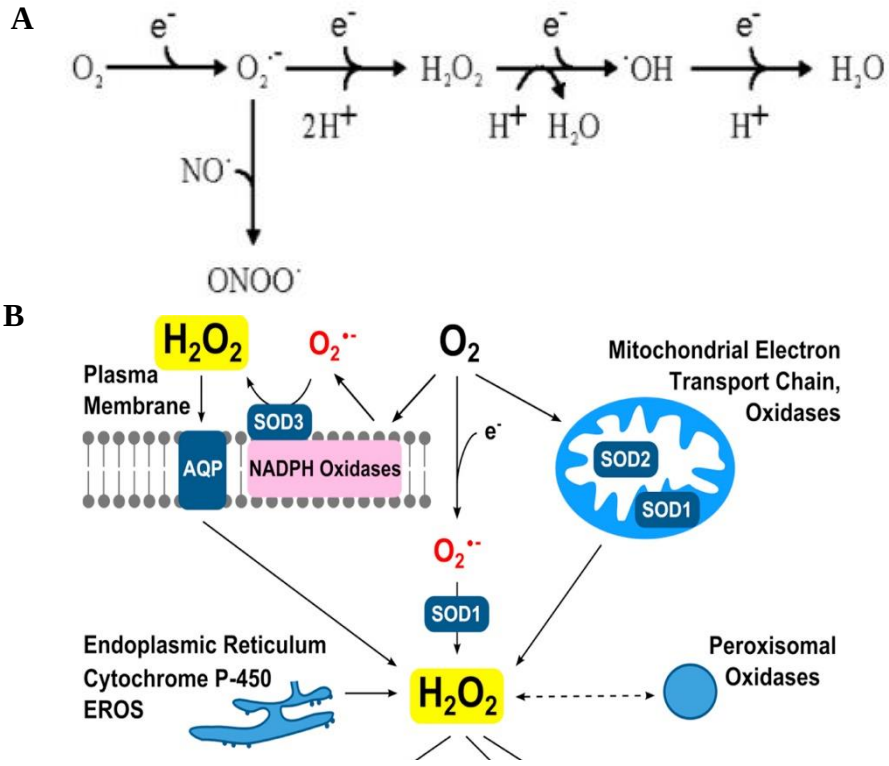

**Figure 1.3 The generation and interconversion of hydrogen peroxide by various biological processes**. Reduction of molecular oxygen by superoxide dismutases 1, 2 and 3 (SOD 1, 2, 3) yields superoxide ($O_2^{\cdot}$) and by sequential addition of electrons will lead to hydrogen peroxide ($H_2O_2$) and hydroxyl radical (°OH) formation respectively. Additionally, superoxide can react with nitric oxide ($NO^{\cdot}$) to form peroxynitrate ($ONOO^{\cdot}$)(A) (Adapted from Mailloux (2015)). The generation of hydrogen peroxide by various cellular processes at different locations in the cell (B) (Adapted from Sies (2017)). (Copyright permission to reproduce these images were obtained from Elsevier).

## 1.3 Hydrogen peroxide antioxidant defense system

Cells contain an array of enzymatic and non-enzymatic effectors to eliminate hydrogen peroxide (Birben *et al*, 2012; Ray *et al*, 2012; Kawagishi and Finkel, 2014). Non-enzymatic antioxidants like vitamins and ascorbate will not be considered here due to their relatively inefficient reaction rates with hydrogen peroxide (Figure 1.4) (Rhee *et al*, 2005). Cellular hydrogen peroxide is detoxified primarily by two types of specialist enzymes: catalases and peroxidases (Figure 1.4) (Rhee *et al*, 2001; Kawagishi and Finkel, 2014).

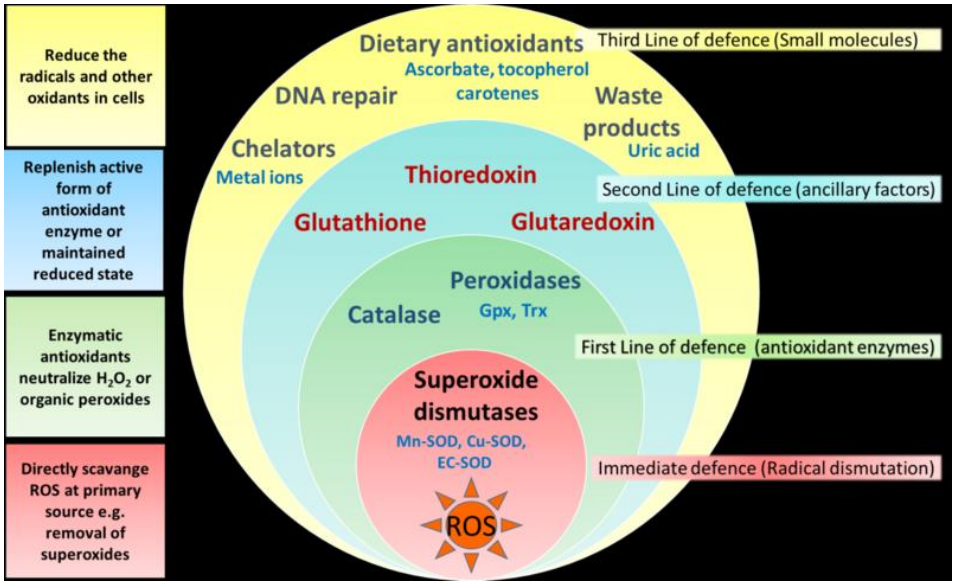

**Figure 1.4: System level response to oxidative stress**. Superoxide dismutases rapidly convert superoxide to less reactive hydrogen peroxide. Antioxidant enzymes like peroxidases that eliminate hydrogen peroxide are coupled with a second line of defence that includes thioredoxins and/or glutaredoxins. Lastly, small molecule antioxidants such as vitamins are also capable of reducing ROS in the cell (Permission to reproduce this figure was obtained by a Creative Commons license https://link.springer.com/chapter/10.1007/978-981-10-4711-4_3).

Catalases reduce two hydrogen peroxide molecules to oxygen and water and are predominantly found in the peroxisomes of eukaryotes (Birben *et al*, 2012; Ray *et al*, 2012). However, these two factors also constrain catalase's effectiveness. First, hydrogen peroxide must be transported into the organelles where catalase is present and second, because two molecules of hydrogen peroxide are required for each catalytic redox cycle, catalase works most effectively at high hydrogen peroxide concentrations (Figure 1.4) (Rhee *et al*, 2005). Peroxidases on the other hand, reduce hydrogen peroxide to water and are in turn reduced by another substrate (Halliwell and Gutteridge, 2015). There are several classes of peroxidases which are characterized by their preferred reductants and/or their active sites. For example, glutathione peroxidases (GPx), reduce hydrogen peroxide by oxidizing glutathione (Dayer *et al*, 2008) while haem-peroxidases react with hydrogen peroxide using iron as a cofactor. Compared to catalases, peroxidases are efficient hydrogen peroxide scavengers at lower hydrogen peroxide concentrations (nM), but can also reduce hydrogen peroxide with relatively high rate constants (Hyun *et al*, 2005; Peskin *et al*, 2013; Rhee, 2016). For example, metal-dependent and selenocysteine peroxidases react with hydrogen peroxide with rate constants in the range of $10^7$ $M^{-1}s^{-1}$ and $10^5$ $M^{-1}s^{-1}$ respectively (Stone and Yang, 2006). However, the requirement for transition metal pools, like iron, or other co-factors, as well as the need for a reductant to complete their redox cycles can limit the effectiveness of these peroxidases. Further, metal-centers increase the likelihood of hydroxyl radical formation via Fenton chemistry (Halliwell and Gutteridge, 2015). On the other hand, thiol-dependent peroxidases, the peroxiredoxins, react with hydrogen peroxide through a deprotonated cysteine thiol. Remarkably, their rate constants with hydrogen peroxide and cysteine thiols are in the range of $10^5$-$10^8$ $M^{-1}s^{-1}$ without the use of transition metals or unusual amino acids (Rhee *et al*, 2005). The thiol-based reactions of peroxiredoxins form the basis of redox signaling and will be discussed in greater detail.

### 1.3.1 Peroxiredoxins: specialist hydrogen peroxide sensors and scavengers

Peroxiredoxins are conserved from archaea to eukaryotes and certain members of this family are found at high intracellular concentrations (Hanschmann *et al*, 2013; Rhee, 2016). There are six peroxiredoxins types that can be grouped into three subgroups based on their protein structure and catalytic mechanism of cysteine: typical 2-cysteine peroxiredoxins (peroxiredoxin types one to four), atypical 2-cysteine peroxiredoxins (type 6 peroxiredoxins) and 1-cysteine peroxiredoxins that include type 5 peroxiredoxins (Rhee, 2016; Toledano and Huang, 2016). Typical 2-cysteine peroxiredoxins form homodimers, are the most abundant peroxiredoxin and are found in all life domains and react with hydrogen peroxide using either their peroxidatic or sulphenic acid catalytic cycles (Figure 1.5) (Rhee, 2016; Toledano and Huang, 2016). During the peroxidatic cycle, an active cysteine is oxidized by hydrogen peroxide leading to an intersubunit disulfide bridge with the resolving cysteine (Dietz, 2016; Rhee, 2016).

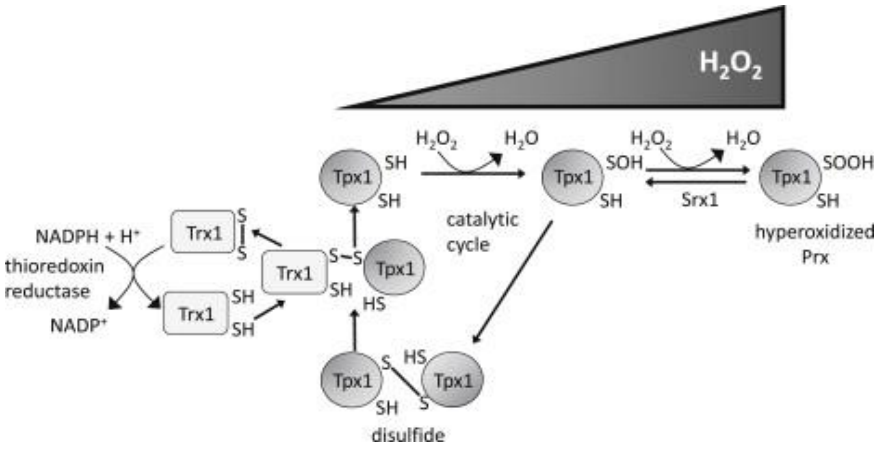


**Figure 1.5: Reaction of typical 2-Cys peroxiredoxin (Tpx1) with hydrogen peroxide in the catalytic cycle with the thioredoxin (Trx1) system to restore peroxiredoxin activity**. During the peroxidatic cycle, the peroxidatic cysteine on Tpx1 reduces hydrogen peroxide, forming a sulfenic (SOH) acid that condenses into a disulfide bond. This bond is reduced by thioredoxin. However, further oxidation of the sulfenic acid with hydrogen peroxide results in hyperoxidation (SOOH) that can be reversed by sulphiredoxin (Srx1). (Day *et al*, 2012) Permission to reproduce this image was obtained from Elsevier.

This disulfide bridge is then reduced by thioredoxin which in turn, is reduced by thioredoxin reductase and NADPH (Figure 1.5) (Day *et al*, 2012; Veal *et al*, 2014). Additionally, many eukaryotes have a conserved loop near the C-terminal that facilitates hyperoxidation which is lacking in prokaryotes (Peskin *et al*, 2013). Under high hydrogen peroxide conditions, the cysteine-sulphenic acid in eukaryotes can react with another hydrogen peroxide molecule resulting in a hyperoxidized peroxiredoxin which can only be reduced by sulphiredoxin (Figure 1.5) (Day *et al*, 2012; Veal *et al*, 2018). The physiological relevance of hyperoxidation remains unclear although two models have been proposed to explain this phenomenon (Veal *et al*, 2018). In the 'floodgate' model, peroxiredoxins act as a barrier preventing hydrogen peroxide from reacting with sensitive targets. However, once the peroxiredoxins are hyperoxidized and inactivated, hydrogen peroxide is free to react with sensitive targets allowing it to regulate signalling events by oxidizing cysteine residues on phosphatases that are found in phosphokinase signalling cascades, for example (Wood *et al*, 2003). A significant limitation with this model is that it cannot adequately explain how the oxidation of such signalling proteins could kinetically outcompete reactions of hydrogen peroxide with other molecules such as glutathione or indeed other peroxidases (Hampton and Connor, 2016).

On the other hand, in the 'signal peroxidase' model, peroxiredoxins transmit oxidizing equivalents allowing for signal propagation via redox relays which are shut down during hyperoxidation. For example, in the fission yeast *Schizosaccharomyces pombe*, the AP-1 like transcription factor, Pap1, is not activated at high hydrogen peroxide concentrations once its cognate peroxiredoxin is hyperoxidized (Vivancos *et al*, 2005). It was also demonstrated that peroxiredoxin hyperoxidation in fission yeast decouples thioredoxin from the peroxidatic cycle allowing thioredoxin to support the repair of proteins damaged by oxidative stress and where enzymes required for further detoxification can be expressed (Figure 1.5) (Day *et al*, 2012).

### 1.3.2 Oxidative stress repair mechanisms

Despite an extensive antioxidant network, proteins can still be damaged by oxidation leading to inactivation and impairment of vital metabolic and signal transduction processes. Therefore, an important aspect of oxidative stress defence is the restoration of inactivated proteins and redox balance in the cell (Figure 1.4) (Fernandes and Holmgren, 2004). For example, methionine residues can be oxidized to methionine sulfoxide, inhibiting protein function which can be reversed by thioredoxin-dependent methionine sulfoxide reductases (Moskovitz, 2005).

Many oxidized cysteine residues become glutathionylated, a process in which the abundant cellular tripeptide glutathione (GSH) binds to thiol residues. This modification also inactivates the proteins which are then deglutathionylated by glutaredoxins to restore activity (Du *et al*, 2012).

## 1.4 Adaptive stress response by transcription factor activation

To ensure that cells adapt to oxidative stress, there are specialized mechanisms that sense hydrogen peroxide and ultimately induce a transcriptional response to oxidative stress (Marinho *et al*, 2014; Rhee, 2016). Biochemical, genetic and kinetic studies have revealed three main types of redox sensors for inducing transcriptional activity viz. direct, sensor-mediated and indirect sensing sensors.

### 1.4.1 Direct sensors

In prokaryotic organisms, hydrogen peroxide is often sensed directly by a transcription factor which leads to the transcription of relevant genes (Aslund *et al*, 1999; Dubbs and Mongkolsuk, 2016). For example, in *Escherichia coli* the transcription factor OxyR has a number of critical cysteine residues, Cys 199 and Cys 208, which are directly oxidized by hydrogen peroxide which changes the transcription factor's conformation allowing it to transduce gene expression (Figure 1.6). Proteins induced by the OxyR regulon include hydroperoxidases (KatG) and alkylhydroperoxide reductase (AhpC) that eliminate hydrogen peroxide (Aslund *et al*, 1999). The oxidized, activated OxyR is reduced by the glutaredoxin system which consists of GSH, glutathione reductase and NADPH.

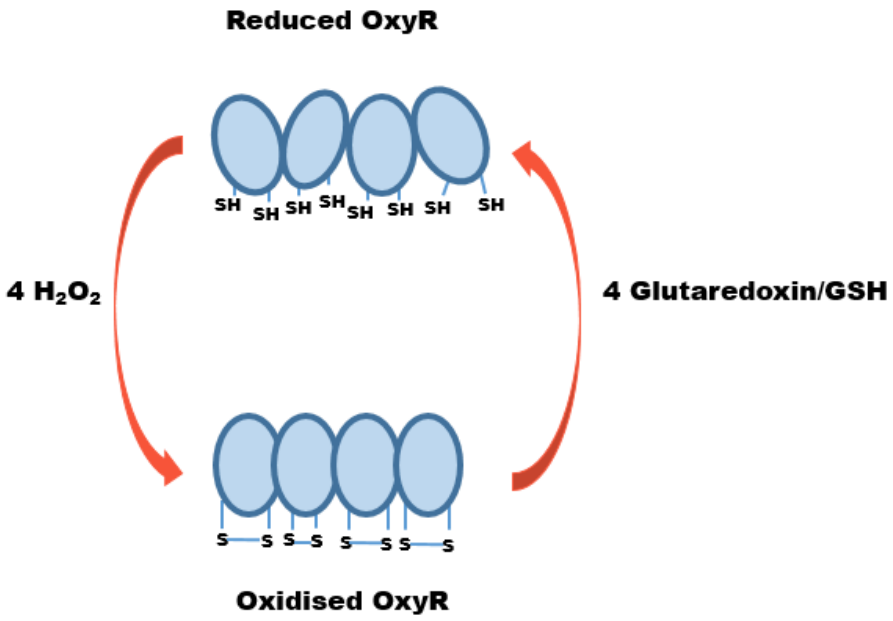


**Figure 1.6**: Direct activation of reduced OxyR by hydrogen peroxide in *E. coli*, oxidized OxyR can then be reduced by glutaredoxin/GSH (Figure created based on Storz and Imlay (1999)).

Many methods have been used to uncover the regulation of OxyR. For example, mutation analysis of OxyR showed that cysteine 199 is critical in transcriptional activation assays *in vitro* which was also confirmed *in vivo* (Kullik *et al*, 1995; Choi *et al*, 2001). The kinetics of OxyR binding to DNA for gene transcription were analysed using chromatin immunoprecipitation (ChIP) analysis (Kim *et al*, 2002; Wei *et al*, 2012). These studies found that OxyR directly activated over 56 genes. Gene knockout studies and redox western blot analysis that were used to determine the phenotype of cells with an *oxyR* deletion which revealed that the oxidative stress response genes, *ahpC* and *katB*, were only induced in the presence of OxyR (Rocha *et al*, 2000). Genome-wide transcript profiles were used with DNA microarray data to determine how OxyR activates genes related to hydrogen peroxide stress response (Zheng *et al*, 2001). Additionally, knockout studies also revealed that glutaredoxin, and not thioredoxin, was required to reduce OxyR *in vivo* (Zheng *et al*, 1998). Redox western blot analysis, in which the oxidized and reduced OxyR isoforms were separated and detected by antibodies, was used to determine how OxyR responded to differing hydrogen peroxide concentrations (Aslund *et al*, 1999; Rocha *et al*, 2000). This study revealed that OxyR was extremely sensitive to hydrogen peroxide concentrations as low as 0.5 μM *in vivo*. These combined approaches have revealed that OxyR is directly activated by low hydrogen peroxide levels suggesting that *E. coli* cells are highly sensitive to hydrogen peroxide (Aslund *et al*, 1999). It therefore appears that in these

cells, early detoxification of hydrogen peroxide is essential for survival which may be relevant as no intracellular membranes are present to shield DNA and other vital cellular components from oxidative stress induced damage (Zheng *et al*, 1998).

### 1.4.2 Sensor-mediated transcription factor activation

In eukaryotes, many transcription factors are not directly oxidized by hydrogen peroxide but rather by a sensor molecule which is the primary hydrogen peroxide receptor. In *Saccharomyces cerevisiae,* hydrogen peroxide oxidizes the active site cysteine in Gpx3 to produce a sulphenic acid which then forms a disulphide bond with Yap1, an AP-1 homologue (Figure 1.7 A) (Delaunay *et al*, 2000; Maeta *et al*, 2004). Under normoxic conditions, Yap1 can dynamically move between the nucleus and cytoplasm, but once oxidized, a disulphide bridge masks its nuclear C-terminal export signal and Yap1 is retained in the nucleus to activate the transcription of target genes (Delaunay *et al*, 2000; Maeta *et al*, 2004). Yap1 induces an antioxidant gene response by transcribing the thioredoxin (*TRX2*, *TRR1*) and glutaredoxin systems (*GSH1*, *GLR1*) as well as superoxide dismutase (*SOD1*, *SOD2*), glutathione peroxidase and the thiol peroxidases (*TSA1*, *AHP1*). Like *S. cerevisiae*, *Schizosaccharomyces pombe* senses hydrogen peroxide through a peroxiredoxin, Tpx1, resulting in sulphenic acid which then forms a disulphide bond with Pap1, the Yap1 homologue (Figure 1.5, 1.7). As with Yap1, oxidized Pap1 cannot be exported from the nucleus as its nuclear export signal is masked (Figure 1.7 B) (Vivancos *et al*, 2005; Day *et al*, 2012). Pap1 initiates an antioxidant response by inducing catalase (*ctt1*), sulphiredoxin (*srx1*) and the thioredoxin system (*trx2*, *trr1*) genes (Calvo *et al*, 2013). Importantly, unlike *S. cerevisiae* which senses hydrogen peroxide using Gpx3 or TSA1 (in ΔYbp1 cells), *S. pombe* has just a single peroxiredoxin that senses and transmits hydrogen peroxide signals.

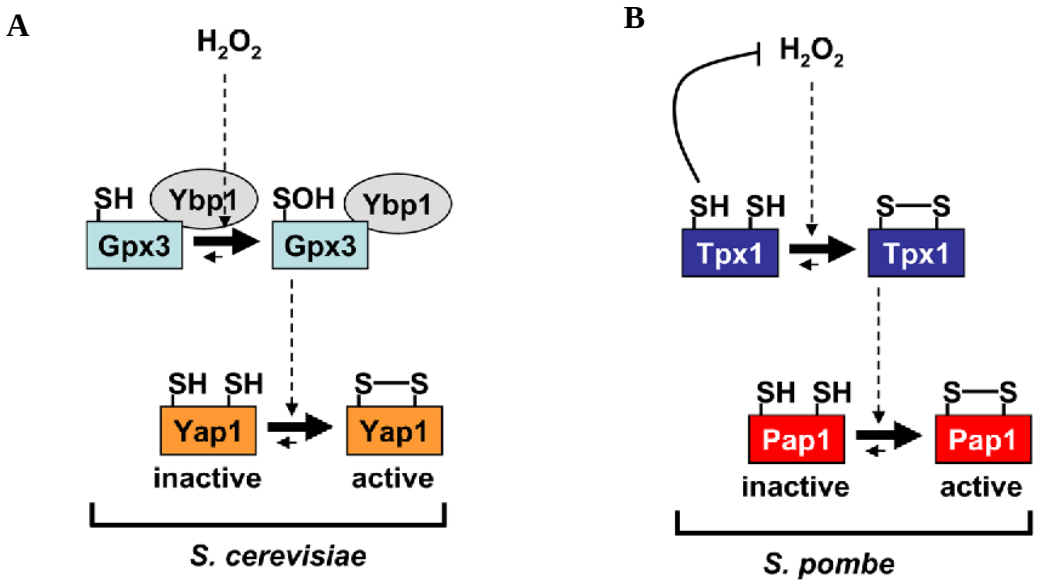

**Figure 1.7: Sensor mediated activation of AP 1-like transcription factors in yeast:** Yap1 of *S. cerevisiae* is activated by Gpx3 and Ybp1 binding protein (A). Pap1 sensor mediated activation in *S. pombe* is enabled by Tpx1 (B). The disulphide, active, forms of Yap1 and Pap1 are then retained in the nucleus (Boronat *et al*, 2014). Permission to reuse these images were obtained from Elsevier.

The tools used to understand redox regulation in eukaryotic transcription factors are similar to those used for prokaryotes like *E. coli*. *In vitro* studies revealed the DNA binding activities of Yap1 for transcription factor activation (Wu and Moye-Rowley, 1994). Mutations in six of the cysteine residues in Yap1 revealed the critical cysteines, Cys 303 and Cys 598, which are required for Yap1 oxidation by hydrogen peroxide *in vivo* (Delaunay *et al*, 2000). Redox western blotting was used to determine the redox status of Yap1 over a time-course following hydrogen peroxide exposure showed that Yap1 is rapidly oxidized but only at hydrogen peroxide concentrations over 100 μM (Okazaki *et al*, 2007). Therefore, this sensor-mediated transcription system appeared to be less sensitive to hydrogen peroxide when compared to direct sensors like OxyR (Okazaki *et al*, 2007). Similarly, in *S. pombe*, site-directed mutagenesis of the seven cysteine residues found in N and C-termini of Pap1 showed that Cys 278 and Cys 501 were critical to the activity of Pap1 (Castillo *et al*, 2002; Calvo *et al*, 2013). Gene knockout studies have also revealed the components of the oxidative stress response pathways in Yap1/Pap1 activation. For example, during western blot analysis Pap1 is usually oxidized when cells are exposed to hydrogen peroxide but when *tpx1* is deleted (Figure 1.7), Pap1 does not become oxidized and therefore antioxidant gene transcription by this transcription factor cannot occur ((Brown *et al*, 2013; Netto and Antunes, 2016). These results clearly demonstrated that Pap1 can only be activated by Tpx1 (Figure 1.7).

cDNA microarray analysis was used to test the transcriptional response of *S. cerevisiae* by deleting peroxidases and glutathione peroxidases (Fomenko *et al*, 2011). This analysis showed that thiol peroxidases regulated the global gene response to oxidative stress (Fomenko *et al*, 2011). mRNA analysis using northern blotting data of gene expression and western blot techniques were also used to understand system level regulation of the Tpx1/Pap1 pathway in

fission yeast (Brown *et al*, 2013). Here, it was observed that a thioredoxin like protein, Txl1, was responsible for Pap1 reduction.

Thus, sensor-mediated redox signaling relies on redox-relays to bring about a cellular response to oxidative stress (Klomsiri *et al*, 2011; Stöcker *et al*, 2018). Additionally the term 'redox switches' has been used to describe redox-sensitive activation of proteins in response to oxidants (Klomsiri *et al*, 2011; Stöcker *et al*, 2018). To date, a plethora of redox switches have been identified mainly through western blot analysis where the redox state of the protein is observed when the protein becomes oxidized; the redox switch is *on* and when it is fully reduced again it is *off* (Stöcker *et al*, 2018) or *vice versa*.

### 1.4.3 Indirect redox sensing

Indirect sensing or secondary redox signaling occurs when other signaling pathways oxidize the thioredoxin or glutaredoxin systems. For example, peroxiredoxins oxidize thioredoxin during cellular detoxification of hydrogen peroxide, reducing the availability of reduced thioredoxin to other pathways (Day *et al*, 2012). Hyperoxidation of peroxiredoxins appears to restore the availability of reduced thioredoxin to the cell (Figure 1.8) (Day *et al*, 2012). For example, under normoxic conditions reduced thioredoxin binds and inhibits the apoptosis signal-regulating kinase 1 (ASK1) but when thioredoxin becomes oxidized, it dissociates from ASK1 which then activates this signaling pathway (Fujino *et al*, 2007).

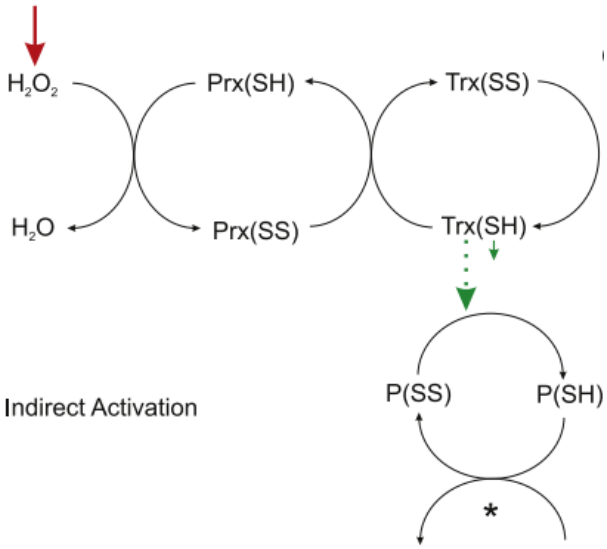


**Figure 1.8: Indirect redox sensing**. In this model, hydrogen peroxide oxidizes a peroxiredoxin which is then reduced by a thioredoxin. However, oxidation of thioredoxin (Trx(SS)) decreases the pool of reduced thioredoxin (TrxSH) available to reduce other oxidized proteins P(SS)/P(SH) involved in various signal cascades (Pillay *et al*, 2016) (Permission to reproduce this image from was obtained from Elsevier).

In summary, several methodologies have been used to uncover the molecular components and the hydrogen peroxide concentrations required to activate signaling targets (Choi *et al*, 2001; Okazaki *et al*, 2007). These studies have been complemented by studies on both specific and global gene expression in response to hydrogen peroxide exposure. Notably however, methods to quantify the redox signal itself, have not been considered.

## 1.5 Can quantification of redox signals resolve conflicting roles of ROS in health and disease?

As described above, a range of biochemical approaches together with mutations in antioxidant activities in model organisms, like *E. coli*, *S. cerevisiae* and *S. pombe*, have revealed information on the sources of oxidative stress, oxidative stress defence components and the mechanisms in which oxidative stressors are sensed by the cells. Additionally, many of the genes and proteins involved have been identified along with most of the proteome in these model organisms. Considerable information has also been gained on the signalling pathways that coordinate the cellular responses to the oxidative stress.

Despite this, application of redox biology to medicine has been elusive. This was highlighted by the failure of antioxidant therapies which were originally believed to cure diseases associated with oxidative stress (Figure 1.1) (Steinhubl, 2008). Additionally, it was envisioned that the discovery of redox-switches would provide novel drug targets to diseases, but little progress has been made in this area (Imber *et al*, 2017; Postovit *et al*, 2018). Therefore, resolving the paradoxical role of ROS in disease and health still remains an open and important question in redox biology. One potential reason is due to the limitation of the current methodologies available. A quote by Hans Selye summarizes the conundrum in the field: "*If only stress could be seen, isolated and measured, I am sure we could enormously lengthen the average human life span."* (Jasmin *et al*, 2000) In-order to achieve this, new methods and measures must be introduced to understand redox regulation in cells. Therefore, we propose that quantitative measures for redox signalling may pave the way for new insights into redox signalling pathways as redox signals could be precisely measured (Buettner *et al*, 2013; Pillay *et al*, 2016).

A mathematical theory was devised to quantify the signaling properties in protein kinase cascades by defining three parameters: signaling time, signal duration and signal amplitude (Heinrich *et al*, 2002). Practically, these parameters can be calculated from western blot time course data during the activation of a signaling pathway. Signal time is the average time it takes to activate a target protein, signal duration is the average time that a signal protein is active for, and, the signal amplitude is the average concentration of active target protein over a given signal interval (Heinrich *et al*, 2002). Intriguingly, this study predicted that the signaling parameters were controlled by different components within a signaling pathway. For instance, the amplitude was controlled by kinases more than by phosphatases, whereas the signaling duration was influenced by phosphatases (Heinrich *et al*, 2002). This theoretical model was subsequently validated in the ERK phosphorylation pathway *in vitro* (Hornberg *et al*, 2005).

The aim of this thesis is to test whether these time-dependent signaling parameters could be used for analyzing redox signaling in the model organism *S. pombe*. By quantifying these signals, we would then have a method to explore the paradoxical roles of oxygen in health and disease.

# Chapter 2: Materials and Methods

## 2.1 Materials

PCR reagents, DreamTaq DNA polymerase and alkaline phosphatase were obtained from Thermofisher Scientific (Johannesburg, South Africa) while PCR primers were obtained from Inqaba Biotech (Johannesburg, South Africa). Hydrogen peroxide was purchased from Laboratory and Analytical Supply (Durban, South Africa) and used within one month of purchase for oxidation experiments. The concentration of hydrogen peroxide was determined at 240 nm using an extinction coefficient of 43.6 $M^{-1}cm^{-1}$ (Hildebrandt and Roots, 1975). Iodoacetamide, PVP, CTAB, acrylamide, N,N' methylene-bisacrylamide, monoclonal (mouse) anti-v5 antibody (α-Pk) (Lot #065M480IV), anti-mouse (rabbit) IgG peroxidase antibody (Lot #106M4870V) were purchased from Sigma Aldrich (Johannesburg, South Africa) and the Clarity™ Western ECL substrate was purchased from Bio-Rad. Bovine serum albumin (BSA) was obtained from Celtic molecular diagnostics (Cape Town, South Africa). TEMED, ammonium persulphate, Coomassie Brilliant Blue R-250 and dithiothreitol (DTT) were purchased from Capital Labs (South Africa).

All other reagents and amino acids were purchased from Saarchem (Merck, South Africa) or Sigma Aldrich (Capital Labs, South Africa). The *S. pombe* strains used in this project were a kind donation from Dr. Elizabeth Veal (Newcastle University, UK).

## 2.2 Preparation of culture media

### 2.2.1 Yeast extract supplemented with 5 amino acids (YE5S)

The YE5S medium consisted of yeast extract (0.5%), glucose (3%), adenine (225 mg/L), histidine (225 mg/L), uracil (225 mg/L), lysine (225mg/L) and leucine (250 mg/L) with agar 2% added for solid growth.

### 2.2.2 Edinburgh Minimal Media (EMM)

Potassium hydrogen phthalate (15 mM), di-sodium hydrogen orthophosphate (15.5 mM), ammonium chloride (93 mM), glucose (2%), magnesium chloride (5 mM), calcium chloride (1 µM), potassium chloride (13 mM), di-sodium sulphate (280 µM), boric acid (0.81 µM), manganese sulphate (0.33 µM), zinc sulphate (0.25 µM), ferric chloride (0.1 µM), molybdic

acid (0.25 µM), potassium iodide (0.6 µM), copper sulphate (0.16 µM), citric acid (0.52 µM), nicotinic acid (81 µM), myo-inositol (56 µM), biotin (41 nM), pantothenic acid (4.6 µM) together with adenine (225 mg/L), histidine (225 mg/L), uracil (225 mg/L), lysine (225mg/L) and leucine (250 mg/L) were combined together and 2% agar was added for a solid growth medium.

## 2.3 Preparation of reagents and buffers

### 2.3.1 Extraction buffer

The extraction buffer consisted of Tris-HCl (200 mM, pH 8.0), NaCl (200 mM), EDTA (25 mM, pH 8.0) and 0.5% SDS in distilled water.

### 2.3.2 CTAB buffer

CTAB buffer was prepared with Tris-HCl (100 mM, pH 8.0), EDTA (20 mM, pH 8.0), NaCl (1.4 M), 2% hexadecyltrimethylammonium bromide (CTAB) and 1% polyvinylpyrrolidene (PVP) in distilled water.

### 2.3.3 TE buffer

TE buffer was prepared with Tris-HCl (1 M) and EDTA (0.5 M) in distilled water and the pH adjusted to 8.0.

### 2.3.4 TAE buffer

1 X TAE buffer consisted of 40 mM Tris-acetate and 1 mM EDTA adjusted to pH 8.0.

### 2.3.5 IAM buffer

1.4% Iodoacetamide was dissolved in 100 mM Tris-HCl (pH 8.0) containing 1% SDS. This solution was freshly prepared before use.

### 2.3.6 Loading buffer

0.25% Bromophenol blue was dissolved into 30% glycerol and stored at - 20°C.

### 2.3.7 Tris Lower Buffer

Resolving Tris buffer was made to a final concentration of 3.0 M Tris-HCl (pH 8.8) and 0.8 % SDS.

### 2.3.8 Tris Upper Buffer

Stacking Tris buffer consisted of 0.5 M Tris-HCl (pH 6.8) and 0.4 % SDS.

### 2.3.9 SDS loading dye

Protein loading dye was prepared to a final concentration of 500 mM Tris-HCl, 10%, glycerol 0.005 % Bromophenol blue and 0.8 % SDS the buffer was adjusted to pH 6.7 and stored at 4°C.

### 2.3.10 SDS tank buffer

SDS tank buffer was prepared to a final concentration of 25 mM Tris (pH 8.0), 200 mM glycine and 1 % SDS.

### 2.3.11 Transfer buffer

Transfer buffer was composed of 25 mM Tris (pH 8.0) and 200 mM glycine, 10 % methanol and 0.8% SDS.

### 2.3.12 Coomassie blue dye

Coomassie blue dye consisted of 0.125 % Brilliant Blue R-250, 50 % methanol and 10 % acetic acid.

### 2.3.13 Destain solution 1

Destain solution was prepared to final concentrations of 50 % methanol and 10 % acetic acid in distilled water.

### 2.3.14 Destain solution 2

The second detain solution consisted of 5 % methanol and 7 % acetic acid in distilled water.

### 2.3.15 Tris Buffered Saline with Tween (TBST) solution

TBST was made to a final concentration of 20 mM Tris (pH 8.0) and 137 mM $NaCl_2$ and 0.1% Tween 20 in distilled water.

### 2.3.16 Primary and secondary antibody dilution

α-Pk monoclonal antibody was stored at -20°C. Before use, it was diluted 5000 X in 5% BSA in TBST containing 0.02 % sodium azide and kept at 4°C for reuse. Secondary antibody was stored at -20°C and was freshly prepared before use by diluting it 5000 X in a 5% BSA in TBST.

## 2.4 Methods

### 2.4.1 Maintenance and cultivation of *Schizosaccarharyomyces pombe*

The strains used in this study, *S. pombe* 972 (h-), SB3 (h-, ade6-M216, pap1+ (3Pk)::ura4, his7-366, leu1-32, ura4-D18) and *S. pombe* SB4 (H+, ade6, pap1+ (3Pk)::ura4, tpx1::ura4+, his7-366, leu1-32) (Bozonet *et al*, 2005), were initially cultivated from frozen stocks on YE5S agar plates for 2 days at 30˚C and then stored at -80˚C in 50% (v/v) glycerol. For short term usage plates were stored at 4˚C and streaked weekly onto fresh YE5S plates. Liquid cultures were cultivated in EMM media by inoculating an overnight culture with a single colony and cells from these cultures were diluted into fresh media to an OD~0.15.

### 2.4.2 Genomic DNA isolation

*S. pombe* strains SB3 and *S. pombe* SB4 were grown to mid-exponential phase OD~0.5 in YE5S. Samples (1 ml) were harvested and pelleted (14 000 x *g*, 5 minutes, 21˚C) and the pellet was resuspended in extraction buffer (400 µl). Cells were lysed by adding 0.5 mm glass beads (750 µl) and homogenized (maximum speed, 15 seconds, 21°C) in a bead beater (Biospec Products), placed on ice for 1 minute, and this process was then repeated. RNase A was added to a final concentration of 10 µg/ml and the lysate was incubated at 80˚C for 2 minutes. CTAB buffer (400 µl) and 400 µl of chloroform: isoamyl alcohol (24:1) with 5 % phenol was added to the lysate and mixed gently. The aqueous layer was separated by centrifugation (14, 000 x *g*, 10 minutes, 21˚C) and the clear supernatant transferred to a fresh microfuge tube containing ice-cold propan-2-ol (600 µl) and the DNA was allowed to precipitate overnight at -20˚C. The DNA was pelleted by centrifugation (16 000 x *g*, 10 minutes, 4˚C), washed twice with 70% ethanol (500 µl), dried for 30 minutes and resuspended in TE buffer (50 µl) (Kang *et al*, 1998). DNA purity and was determined by spectroscopy ($A_{260}/A_{280}$) and agarose gel electrophoresis.

PCR primers for *tpx1* and *ura4* (Table 1) were developed from sequences obtained from Pombase (https://www.pombase.org/) and evaluated using Primer3 (http://primer3.ut.ee/), BlastN (https://blast.ncbi.nlm.nih.gov) and Oligoanalyser (https://eu.idtdna.com/calc/analyze).

A reaction mix of 1X DreamTaq buffer with 20 mM $MgCl_2$, 200 µM dNTPs, 500 nM of the forward and reverse primers, 2.5 mM $MgCl_2$ and 1U/50 µl DreamTaq polymerase was made-up to 10 µl with nuclease-free water. Cycling conditions consisting of 94˚C for 2 minutes for initial denaturation and 25 cycles of 94˚C for 30 seconds (denaturation), 30 seconds at 50 or 55˚C (annealing), 72˚C for 1 minute (extension) and a final extension step of 72˚C for 4 minutes were used and the PCR products were analyzed by gel electrophoresis.

**Table 2.1: List of oligonucleotide primers used to amplify tpx1 and ura4 to confirm the genotypes of the S. pombe SB3 and SB4 strains.**

| Primer | Sequence | Annealing temperature | Expected Product size |
|---|---|---|---|
| Tpx1 Left | ATG AGT TTG CAA ATC GGT AA | 50°C | 579 bp |
| Tpx1 Right | CTA GTG CTT GGA AAA GTA CT | 50°C | |
| Ura4 Left | TGA GGA TCG CAA ATT CGC AG | 55°C | 211bp |
| Ura4 Right | ACC AGT AGC CAA AGA GCC TT | 55°C | |

### 2.4.3 Agarose Gel Electrophoresis

Agarose was dissolved into 1 X TAE (50 ml) to 1% (w/v) or 2% (w/v) by heating in a conventional microwave. Once cooled, ethidium bromide was added to a final concentration of 5 µg/ml and the gel cast in a tray and left to polymerize for 1 hour. Loading buffer (5 µl) was added s and mixed by pipetting and a sample (2 µl) was loaded onto the gel and electrophoresed (80 V, 1 hour). DNA was then imaged under UV light using a DNR MiniBIS Pro Versadoc, (Bio-Rad).

### 2.4.4 Sensitivity of *S. pombe* SB3 and SB4 cells to hydrogen peroxide

*S. pombe* strains were cultured in EMM (100 ml) to an OD~0.5 and pipetted in separate lines onto YE5S plates. A disk of Whatman filter paper was soaked in 10 µl of different concentrations of hydrogen peroxide (0.1 – 10 mM) and placed into the center of the plate. The plates were incubated at 30°C for 2 days and imaged under white light.

### 2.4.5 Hydrogen peroxide challenge to *S. pombe* cells

*S. pombe* cells were cultured in EMM (100 ml) overnight (30°C, 250 rpm) and their optical density (OD) was measured at 595 nm. The cells were diluted into fresh EMM media to an OD~0.15 and then cultured (30°C, 250 rpm) to an OD~0.5. Hydrogen peroxide (100 – 1000 μM) was then added to these exponentially growing cultures which were grown for one hour (100 - 200 μM of hydrogen peroxide) or 2 hours (500 - 1000 μM hydrogen peroxide). 2 ml of culture was harvested at different time points over the 60 or 120 minute time course and added to 2 ml of ice-cold 20% trichloroacetic acid (TCA) in 15 ml falcon tubes. The cells were then pelleted by centrifugation (2, 000 x *g*, 5 minutes, 4°C), snap frozen in liquid nitrogen and stored at – 80°C.

### 2.4.6 Protein isolation

Pelleted cells were thawed on ice and resuspended in 10% TCA (200 μl) and 0.5 mm glass beads (750 μl) were added into a 2 ml Ribolyser tube. The cells were lysed in a bead beater (maximum speed, 15 seconds, 21°C) placed on ice for 1 minute, and this process was then repeated. 10% TCA (500 μl) was added to the tubes which were vortexed briefly. The Ribolyzer tubes were pierced at the bottom with a hot needle and secured in a sterile 1.5 ml tube and both tubes were then placed into a 50 ml Falcon tube and centrifuged (2, 000 x *g*, 1 minute, 21°C) to collect the solution. Protein was pelleted (13, 000 x *g*, 10 minutes, 4°C) and washed 3 times with 100% acetone and allowed to air dry for 10 minutes. Protein pellets were resuspended in freshly-prepared IAM buffer (30 μl) for 20 minutes at 25°C to allow for alkylation. The protein samples were then centrifuged (13000 x *g*, 3 minutes, RT) and the supernatant pipetted into a fresh tube. For the DTT controls (section 2.4.8), protein samples were resuspended in TE buffer (30 μl) and 0.1M DTT. The samples were then treated with alkaline phosphatase (1 hour at 37°C) to remove phosphoryl groups from Pap1 (Day *et al*, 2012). Protein concentration was determined using a Pierce BCA protein assay kit (Thermofisher) to ensure an equal protein concentrations were used for subsequent analyses.

### 2.4.7 SDS-PAGE Electrophoresis

A 30% acrylamide solution was prepared by mixing acrylamide (29 g) with N, N' methylene-bisacrylamide (1 g) in 100 ml distilled water and the mixture filtered through Whatman filter paper (0.5 mm) into an amber bottle and stored at 4°C. A resolving gel was prepared by combining 30% acrylamide with Tris Lower Buffer, 10% Ammonium persulfate (APS), freshly prepared) and TEMED (Table 2). The stacking gel was prepared with 30% acrylamide, Tris Upper Buffer, APS and TEMED (Table 2).

**Table 2. 2: Preparation of resolving and stacking solutions for an 8 % SDS-PAGE gel**

| Reagent | Resolving (ml) | Stacking (ml) |
|---|---|---|
| 30% acrylamide | 4 | 0.65 |
| Tris lower buffer | 3.75 | - |
| Tris upper buffer | - | 1.25 |
| Water | 7.25 | 3.05 |
| APS | 0.1 | 0.05 |
| TEMED | 0.03 | 0.001 |

SDS loading dye (10 µl) was added to each protein samples and DTT controls which were then boiled at 100°C for 5 minutes and then cooled to 4 °C before electrophoresis (200 V, 50 minutes) in 1 X SDS tank buffer.

### 2.4.8 Protein transfer to nitrocellulose membrane

Following SDS-PAGE electrophoresis the protein gel was placed underneath a nitrocellulose membrane (0.2 µm) and sandwiched between transfer stacks (Trans-blot, Bio-rad). Protein was transferred for 3 hours in ice-cold transfer buffer. An ice-pack was placed in the tank and changed after 1.5 hours to keep the transfer buffer cold. Effective transfer was checked by staining the gel post transfer with Coomassie blue (50 ml) overnight (21°C, 50 rpm) and the gel was then destained with destain solution 1 (100 ml) followed by destain solution 2 (100 ml).

### 2.4.9 Western blot development

Following protein transfer, the nitrocellulose membrane was blocked with 10% (w/v) BSA in TBST and then incubated with 5000 X diluted α-pk primary antibody (30 ml) overnight (4°C, 50 rpm). The membrane was washed 4 times with TBST for 5 minutes and then incubated with diluted (5000 X) secondary antibody (30 ml) for 1 hour. The membrane was then washed 4 times with TBST for 5 minutes, and dried (10 minutes, 21°C). The membrane was then incubated with ECL reagent for 5 minutes and imaged using the G-BOX Chemi-XR5 Gene*Sys* imaging system. The bands were sized according to Precision Plus Protein™ WesternC™ standard (Bio-Rad).

### 2.4.10 ImageJ analysis of Pap1 oxidation

Western blot images were contrasted to black and white and the reduced Pap1 bands ($Pap1_{red}$) were selected. The gel analysis function was selected to measure the intensity of these bands and this was repeated for the oxidized Pap1 bands ($Pap1_{ox}$). The intensities were added together giving '$Pap1_{total}$'. The oxidized Pap1 intensity reading was then divided by $Pap1_{total}$ to give the fractional Pap1 activation which was then plotted over the time course period and signaling parameters was calculated from the area under this curve (section 2.4.11).

### 2.4.11 Signal quantification

Signaling time ($\tau_i$), average time taken to oxidize Pap1, was calculated using equation 1 where ($I_i$) is the fraction of activated target (i.e. $Pap1_{ox}$ /$Pap1_{total}$) protein and $T_i$ is the area underneath the curve. $I_i$ and $T_i$ were calculated using time course data during activation of a signaling pathway from the target product ($P_i$) over a signal interval ($t$) (Heinrich *et al*, 2002; Pillay *et al*, 2016).

$$\tau_i = \frac{T_i}{I_i} \quad (1)$$

Signal duration ($\vartheta i$), average time that oxidized Pap1 is present, was calculated using equation (2)

$$\vartheta_i = \sqrt{\frac{\int_0^\infty t^2 P_i(t)dt}{I_i} - \tau_i^2} \quad (2)$$

Lastly, signal amplitude, average concentration of Pap1 over a time period, was determined ($S_i$) using equation (3)

$$S_i = \frac{I_i}{2\,\vartheta_i} \quad (3)$$

# Chapter 3: Quantifying Redox Signal Pathways

## 3.1 Introduction

*S. pombe* has been extensively used as a model organism to study redox systems for a number of reasons. First, *S. pombe* contains only a single 2-Cys peroxiredoxin, Tpx1, making its redox signal transduction system much simpler to investigate than those of other eukaryotic systems such as *S. cerevisiae* which has five peroxiredoxins (Brown *et al*, 2013; Peskin *et al*, 2013; Marinho *et al*, 2014; Santos *et al*, 2017). Second, and in common with most other eukaryotic cells, Tpx1 can become hyperoxidized at high hydrogen peroxide concentrations and is reduced by a native sulphiredoxin and therefore studies in this yeast are comparable to other eukaryotes (Day *et al*, 2012; Veal *et al*, 2018). Third, detailed genomic and proteomic data on *S. pombe* are readily available (Marguerat *et al*, 2012) although kinetic data on many of these proteins is lacking (Chapter 4). Fourth, *S. pombe* is genetically amendable and an extensive mutant library is available. Further, virtually all genes in this yeast can have a short sequence added to them, resulting in proteins that are specifically labelled with a short peptide *in vivo* (Gadaleta *et al*, 2014). For example, target proteins can be labelled with a Pk-tag which consists of a 14 amino acid (GKPIPNPLLGLDST) epitope (Gadaleta *et al*, 2014). Antibodies developed to recognise this epitope can identify target proteins through western blot analysis obviating the requirement to generate multiple antibodies against the individual targets in the yeast (Bozonet *et al*, 2005). However, the precise effect of these tags on redox signalling processes is not known. Finally, the hydrogen peroxide signal transduction pathway in this yeast has been comprehensively described and will be discussed further below (Toone *et al*, 1998; Vivancos *et al*, 2005; Boronat *et al*, 2014; Rhee, 2016; Domènech *et al*, 2018).

*S. pombe* cells initiate two different cellular responses depending on the hydrogen peroxide concentration (Veal *et al*, 2014). The first is adaptation where cells are able to continue proliferating despite being exposed to hydrogen peroxide (Figure 3.1). For example, at relatively low hydrogen peroxide concentrations (<1 mM), Tpx1 is primarily responsible for hydrogen peroxide detoxification, but also transmits signals to the transcription factor Pap1 which becomes oxidized (Figure 3.1). The oxidized form of Pap1, together with the transcription factor Prr1 initiates gene transcription of antioxidant genes like *trr1*, *trx1* and *tpx1*

(Calvo *et al*, 2012; Veal *et al*, 2014). However, at hydrogen peroxide concentrations exceeding (1 mM), Tpx1 becomes hyperoxidized and can no longer transduce signals to Pap1 hence, Pap1 remains in the reduced, transcriptionally inactive form (Figure 3.1) (Castillo *et al*, 2002; Karplus and Poole, 2012).

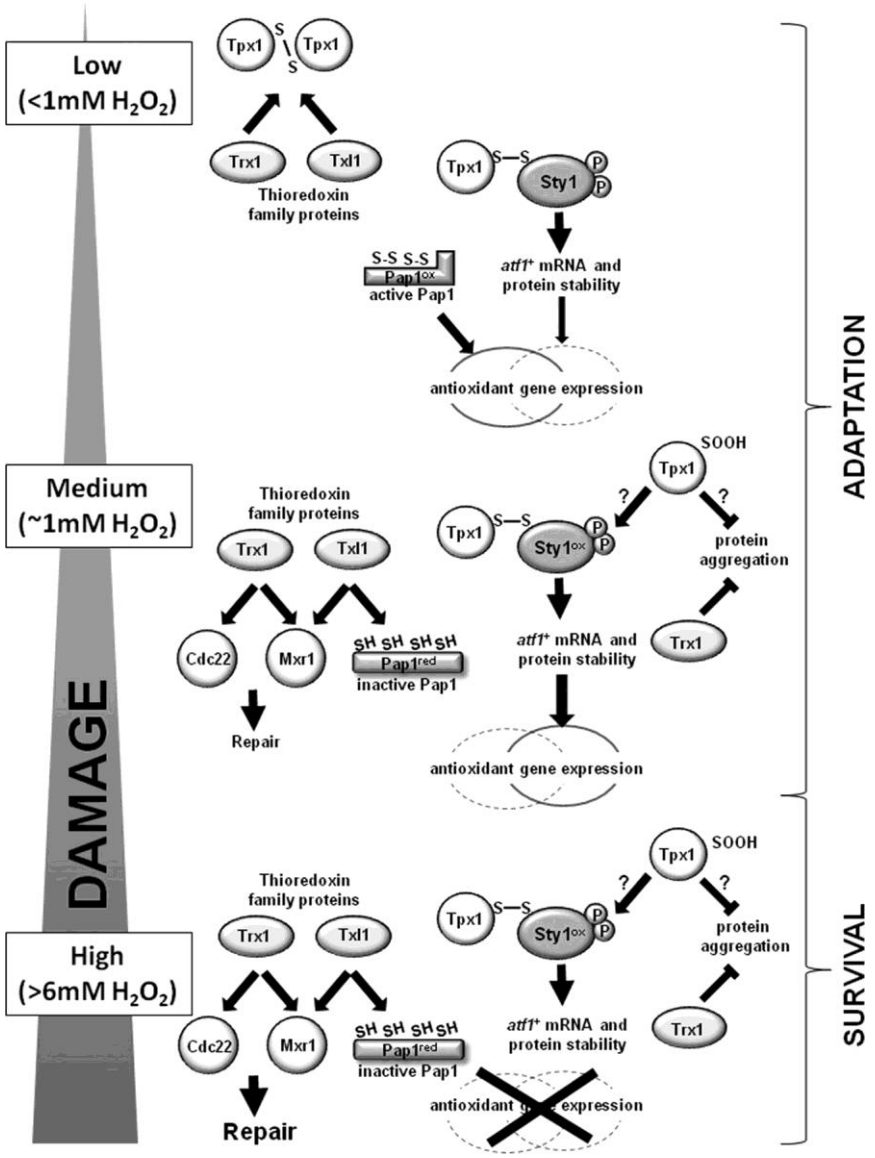


**Figure 3.1: Distinct cellular responses of *S. pombe* to low and high concentrations of hydrogen peroxide.** At low hydrogen peroxide levels, Pap1 is activated and couples with Prr1 to induce antioxidant gene response. Hydrogen peroxide concentrations greater than 1 mM inhibit Pap1 activation, but the Sty1 pathway is activated to induce antioxidant gene transcription. These responses are considered adaptive whereas at hydrogen peroxide concentrations greater than 6 mM, gene expression is inhibited and cellular repair mechanisms are initiated. Veal *et al*, (2014) Copyright permission to reproduce this image was obtained from Elsevier.

At higher hydrogen peroxide concentrations ( >1 mM), the Sty1 pathway initiates a general stress response (Quinn *et al*, 2002). Sty1 phosphorylates and regulates Atf1 which induces the transcription of catalase, Ctt1, and the sulphiredoxin, Srx1, which is then able to reduce hyperoxidized Tpx1 thus restoring the Pap1 pathway (Chen *et al*, 2008; Veal *et al*, 2014). However, if hydrogen peroxide concentrations exceed 6 mM, the cell stops antioxidant gene expression and the oxidative stress repair mechanisms are then activated (Veal *et al*, 2014).

Despite the components of this system being well understood, how these pathways are dynamically regulated in response to various hydrogen peroxide concentrations has not been explored. Further, only a few studies have even attempted quantification of redox signaling pathway. Notably Domènech *et al* (2018) quantified the reduced forms of Pap1, Tpx1 and Trx1 to determine how these redox-species responded to various hydrogen peroxide concentrations over a 50 minute time-course. However and surprisingly, the oxidized Pap1 isoform was not quantified and analysed in this study. In this chapter, the utility of a method to quantify time-dependent redox signalling (Heinrich *et al*, 2002) by hydrogen peroxide was tested.

## 3.2 Results

### 3.2.1 Genotypic confirmation of the *tpx1* delete strain and Pk-tag Pap1 in *S. pombe* SB3 and SB4 strains respectively

The two *S. pombe* strains used in this study were SB3, which contained a Pk-tag on Pap1, and SB4 which contained a Pk-tagged Pap1 and a Tpx1 deletion. A *ura4* marker was used to select cells with the Pk-tag and could therefore be used to identify these strains. Genomic DNA was first isolated from these strains and its quality determined through agarose gel electrophoresis and spectroscopy ($A_{260/280}$). PCR amplification of *tpx1* and *ura4* genes was carried out and the *ura4* marker was detected in both SB4 and SB3 strains indicating that these strains had been genetically modified (Figure 3.1A). *Tpx1* was successfully amplified in the SB3, but was not present in SB4 indicating that this strain was indeed lacking this peroxiredoxin (Figure 3.2B).

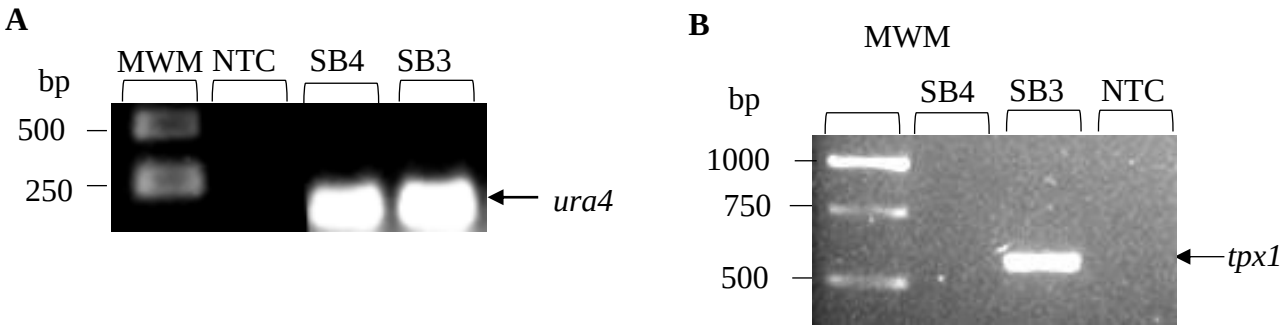


**Figure 3.2: Genotype confirmation of the *S. pombe* strains used in this study**. The *ura4* marker was successfully amplified in the SB3 and SB4 strains indicating genetic changes in these strains (A). Positive amplification of *tpx1* in SB3 and no amplification in SB4 reveal that *tpx1* was deleted in the SB4 strain (B). A no template control (NTC) served as a negative control.

### 3.2.2 Determining the hydrogen peroxide sensitivity range for *S. pombe* SB3 and SB4 strains

As discussed above, Pap1 initiates a cellular response to low and medium hydrogen peroxide concentrations up to 1 mM and is inactivated at high concentrations, but our analysis could be skewed if hydrogen peroxide killed the cells. Therefore, a cell sensitivity test was done to ensure that the hydrogen peroxide concentrations used in this study were not lethal to the SB3 and SB4 strains. Fresh liquid culture was pipetted onto agar together with a disc soaked in hydrogen peroxide (0.1-10 mM) and then incubated at 30°C for two days. Cells sensitivity was determined if a zone of inhibition was observed around the disc. Hydrogen peroxide concentrations from 0.1-1 mM had no effect on the cell viability even when the SB3 strains were diluted 10-fold (Figure 3.3). A concentration of 5 mM hydrogen peroxide began to slightly inhibit growth of the SB4 strain whereas 10 mM sufficiently inhibited the growth of SB4 but the SB3 strain showed no growth inhibition (Figure 3.3). Thus and in agreement with the literature (Chen *et al*, 2008; Calvo *et al*, 2013; Boronat *et al*, 2014), it was concluded a range of hydrogen peroxide concentrations between 0.1-1 mM would not affect cell viability in this study.

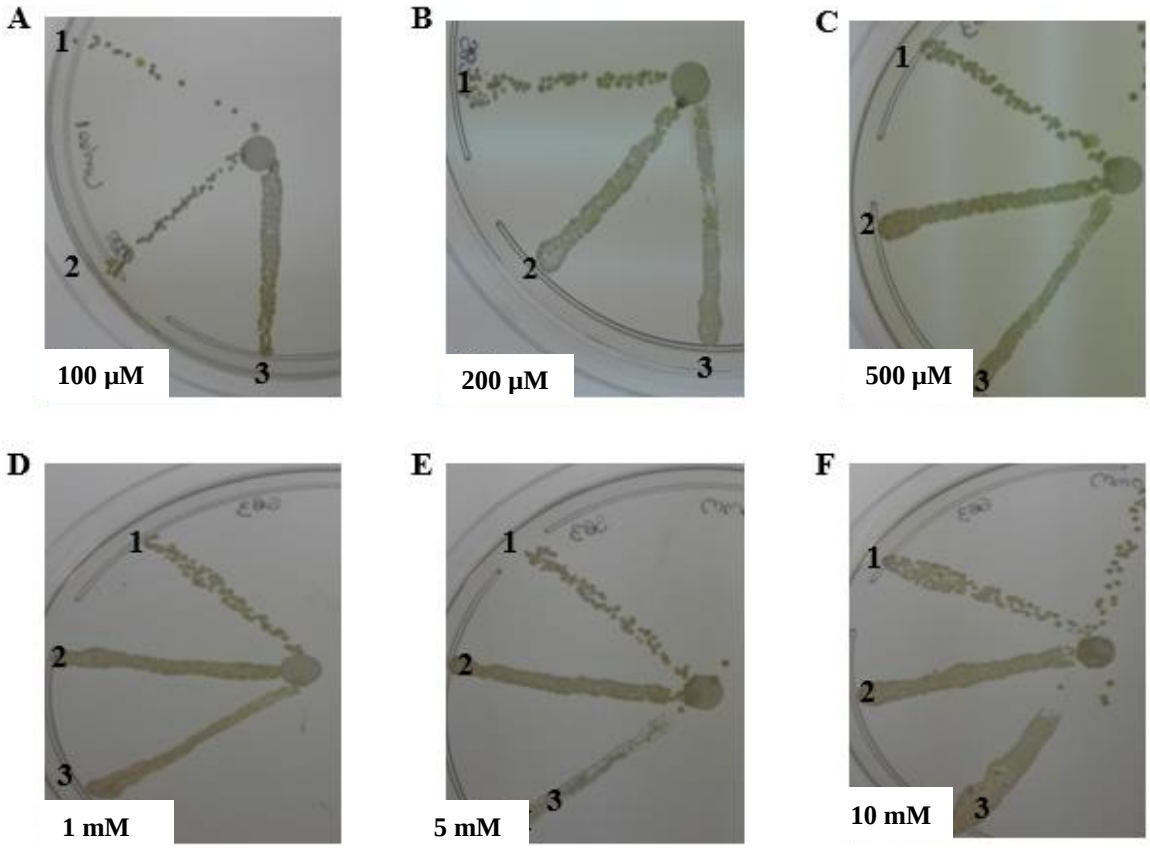


**Figure 3.3: The hydrogen peroxide concentration range of 0.1-1 mM did not affect the viability of *S. pombe* SB3 and SB4 strains.** Wildtype strain SB3 diluted 10-fold (1) or undiluted (2) were exposed to 100 µM–10 mM hydrogen peroxide and no halos around the discs were observed. The *tpx1* delete SB4 strain (3) showed sensitivity to hydrogen peroxide at 5 mM and 10 mM as an inhibition zone was observed at these concentrations.

### 3.2.3 Antibody optimisation for western blot analysis of Pap1 (Pk-tag) *in vivo*

Protein was extracted from *S. pombe* SB3 cells before and after exposure to 200 µM hydrogen peroxide and subjected to western blot analysis with a commercial α-Pk antibody (See Chapter 2.4.6-2.4.10 for experimental details). The antibody was successful in identifying the presence of a reduced Pap1 band at ~90 kDa the smaller ~70 kDa oxidized Pap1 band which results from intramolecular disulphide bridge formation causing the protein to migrate further during SDS-PAGE electrophoresis (cf. Figures 1.7, 3.1) (Bozonet *et al*, 2005). Some non-specific bands were observed indicated by an asterisk (*) but these bands did not appear to be redox-regulated as the migration of these bands were the same over the time course in the

presence of hydrogen peroxide (Figure 3.4). Hence, the blotting images throughout the rest of this thesis were cropped to show the reduced and oxidized Pap1 bands only.

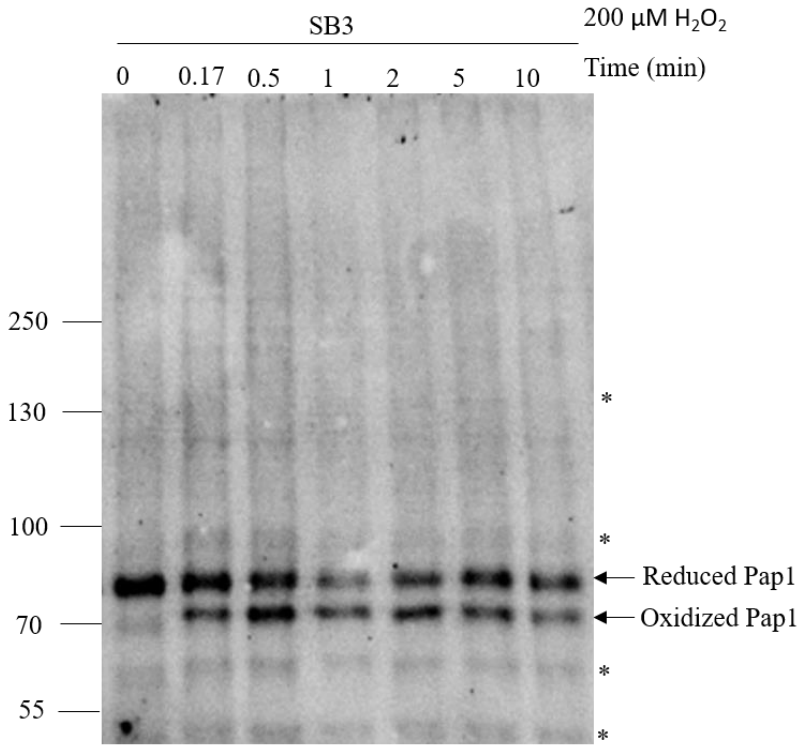


**Figure 3.4: α-Pk antibodies were specific in identifying oxidized and reduced Pk-tagged Pap1 in the *S. pombe* SB3 strain**. The SB3 strain was exposed to 200 μM hydrogen peroxide for 10 minutes. Protein was extracted and alkylated with IAM and subjected to western blot analysis. The specificity of α-Pk antibodies was assessed to identify the reduced (~91 kDa) and oxidized (~70 kDa) forms of Pap1. Asterisks (*) indicate non-specific binding of antibodies, but these bands do not change upon addition of hydrogen peroxide compared to the 0 minute time point.

### 3.2.4 Quantification of redox signalling in Tpx1/Pap1 pathway at different hydrogen peroxide concentrations (0.1-1 mM)

To confirm that Tpx1 was responsible for transducing redox signals to Pap1, the SB4 strain containing a *tpx1* deletion, was exposed to four hydrogen peroxide concentrations and the oxidation state of Pap1 was examined through western blot analysis (Figure 3.5). All four hydrogen peroxide concentrations 100—1000 μM showed no Pap1 oxidation and therefore

690 Tpx1 was required for Pap1 oxidation (Figure 3.5) confirming previous studies (Castillo *et al*,
691 2002; Bozonet *et al*, 2005; Brown *et al*, 2013). The redox signal in the SB3 strain could now
692 be quantified as the correct range of hydrogen peroxide concentration range had been identified,
693 the α-Pk antibody was sufficiently specific to Pap1-Pk and, the Pap1 activation depended solely
694 on Tpx1 transducing the redox signal

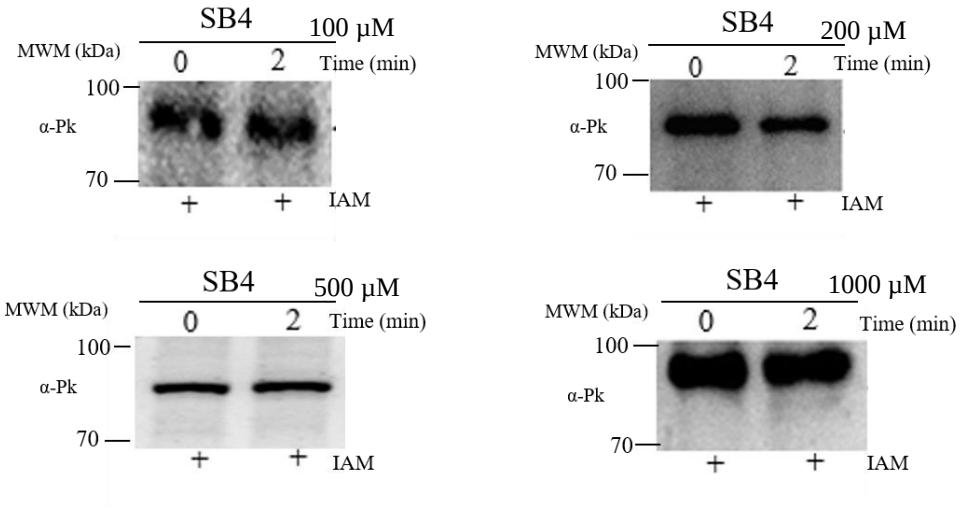


**Figure 3.5: Confirmation that Pap1 was exclusively oxidized by Tpx1.** The *S. pombe tpx1* delete strain was challenged with four hydrogen peroxide concentrations (100, 200, 500 and 1000 µM) for two minutes. Protein was extracted and Pap1 oxidation was examined by western blot analysis and showed no oxidation of Pap1 confirming that Tpx1 was required for Pap1 oxidation.

695 Western blot analysis was undertaken in the *S. pombe* SB3 cells exposed to 100 and 200 µM
696 hydrogen peroxide over 60 minutes which captured the oxidation and subsequent reduction of
697 Pap1 (Figure 3.6A, C). Rapid Pap1 oxidation was observed just 10 seconds after hydrogen
698 peroxide exposure and Pap1 was fully reduced at 30 minutes for 100 µM hydrogen peroxide
699 and by 60 minutes for a 200 µM hydrogen peroxide exposure. To capture Pap1 reduction
700 dynamics, two additional time points were taken at 15 minutes and 20 minutes for 200 µM
701 hydrogen peroxide (Figure S1C-D). These experiments were all done in triplicate with all

replicates showing similar oxidation patterns (Figure S1A, B; Figure S2A, B) which corresponded to other published data (Vivancos *et al*, 2005; Calvo *et al*, 2013).

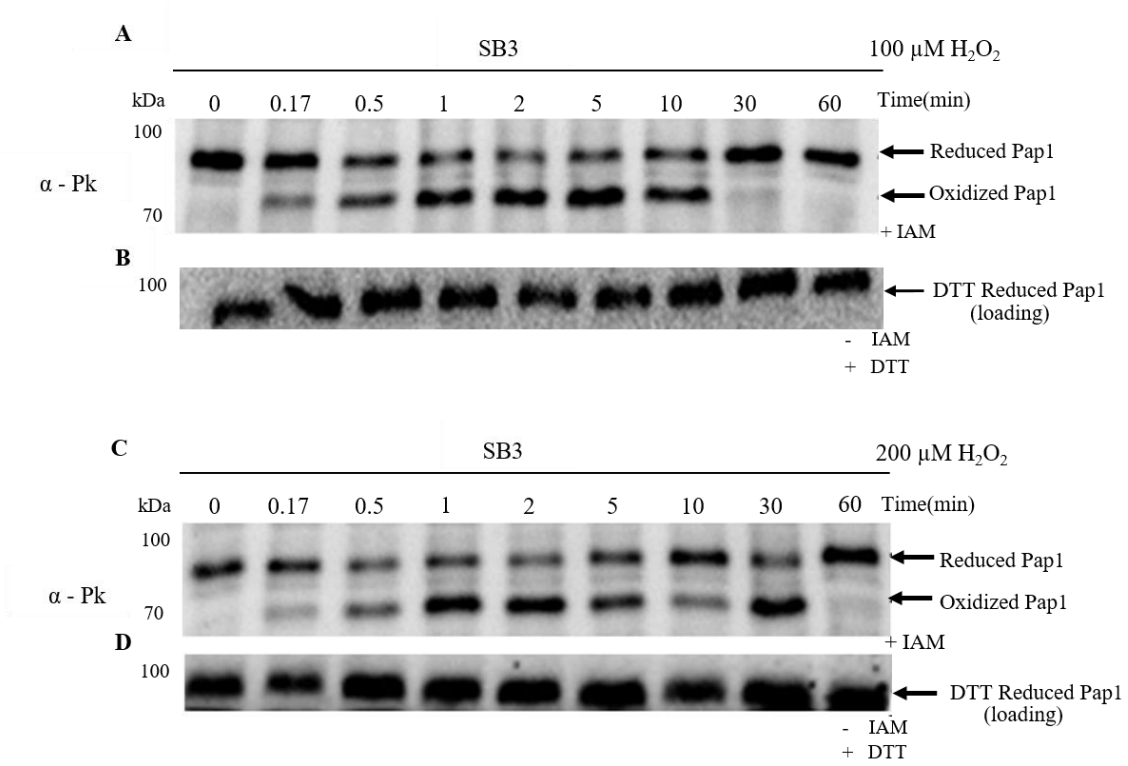


**Figure 3.6: Western blot analysis of SB3 strain exposed to low hydrogen peroxide concentrations of 100 and 200 µM for 60 minutes**. *S. pombe* cells were cultured to OD~0.5 and challenged with hydrogen peroxide for a time-course of 60 minutes. Protein samples were extracted and treated with IAM to inhibit oxidation of free thiol groups and then subjected to western blot analysis. The oxidation state of Pap1 was detected using α-Pk antibodies for 100 µM hydrogen peroxide (A) and for 200 µM hydrogen peroxide (C). Additional time points for cells exposed to 200 µM hydrogen peroxide were also obtained at 15 and 20 minutes (Figure S1C, D; Figure S2C, D). DTT was used as a loading and alkylation control (B, D) and all blots are representative of at least three independent experiments.

To convert the blotting data into graphical form, the intensity of the oxidized Pap1 band was divided by the sum of the intensity of the reduced and oxidized bands (Figure 3.7) and standard error for the data points were determined (Table S1). The signal profile of Pap1 activation at 100 μM hydrogen peroxide showed rapid oxidation with the highest oxidation at 2 minutes which was sustained for 10 minutes and then started to decrease rapidly from 15 minutes to 30 minutes and Pap1 was fully reduced after 60 minutes of exposure. From this graph, the time-dependent signalling parameters were then calculated. Pap1 oxidation at 200 μM hydrogen peroxide was also graphically represented and appeared to have a different signalling profile compared to 100 μM hydrogen peroxide (Table S2). At this concentration, there was rapid activation of Pap1 oxidation but oxidation was sustained for a longer period compared to 100 μM hydrogen peroxide and then returned to the reduced state by 60 minutes (Figure 3.7 B).

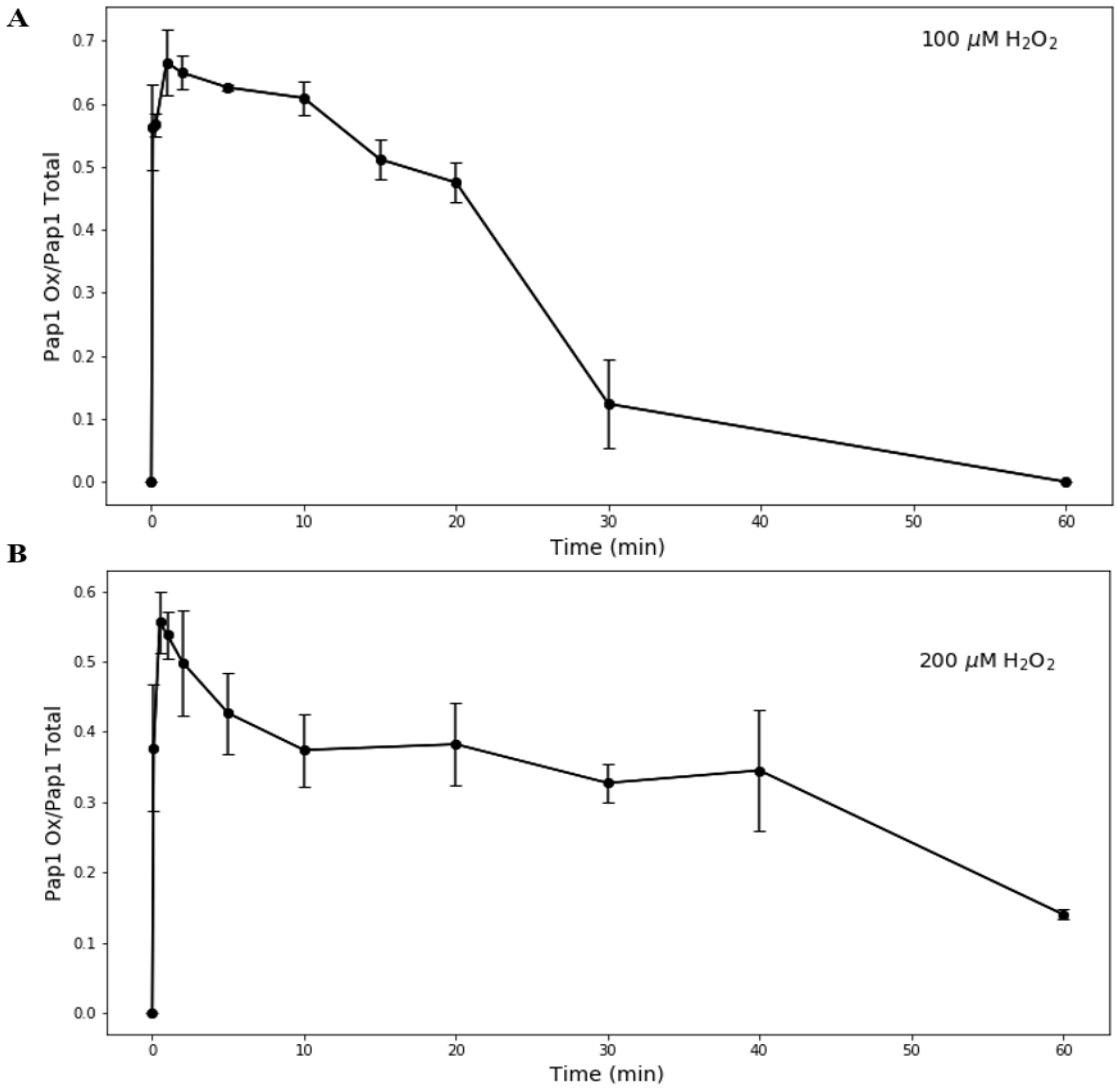


**Figure 3.7: Signalling profiles generated for Pap1 oxidation after exposure to 100 (A) and 200 μM (B) hydrogen peroxide**. These profiles were generated by digitizing western blotting data obtained in Figure 3.6. Standard error bars are indicated for the independent samples at each time point (*n*=3).

Increasing the hydrogen peroxide concentration to 500 and 1000 µM moved the cell into the top-end of adaptation (Figure 3.1) and therefore the response of Pap1 at the upper-limit of adaptation was tested. The SB3 strain was exposed to 500 and 1000 µM hydrogen peroxide and Pap1 oxidation was examined over a longer time period (120 minutes) as a higher hydrogen peroxide concentration was expected to lead to sustained oxidation. Western blot analysis showed that Pap1 oxidation began as early as 10 seconds and was sustained up to 100 minutes for both concentrations before returning to the reduced form by 120 minutes (Figure 3.8A, C). These experiments were carried out in three independent experiment with similar banding patterns observed in each replicate (Figure S3; Figure S4). Published data available for Pap1 oxidation at these concentrations only tracked the oxidation to 60 minutes and did not include many time points (Bozonet *et al*, 2005; Brown *et al*, 2013; Domènech *et al*, 2018) but the Pap1 oxidation patterns observed were consistent with previous results (Veal *et al*, 2014).

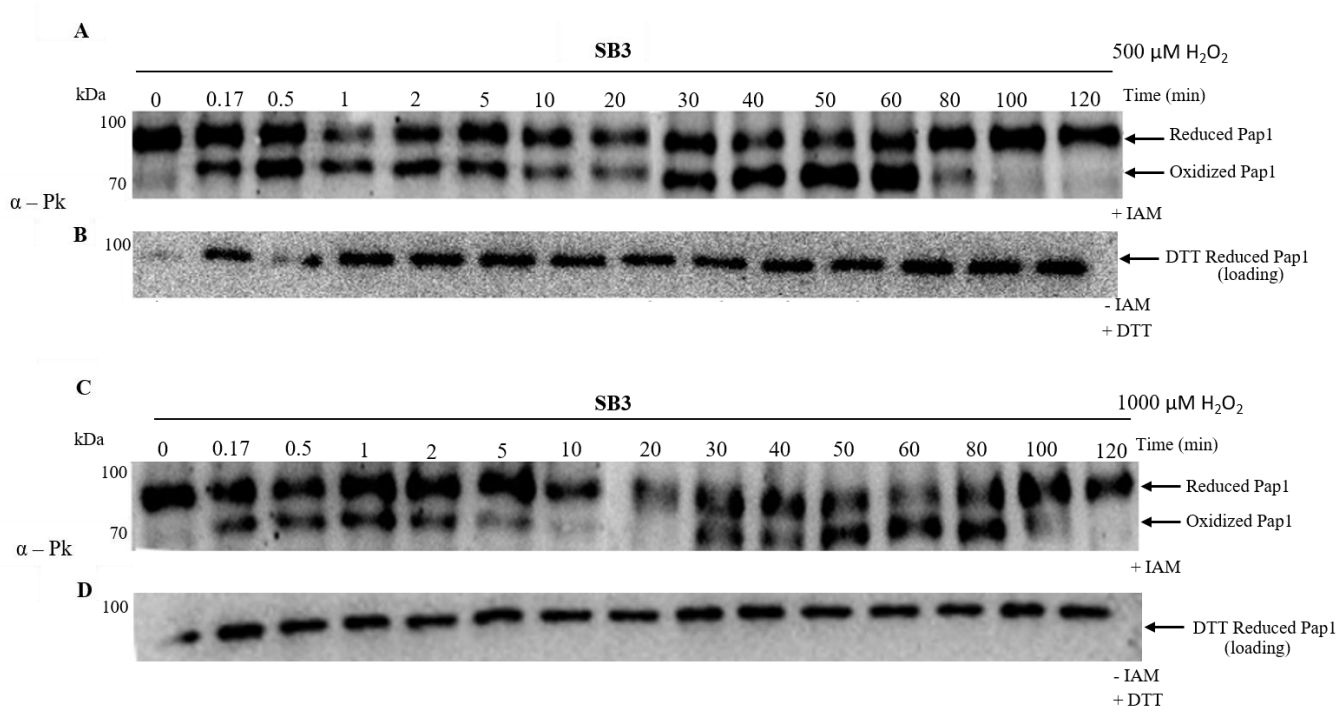


**Figure 3.8: Western blot analysis of Pap1 oxidation after exposure to 500 (A) and 1000 µM (C) hydrogen peroxide.** *S. pombe* cells were cultured to OD~0.5 and challenged with 500 and 1000 µM hydrogen peroxide for 120 minutes. Protein was extracted and alkylated with IAM and examined by western blot analysis using α-Pk antibodies. DTT was used as a loading and alkylation control (B, D) and all blots represent one of at least three independent replicates (*n*=3).

Western blot data obtained for Pap1 oxidation at 500 and 1000 μM hydrogen peroxide was converted using ImageJ and plotted against the time (Table S3; Table S4). The signalling profiles revealed the rapid oxidation of Pap1 which peaked at 2 minutes for both concentrations (Figure 3.8A, B). Oxidation then decreased until 10 minutes but then steadily increased again and peaked at 60 minutes for 500 and 1000 μM hydrogen peroxide (Figure 3.9A, B). From 60 minutes onward Pap1 oxidation decreased until it was fully reduced after 120 minutes (Figure 3.9). Interestingly, for the 1 mM hydrogen peroxide-treated cultures, Pap1 oxidation did not decrease as rapidly when compared to 500 μM hydrogen peroxide-treated cultures. These signalling profiles of Pap1 oxidation had a different oxidation trend compared to the signalling profiles of Pap1 oxidation at 100 μM and 200 μM hydrogen peroxide. At these lower hydrogen peroxide concentrations, Pap1 oxidation occurred rapidly and was sustained for approximately 20 minutes and then returned to the reduced form by 60 minutes. By contrast, at the higher hydrogen peroxide concentrations (500 and 1000 μM), Pap1 was also oxidized rapidly, showed decreased oxidation between 10 and 20 minutes and then oxidation increased again until 60 minutes. This second peak in Pap1 oxidation appeared to be specific to the higher hydrogen peroxide concentrations (Figure 3.9A, B).

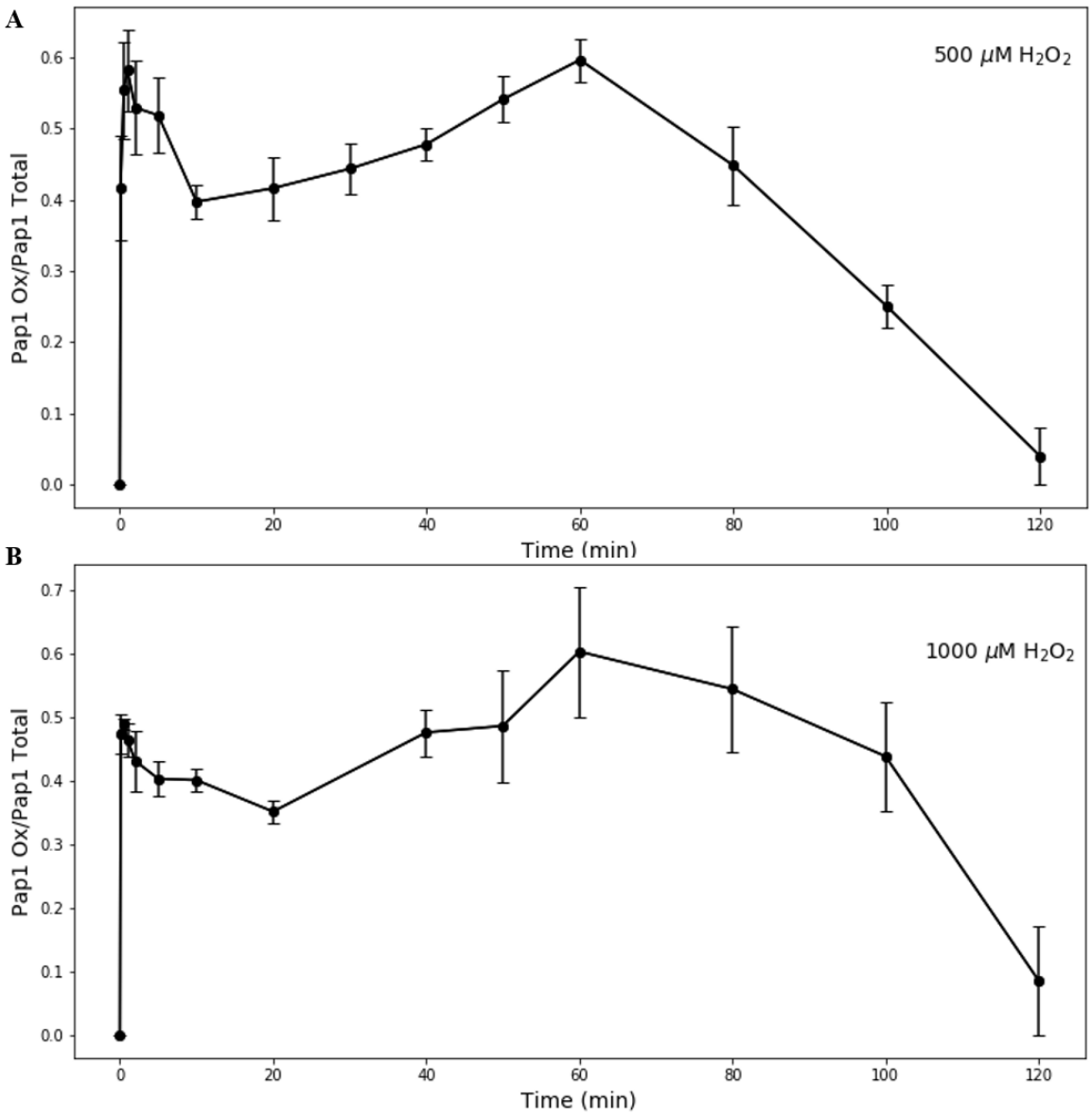


**Figure 3.9: Signalling profiles of Pap1 oxidation after exposure to 500 (A) and 1000 µm (A) hydrogen peroxide for 120 minutes.** Western blotting obtained for Pap1 oxidation after exposure to 500 and 1000 µM hydrogen peroxide (Figure 3.8) was digitized and plotted over the time-course duration of 120 minutes. Standard error bars indicate independent samples taken for each time-point (*n*=3).

Using the fractional values of Pap1 oxidation from time course data, the signalling parameters could then be calculated (See Chapter 2.4.11). Where signaling time was the average time taken to oxidize Pap1, signal duration the average time that oxidized Pap1 was present and signal amplitude the average concentration of oxidized Pap1 over a time period. The values for signalling time, duration and amplitude were calculated for Pap1 oxidation at 100, 200, 500 and 1000 μM and are summarized into Table 3.1 with the respective standard errors.

**Table 3.1: Time-dependent signalling parameters of Pap1 oxidation at various hydrogen peroxide concentrations (0.1-1 mM).** Values for signal time, average time to oxidize Pap1, signal duration, average time that oxidized Pap1 is present, and signal amplitude, average concentration of Pap1 over a time period that were obtained from the Pap1 signalling profiles.

| Hydrogen peroxide concentration (μm) | Signal time (min) | Signal duration (min) | Signal amplitude |
|---|---|---|---|
| 100 | 11.62 ± 2.03 | 8.53 ± 1.54 | 0.94 ± 0.11 |
| 200 | 26.62 ± 1.17 | 17.78 ± 1.77 | 0.6 ± 0.10 |
| 500 | 51.35 ± 2.96 | 29.56 ± 1.29 | 0.85 ± 0.05 |
| 1000 | 56.85 ± 2.15 | 30.57 ± 1.13 | 0.89 ± 0.11 |

It was found that changing the hydrogen peroxide concentration from 100 to 200 μM had a significant effect on signalling time which increased from 11.62 to 26.62 minutes respectively (Figure 3.10A). The addition of 500 μM hydrogen peroxide to the cells also resulted in a significant increase in the Pap1 signalling time, but increasing the hydrogen peroxide from 500 to 1000 μM did not significantly increase the signalling time (Figure 3.10A). As the hydrogen peroxide concentration was increased from 100 to 500 μM there was a significant increase in signal duration (Figure 3.10B) but as the hydrogen peroxide concentration was increased from 500 to 1000 μM there was no significant increase in signal duration. (Figure 3.10C).

The signal amplitude significantly decreased from 100 to 200 μM hydrogen peroxide, but as the hydrogen peroxide concentration was increased to 500 μM the increase in signal amplitude was not significant. Furthermore, increasing the hydrogen peroxide concentration 2-fold between 500 and 1000 μM resulted in no significant difference on signal amplitude (Figure 3.10C). Of all the signalling parameters, increased oxidation of a signalling protein (which approximates the amplitude) is the most readily observed on blots and therefore reported (see

for example Vivancos *et al*, 2005; Poole *et al* 2011; Brown *et al*, 2013). These results suggest that using this qualitative measure alone may be misleading.

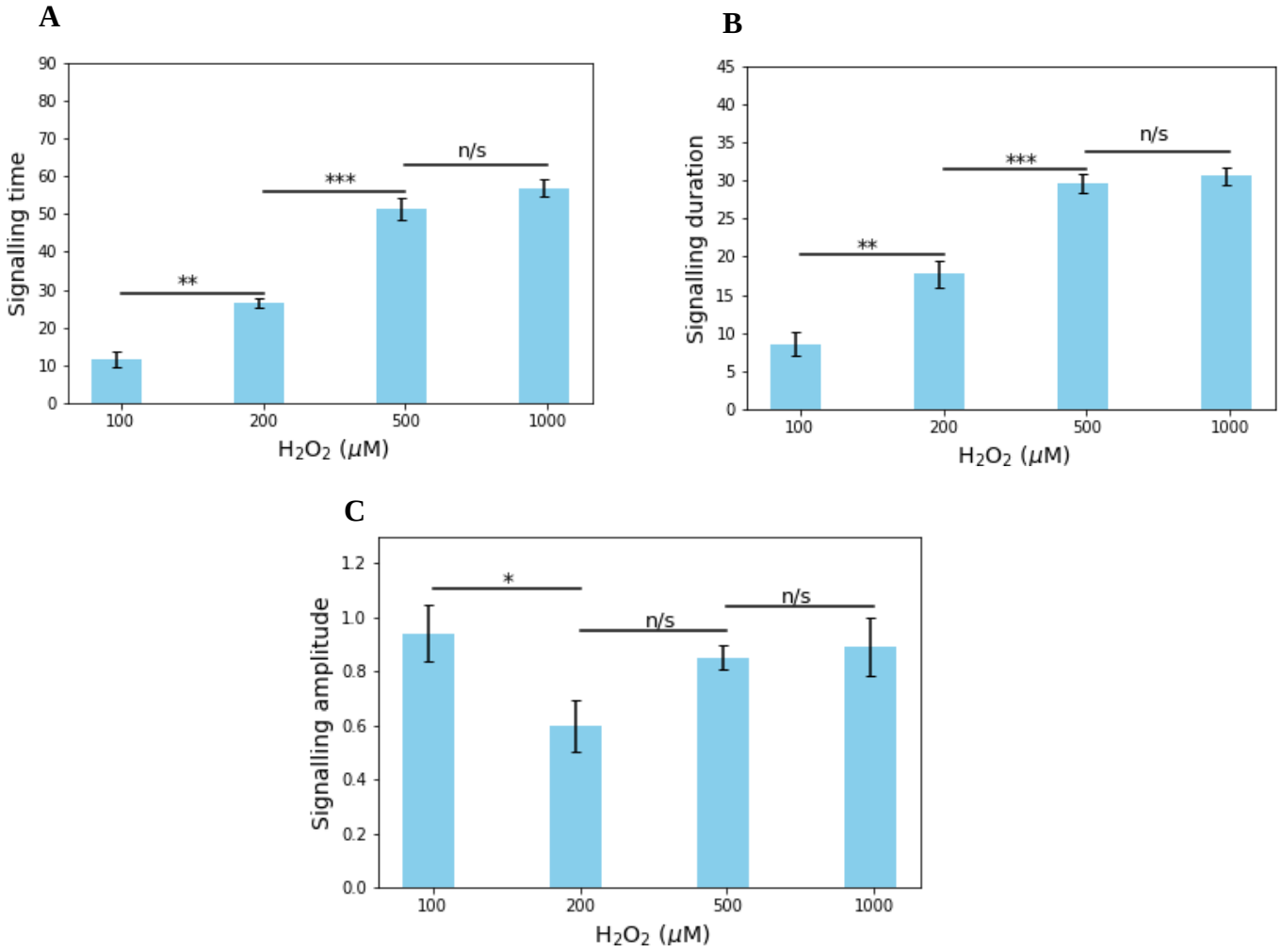


**Figure 3.10: The effect of different hydrogen peroxide concentrations on time-dependent redox signalling in the Tpx1/Pap1 pathway**. Here, the activation of Pap1 was used to calculate signal time (Equation 1, section 2.4.11), signal duration (Equation 2) and signalling amplitude (Equation 3). Significance was calculated using a *t*-test with one-tailed distribution and unequal variance and denoted as * $p<0.05$, ** $p<0.01$, *** $p<0.001$ and n/s is not significant.

### 3.2.6 Effect of a Pk-tag on Pap1 oxidation

Next, the utility of using the signalling parameters to test other redox signalling experiments was assessed. For example, many studies use protein tags for western blot analysis as most of the antibodies against these tags are commercially available and therefore, generation of protein-specific antibodies are not required (Bozonet *et al*, 2005). However, it is unclear if these tags have an effect on the signalling capability of proteins. Therefore, quantification of Pap1 oxidation in the *S. pombe* SB3 Pk-tag strain was compared to a wildtype *S. pombe* 972 strain to determine the effect of the Pk-tag on signalling parameters *in vivo*. These strains were both exposed to 200 μM hydrogen peroxide for 10 minutes and native Pap1 antibodies were used to determine the oxidation state of the transcription factor (Figure 3.11). Pap1 in the SB3 strain appeared to be mostly in the reduced form at 10 minutes whereas Pap1 in the 972 strain was largely in the oxidized form (Figure 3.11). From this western blot it appeared as though the Pk-tag did affect Pap1 oxidation and the precise effect on the signalling parameters could now be quantified from graphs of SB3 and 972 Pap1 oxidation.

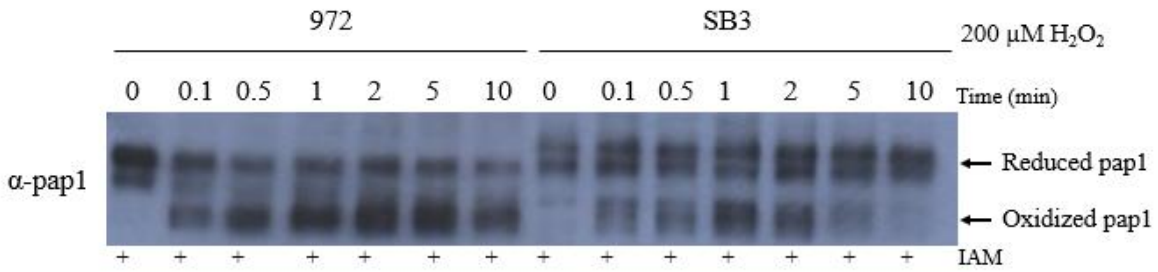


**Figure 3.11: The effect of 200 μM hydrogen peroxide on Wildtype 972 and SB3 *S. pombe* strains.** The *S. pombe* strains were cultivated to OD~0.5 in YE5S media and challenged with 200 μM hydrogen peroxide for 10 minutes. Protein samples were extracted from whole cell lysate and subjected to western blot analyses. Pap1 oxidized and reduced bands were detected using an α-Pap1 antibody.

**Table 3.2: Summarized signalling parameters for Pk-tag effect on Pap1 oxidation in the SB3 strain compared to the wildtype 972.** The 972 and SB3 strains were cultured in YE5S and Pap1 oxidation was evaluated using a specific Pap1 antibody the signalling parameters for Pap1 oxidation were then calculated from western blotting data (Figure 3.11). These parameters were compared to the SB3 strain cultured in EMM media and Pap1 oxidation was determined using the Pk-tag antibody (Figure 3.6). To make a fair comparison the signalling parameters were only calculated for 10 minutes of the 60 minute time-course.

| | α-Pap1 | | α-Pk |
|---|---|---|---|
| **Signalling parameter** | **972 (YE5S)** | **SB3 (YE5S)** | **SB3 (EMM)** |
| **Time (min)** | 5.28 | 3.55 | 4.65 |
| **Duration (min)** | 3.31 | 2.63 | 3.22 |
| **Amplitude** | 1.08 | 0.58 | 0.68 |

Due to the scarce availability of the native Pap1 antibody, this experiment could not be repeated and statistically analysed. Signalling parameters for Pap1 oxidation in *S. pombe* 972 and SB3 cultured in YE5S indicated that the Pk-tag slightly reduced the signal time and duration of Pap1 in SB3 compared to 972 (Table 3.2). However, the signal amplitude of Pap1 was almost half of in the 972 strain (Table 3.2). This was consistent with western blot analysis which showed that the Pk-tag affected Pap1 oxidation (Figure 3.11). In an attempt to counteract the effect of a Pk-tag on Pap1 oxidation on signal amplitude, cells were cultured in EMM media to promote Pap1 oxidation as complex media can degrade hydrogen peroxide (Bozonet *et al*, 2005). The signal parameters were 4.65 minutes for signal time, 3.22 minutes for signal duration and 0.68 for signal amplitude for Pap1 in SB3 cells cultured in EMM (Table 3.2). These results show indicate that a Pk-tag does have an effect on the signalling parameters and that the culture medium can also influence the redox signal time, duration and amplitude. Antibodies against Pap1 will need to be made to statistically verify this result as the native Pap1 antibody was not commercially available.

### 3.2.5 Effect of tert-butyl hydroperoxide (tBOOH) on Pap1 oxidation

Hydroperoxides like the tertiary butanol (tBOOH), are also commonly used to induce oxidative stress responses in cells (Calvo *et al*, 2013; Hampton and Connor, 2016). These oxidants are believed to work similarly to hydrogen peroxide, but for the first time the effect of these oxidants on the Pap1 signalling pathway could be quantified. When compared to the rapid Pap1 oxidation by hydrogen peroxide, tBOOH-induced oxidation of Pap1 took 5 minutes (Figure 3.12A). The tBOOH-induced Pap1 oxidation curve was also more bell-shaped and there was no sustained Pap1 oxidation compared to the hydrogen peroxide signalling profiles of Pap1 (Figure S5). To determine the exact effect of tBOOH on the Tpx1/Pap1 pathway, the signalling parameters were determined (Table S5).

The signalling time for Pap1 oxidation exposed to tBOOH was 12.12 minutes, almost half that of hydrogen peroxide (26.62 minutes) while signal duration with tBOOH was three times as short at 6.69 minutes compared to 17.78 minutes for Pap1 oxidation with hydrogen peroxide and these differences were statistically significant (Figure 3.13A, B). By contrast, the difference between the signal amplitudes for tBOOH and hydrogen peroxide were not statistically significant (Table 3.3, Figure 3.12 C).

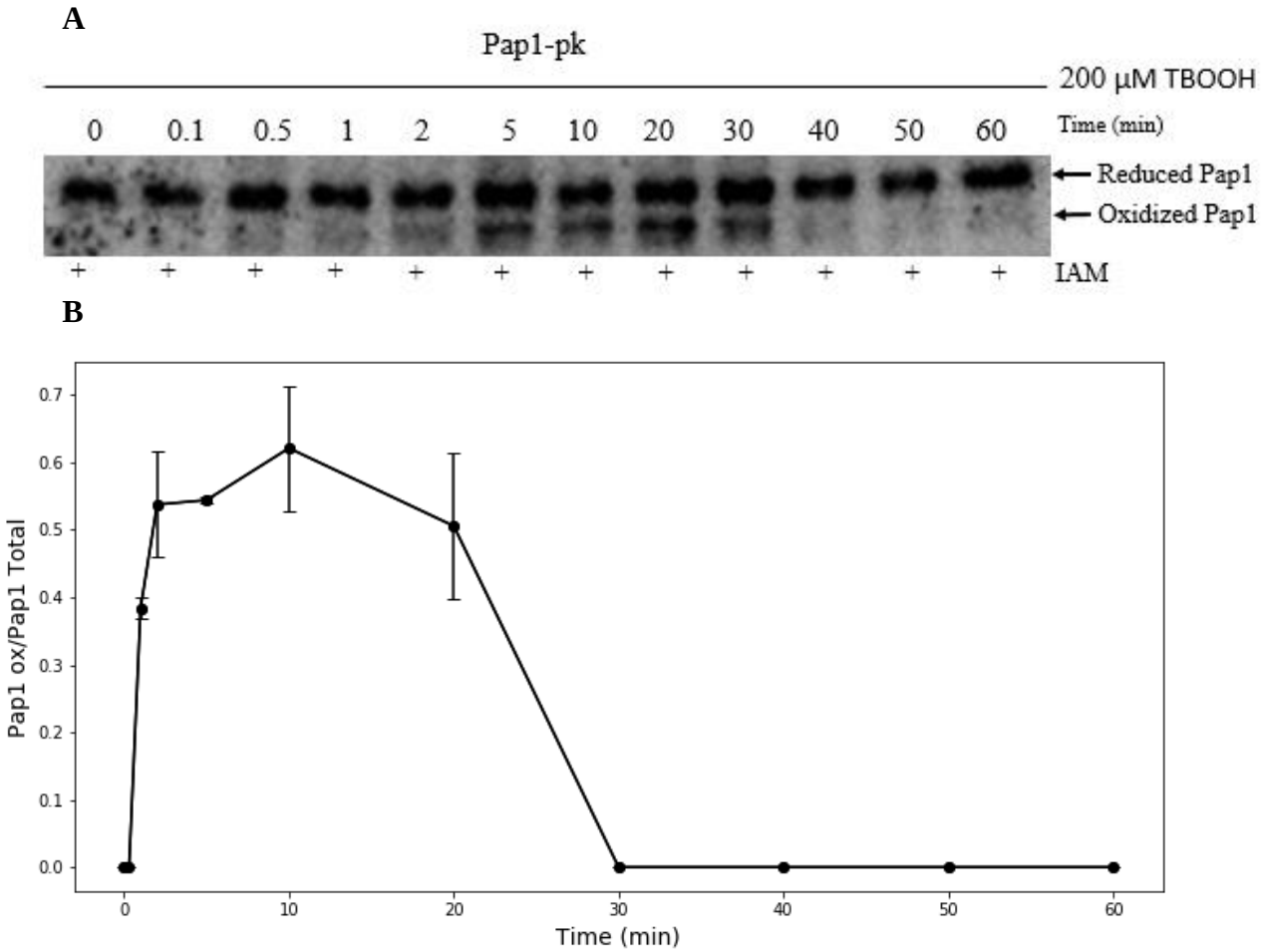


**Figure 3.12: Western blot analysis of Pap1 oxidation after exposure of *S. pombe* cells to 200 µM tBOOH for 60 minutes (A) and the Pap1 signalling profile by tBOOH (B).** The *S. pombe* SB3 strain was challenged with tBOOH for 60 minutes and protein samples were extracted and treated with IAM. Western blot analysis was carried out and α-Pk antibodies detected the Pap1 banding pattern (A). The signalling profile was then generated, error bars indicate independent samples taken for each time-point (B) (*n*=2).

**Table3.3: Summarized signalling parameters for OxyR, Yap1, Pap1 exposed to tBOOH and Pap1 exposed to hydrogen peroxide.**

| Signalling parameter | Pap1 (tBOOH) | Pap1 ($H_2O_2$) | OxyR | Yap1 |
|---|---|---|---|---|
| **Time (min)** | 12.06 ± 0.39 | 26.62 ± 1.17 | 7.21 | 24.59 |
| **Duration (min)** | 6.68 ± 0.01 | 17.78 ± 1.77 | 8.26 | 15.65 |
| **Amplitude** | 0.995 ± 0.15 | 0.6 ± 0.10 | 0.42 | 1.2 |

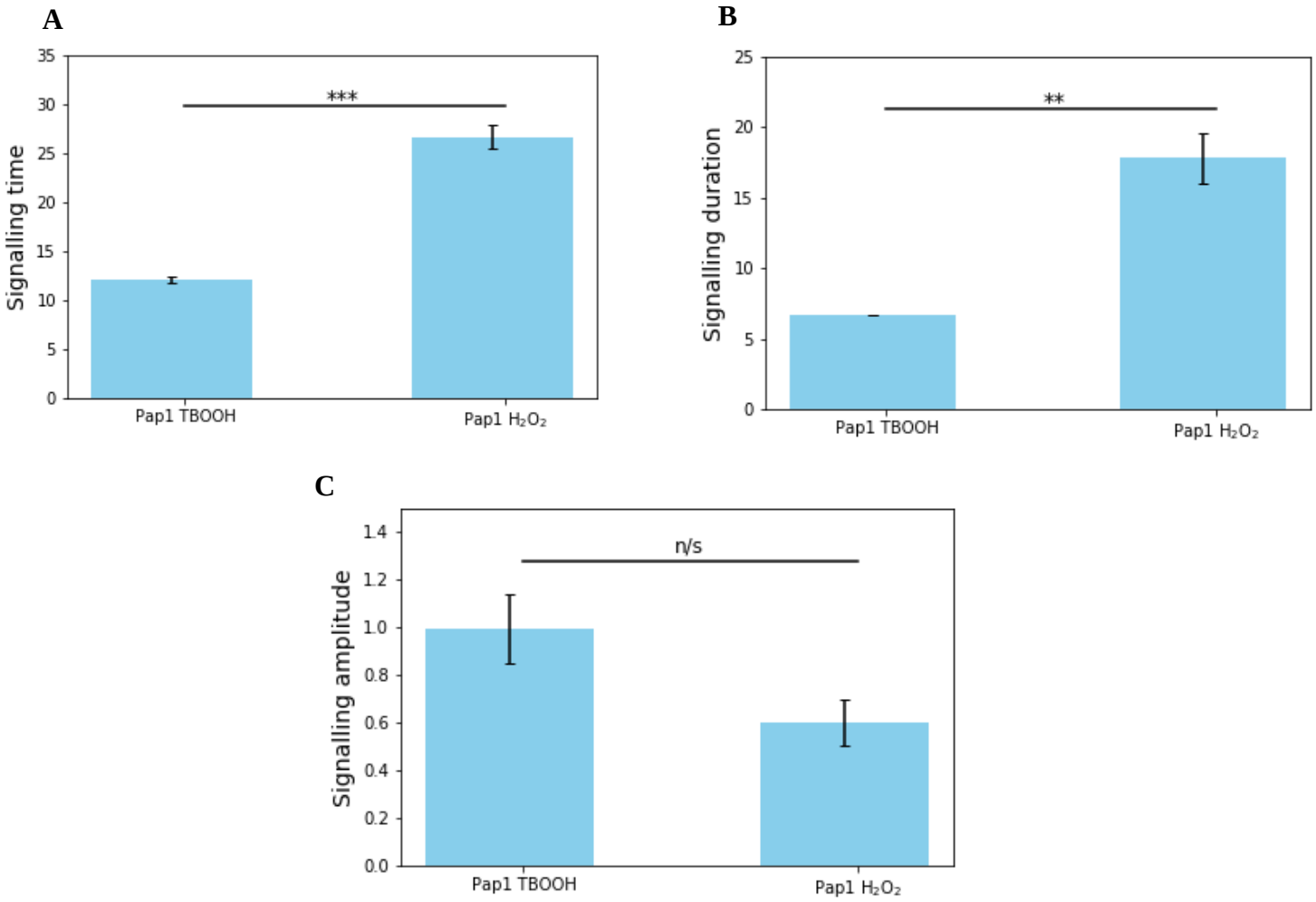


**Figure 3.13: Comparison of signalling parameters of Pap1 oxidation between tBOOH compared to hydrogen peroxide**. Signalling time, duration and amplitude were calculated according to equations 1-3 (See section 2.4.11) from digitized western blotting data obtained in Figure 3.12 and were significantly compared using a *t*-test with a one-tailed distribution and unequal variance. Significance was denoted as **p*<0.05, ***p*<0.01, ****p*<0.001 and n/s is not significant.

### 3.2.6 Quantification of redox signalling by transcription factors

An additional application of this time-dependent quantification method was that it could be used to compare the signal parameters of different redox transcription factors. Western blotting data was obtained for the oxidation of OxyR in *E. coli* (Aslund *et al*, 1999) and the signalling parameters were calculated (Figure 3.14, Table 3.3, Table S6). Rapid oxidation of OxyR was observed after one minute of exposure to 200 µM hydrogen peroxide and then rapidly decreased after 5 minutes and was fully reduced at 10 minutes. The signalling parameters were quantified and were as follows: 7.21 minutes for signalling time, 8.26 minutes for signal duration and 0.42 for signal amplitude (Table 3.3). This oxidation profile of OxyR and the signalling parameters are vastly different to that obtained for Pap1 oxidation with hydrogen peroxide at the same concentration (Table 3.3). Unfortunately, replicate samples of OxyR oxidation were not available and therefore could not be statistically analysed.

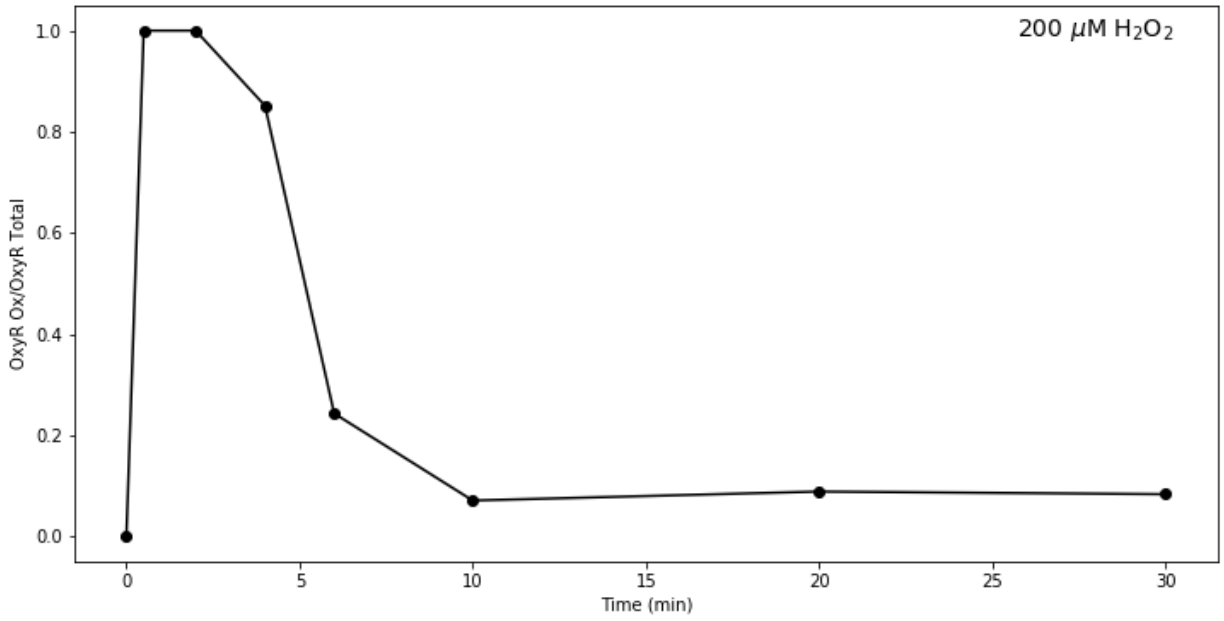


**Figure 3.14: Quantification of the OxyR transcription factor in *E. coli* after 30 minutes of 200 µM hydrogen peroxide exposure**. Exponentially growing *E. coli* cells were challenged with 200 µM hydrogen peroxide and samples taken over a 30 minute time-course. Protein was extracted and alkylated with AMS and subjected to western blot analysis. Reduced and oxidized forms of OxyR were detected using polyclonal antibodies (Aslund *et al*,1999).

Western blotting data was also obtained for the oxidation of Yap1, a Pap1 homologue, in *S. cerevisiae*. Yap1 western blotting data was obtained from Delaunay *et al* (2000), the bands were quantified using ImageJ and fractional Yap1 oxidation was plotted. Yap1 oxidized rapidly after 2.5 minutes of hydrogen peroxide exposure and Yap1 oxidation was sustained until 30 minutes and was fully reduced by 60 minutes (Figure 3.15). The signalling parameters were then quantified and were 24.59 minutes for signal time, signal duration was 15.65 minutes and signal amplitude was 1.2 (Table 3.3).

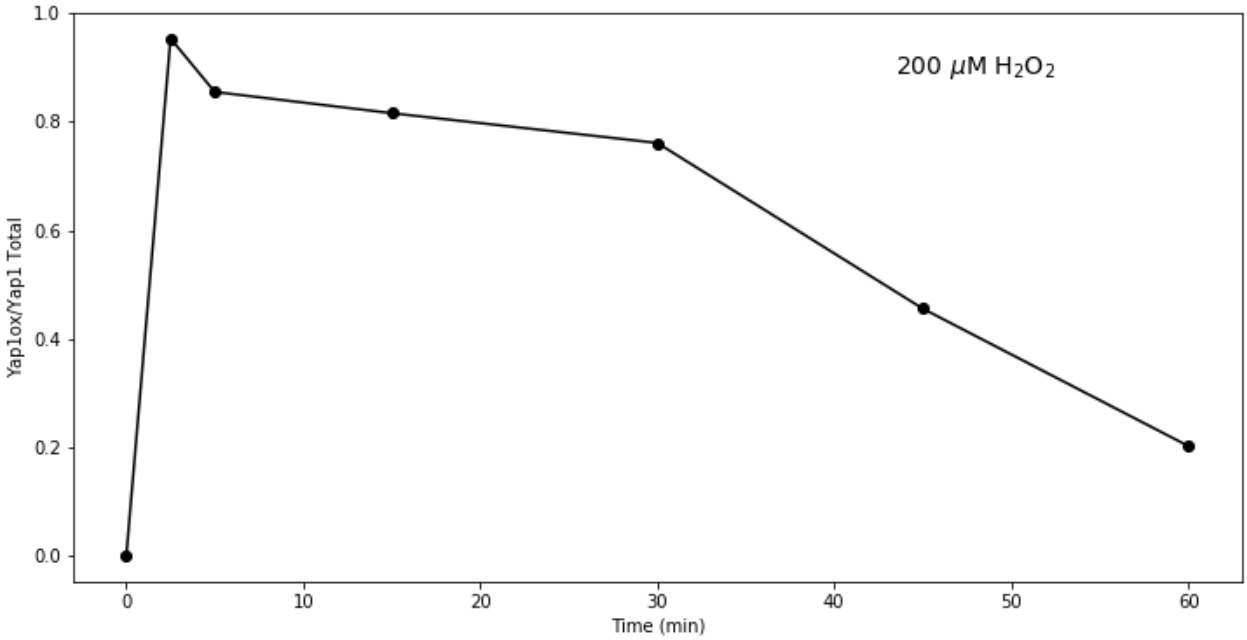


**Figure 3.15: Quantification of Yap1 in *S. cerevisiae* after 60 minutes of 200 μM hydrogen peroxide exposure.** *S. cerevisiae* was cultured to mid-log phase and exposed to 200 μM hydrogen over a 60 minute time-course. Protein samples were extracted and treated with IAM and subjected to western blot analysis from which the oxidized and reduced forms of Yap1 were detected using α-Myc monoclonal antibodies (data from Delauney *et al* (2000)).

The signalling time and duration for Yap1 and Pap1 appeared to be greater than for OxyR (Figure 3.16A, B). Interestingly, this pattern was not observed for the signal amplitude as Yap1 appeared to have a greater amplitude compared to OxyR and Pap1 (Figure 3.16 C). Unfortunately no replicates were available for OxyR and Yap1 therefore the significant differences between these signalling regimes could not be established.

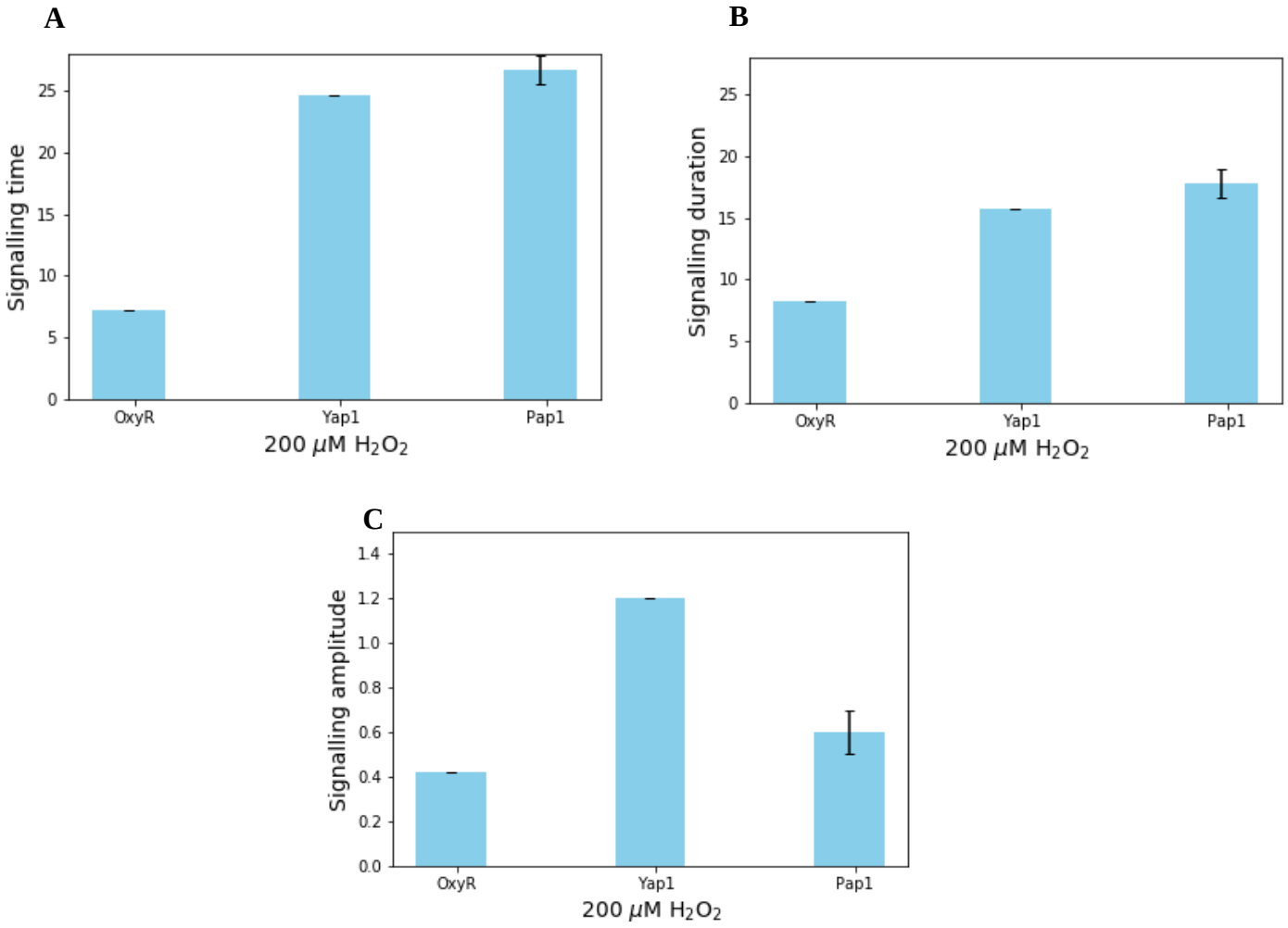


**Figure 3.16: Comparison of signalling parameters of the prokaryotic transcription factor OxyR and the eukaryotic transcription factors Yap1 and Pap1.** From the available western blotting data the oxidation states of OxyR (Figure 3.14) and Yap1 (Figure 3.15) were digitized and the signalling parameters calculated using equations 1-3 (See section 2.4.11). No replicates were available for OxyR and Yap1 data, hence no standard errors for these two transcription factors were calculated. Standard error indicated for Pap1 (*n*=3).

### 3.2.7 Evaluating the effect of gene replacement technologies on signalling parameters

Many studies use gene knockout or knockin technologies to assign functions to antioxidant proteins that maintain the redox balance in cells. For example, to evaluate the differences in direct sensing and sensor-mediated activation of transcription factors (See chapter 1.4), the direct hydrogen peroxide sensor, OxyR, from *E. coli* was cloned into *S. pombe* creating the strain AD29 (Domènech *et al*, 2018). Using the quantification method developed in this chapter, we aimed to determine if this gene knockin had an effect on the Pap1 signalling parameters when compared to the signalling parameters obtained in Figure 3.7.

Pap1 oxidation from the AD29 strain was quantified and plotted together with Pap1 oxidation from SB3 at 100 µM hydrogen peroxide and the signalling parameters were then compared to determine if the presence of OxyR impacted Pap1 signalling (Figure 3.17). The oxidation of Pap1 in both data sets showed rapid oxidation that was sustained for 10 minutes and then Pap1 returned to the reduced form by 50 minutes (Figure 3.17; Table S7). The only notable difference was that the Pap1 data in the AD29 appeared to be more oxidized when compared to the SB3 strain.

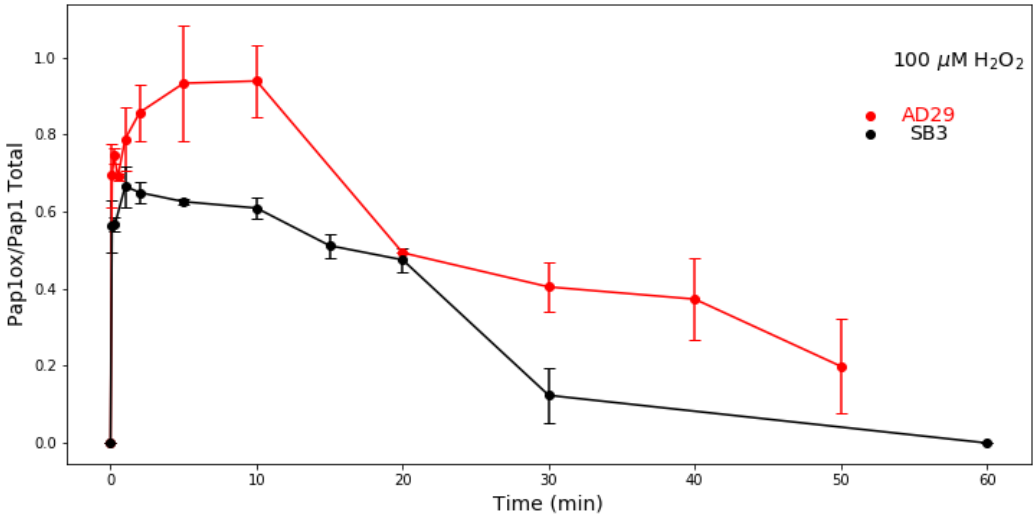


**Figure 3.17: Signalling profiles of Pap1 oxidation after exposure to 100 µM hydrogen peroxide for *S. pombe* AD29 and SB3 strains.** Western blotting data for Pap1 oxidation exposed to 100 µM obtained from Doménech *et al* (2018) was digitized using ImageJ and plotted against the 50 minute time-course (red). This data was also plotted with Pap1 oxidation data obtained in Figure 3.6 (black). Standard error bars indicate triplicate samples taken for each time point ($n$=3).

Doménech *et al* (2018) followed Pap1 oxidation after the addition of 500 µM hydrogen for 50 minutes whereas Pap1 oxidation for the SB3 strain was tracked for 120 minutes. Interestingly, both oxidation profiles was similar for the initial oxidation to 10 minutes but the AD29 strain showed no Pap1 oxidation between 20-40 minutes unlike Pap1 oxidation in SB3. Furthermore, after 40 minutes, Pap1 in the AD29 strain started to oxidize again but Pap1 oxidation was no longer tracked after this time point and consequently the complete Pap1 signalling profile in the AD29 strain is not known. Signalling parameters were therefore only compared up to 20 minutes for the initial oxidation of Pap1 in *S. pombe* AD29 and SB3 strains (Figure 3.18; Table S7).

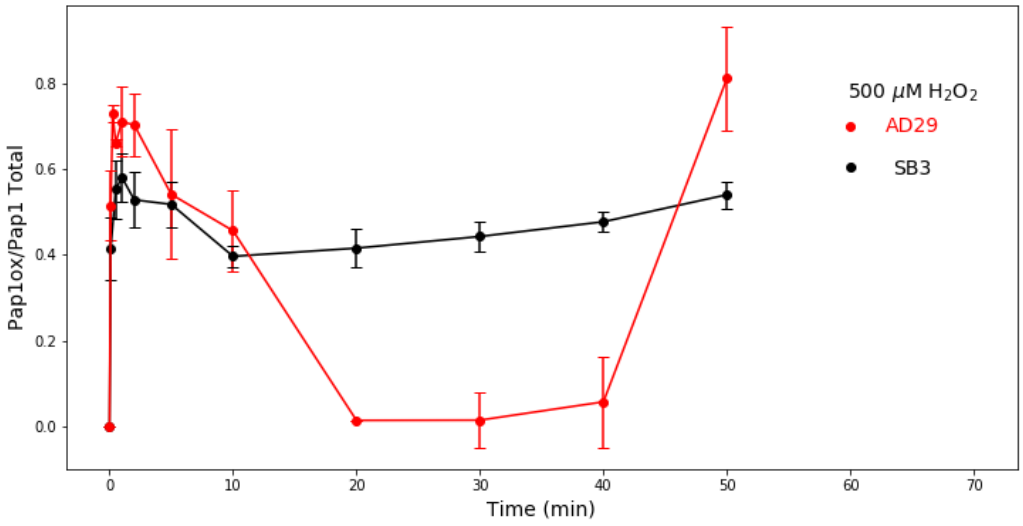


**Figure 3.18: Signal profiles for Pap1 oxidation after 500 µM hydrogen peroxide exposure for AD29 and SB3 strains.** Western blotting data was obtained for Pap1 oxidation in this study (black) and in the AD29 strain (red) and were plotted together. Standard error bars indicate independent samples for AD29 (*n*=2) and for SB3 (*n*=3).

The signalling time at 100 and 500 µM hydrogen peroxide was compared after 20 minutes of Pap1 oxidation and showed no significant difference between the AD29 and SB3 strains (Figure 3.19A). Signal duration also showed no significant difference at 100 µM or 500 µM hydrogen peroxide for the two strains at 20 minutes (Figure 3.19B). Lastly, the signalling amplitude showed no significant difference for the two strains for both 100 and 500 µM hydrogen peroxide exposure (Figure 3.19C). However, the experimental variation observed for the AD29 strain indicates that the data may not be completely reliable (Figure 3.19A-C).

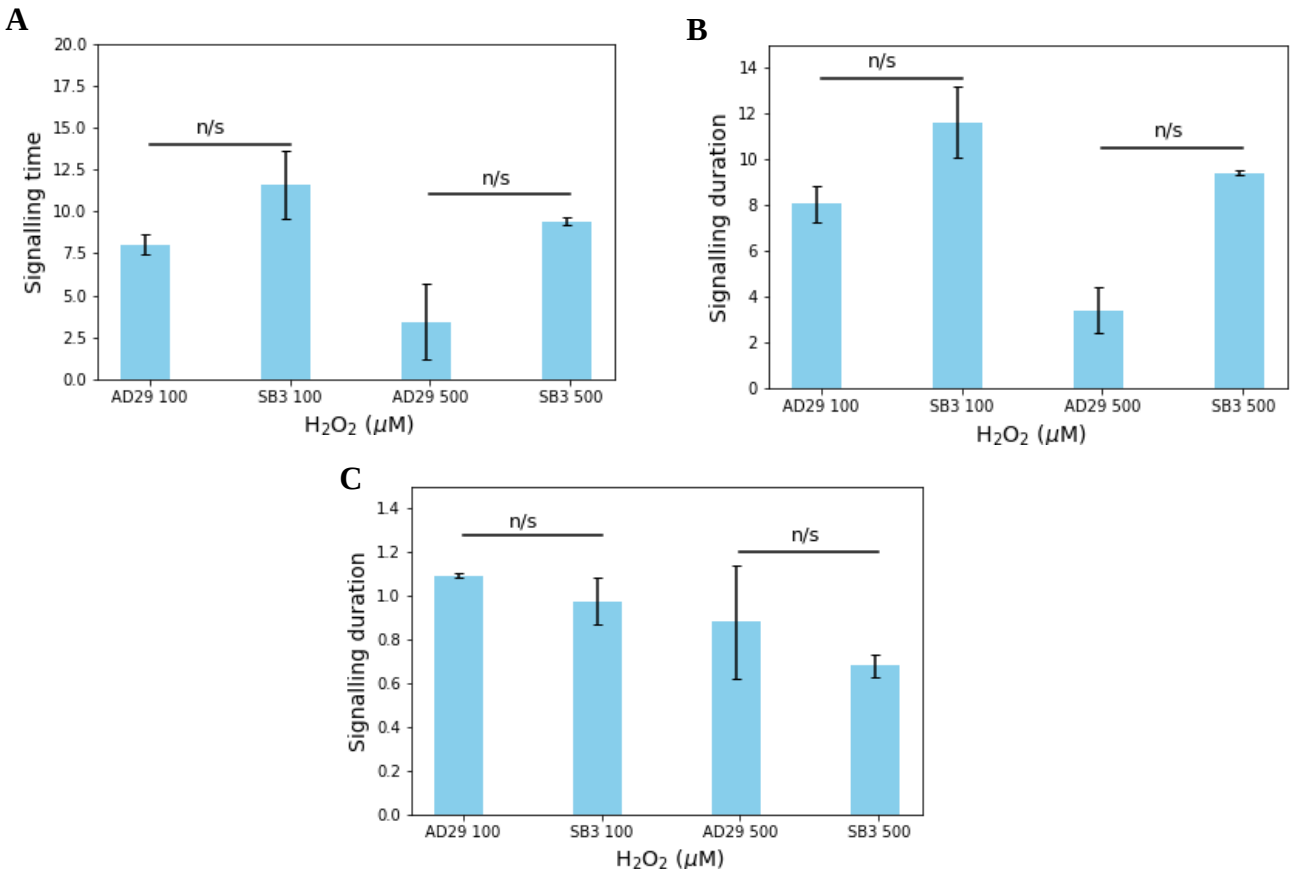


**Figure 3.19: Signalling parameters for *S. pombe* AD29 and SB3 strains exposed to 100 and 500 µM hydrogen peroxide.** Pap1 signal time, duration and amplitude were compared for the AD29 strain (Domènech *et al*, 2018) and SB3 strain. Standard errors indicate triplicate experiments for 100 µM and duplicate experiments for strains exposed to 500 µM hydrogen peroxide. No significance is indicated by n/s.

## 3.2 Discussion

Understanding how redox signalling pathways are dynamically regulated has remained elusive as current measures of signalling are limited. Therefore, time-dependent quantification of the Tpx1/Pap1 pathway was proposed using the mathematical framework developed by Heinrich *et al* (2002) to provide further insights into signal regulation by determining the signalling time, duration and amplitude of Pap1 activation.

It was shown that increasing the hydrogen peroxide concentration from 100 to 500 μM significantly increased the signal time and duration. However, an increase in concentration from 500 to 1000 μM hydrogen peroxide did not have a significant effect on signalling time or duration. This may be due the fact that Tpx1 becomes hyperoxidized and the signalling system becomes saturated (Vivancos *et al*, 2005). Signalling amplitude did not show significant changes upon increasing the hydrogen peroxide concentration which was intriguing as many studies rely on the intensity of the oxidized band on western blots to infer the cellular function of signals (Toone *et al*, 1998; Delaunay *et al*, 2000; Brown *et al*, 2013). With the quantification method being verified its utility to compare other redox signalling experiments was assessed.

The incorporation of a Pk-tag on Pap1 signalling was shown to have an effect upon quantification of time-dependent signalling parameters but this significance could not be tested. The use of 200 μM tBOOH as an oxidant compared to 200 μM hydrogen peroxide resulted in a significant decrease in signal time and duration for Pap1 oxidation. Additionally, the signalling pathways of different types of transcription factors could also be compared which revealed that the signal time and duration of sensor-mediated transcription factors like Yap1 and Pap1 was greater than for the direct sensor OxyR. This may be significant as transcription and translation of new proteins in *E. coli* takes ~20 minutes when compared to yeasts that take ~50-120 minutes for these processes (Cokus *et al*, 2006). Surprisingly, this pattern was not observed for signal amplitude where Yap1 appeared to have a greater amplitude compared to OxyR and Pap1. Finally, the effects of gene knockin technology was also assessed. This was relevant as the use of genetically encoded redox sensors has become a popular technique to monitor the thiol redox state in live cells (Fan *et al*., 2017; Lukyanov and Belousov, 2014). These studies often insert a redox regulated gene into the genome through gene replacement methods (Lukyanov and Belousov, 2014). For example, a hydrogen peroxide sensor (HyPer) was developed based on the fast activation of OxyR to detect intracellular hydrogen peroxide generation (Lukyanov and Belousov, 2014). Time-dependent quantification was used to test

whether incorporation of OxyR into the *S. pombe* genome affected the signalling of Pap1 (Domènech *et al*, 2018) and revealed that there was no significant difference between the signalling parameters. In summary, quantitative comparisons of redox signals can be made using the methodology proposed in this thesis.

An interesting consideration for future work would be to explore how these quantitative measures relate to gene expression studies. It was found that low and medium levels of hydrogen peroxide differentially regulated 127 genes known as the core oxidative stress genes. It was demonstrated that Pap1 regulated most of these genes at low hydrogen peroxide concentrations and the stress response was rapid and transient (Chen *et al*, 2008). In contrast, at medium hydrogen peroxide concentrations of 500 μM Pap1 regulation of core stress response genes was diminished with Atf1 and Sty1 beginning to regulate gene expression (Figure 3.1). Indeed, higher concentrations of hydrogen peroxide are known to hyperoxidize Tpx1, inhibiting the Pap1 pathway, and the Sty1 pathway must be activated to induce sulphiredoxin transcription to recycle hyperoxidized Tpx1 back into the Pap1 pathway (Quinn *et al*, 2002). Precisely how the signalling parameters correlate to gene expression levels is an interesting question but was beyond the scope of this study and would need to be tested in future work. Lastly, the signal amplitude was the only parameter that did not significantly change dependent on the hydrogen peroxide concentration. Unfortunately, this measure is often captured in the band intensity from western blotting data and is currently the most used measure of comparison between different experimental conditions for redox activated proteins.

To conclude, we have tested whether time-dependent quantification of redox signals can provide further insight into stress responses of *S. pombe* cells. This method was useful in identifying the precise effects of increasing hydrogen peroxide concentrations on the Tpx1/Pap1 pathway. Additionally, quantification could measure if protein tags had an effect on signalling. Furthermore, how other oxidants differentially oxidized Pap1 could also be quantified and this method also provides measures to distinguish between transcription factors. Importantly, for the first time, this method allows for accurate comparisons of western blotting data obtained from other research groups.

# Chapter 4: Computational modelling of Tpx1/Pap in fission yeast

## 4.1 Introduction

The ability to quantify time-dependent redox signalling as outlined in Chapter 3 provided a method to ask further questions. An interesting consideration would be to investigate which components of the redox signal machinery controlled the signalling time, duration or amplitude. For example, quantification of MAPK signalling revealed that phosphatases affect signal duration, whereas signal amplitude was regulated by kinases (Hornberg *et al*, 2005). Similarly, we wanted to investigate how the redox signalling parameters are controlled by the Tpx1/Pap1 pathway in *S. pombe*. Computational modelling offered an integrated method to test this as the components, kinetics and reactions of proteins could be simulated *in silico* providing a facile way of testing time-dependent regulation before *in vivo* experiments are undertaken.

As a first step, it was necessary to model the 2-Cys peroxiredoxin redox cycle which was previously described (Section 1.3.1), but this cycle involves a number of additional molecular events which are described below (Figure 4.1A) (Pace *et al*, 2013). Reduced 2-cysteine peroxiredoxins form decameric structures that consist of five dimers in a ring-like structure and are present at high concentrations in most cell types under normoxic conditions (Figure 4.1B) (Cao *et al*, 2011). Upon oxidation, structural rearrangements at the dimer interface results in decamer dissociation (Figure 4.1B). Interestingly, hyperoxidized peroxiredoxins accumulate and reassociate into a decamer and then a dodecamer (20-mer structure made from two decamers). The dodecamer has no peroxidase activity but gains chaperone activity and assists in folding of proteins without the need for ATP (Pace *et al*, 2013).

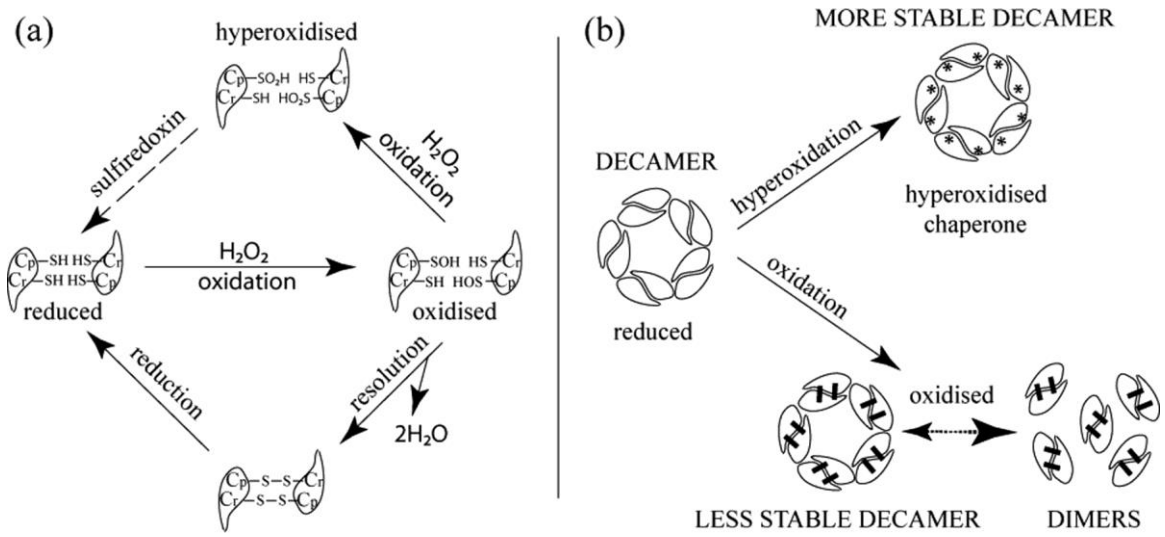


**Figure 4.1: Complexity of the 2-cysteine peroxiredoxin redox cycle.** 2-cysteine peroxiredoxins have two catalytic cysteine residues that degrade hydrogen peroxide and form sulfenic acid that resolves into disulphide bridges. Alternatively, the peroxiredoxins are hyperoxidized by hydrogen peroxide and require sulphiredoxin to return it the reduced form (A). 2-cysteine peroxiredoxins form decamer structures that are more stable once hyperoxidized (B) (Pace *et al,* (2013) Copyright permission to reproduce this image was obtained by Elsevier).

Fortunately, a Tpx1 model for *S. pombe* was developed by Tomalin *et al* (2016). This model was able to accurately simulate hydrogen peroxide transport across the cell membrane and revealed a bi-phasic relationship between extracellular hydrogen peroxide and intracellular hydrogen peroxide consumption. Further, this model was also able to predict Tpx1 oxidation states from experimental data, providing support for the computational model (Figure 4.2) (Tomalin *et al*, 2016). We therefore used this model to further explore Pap1 oxidation *in silico*.

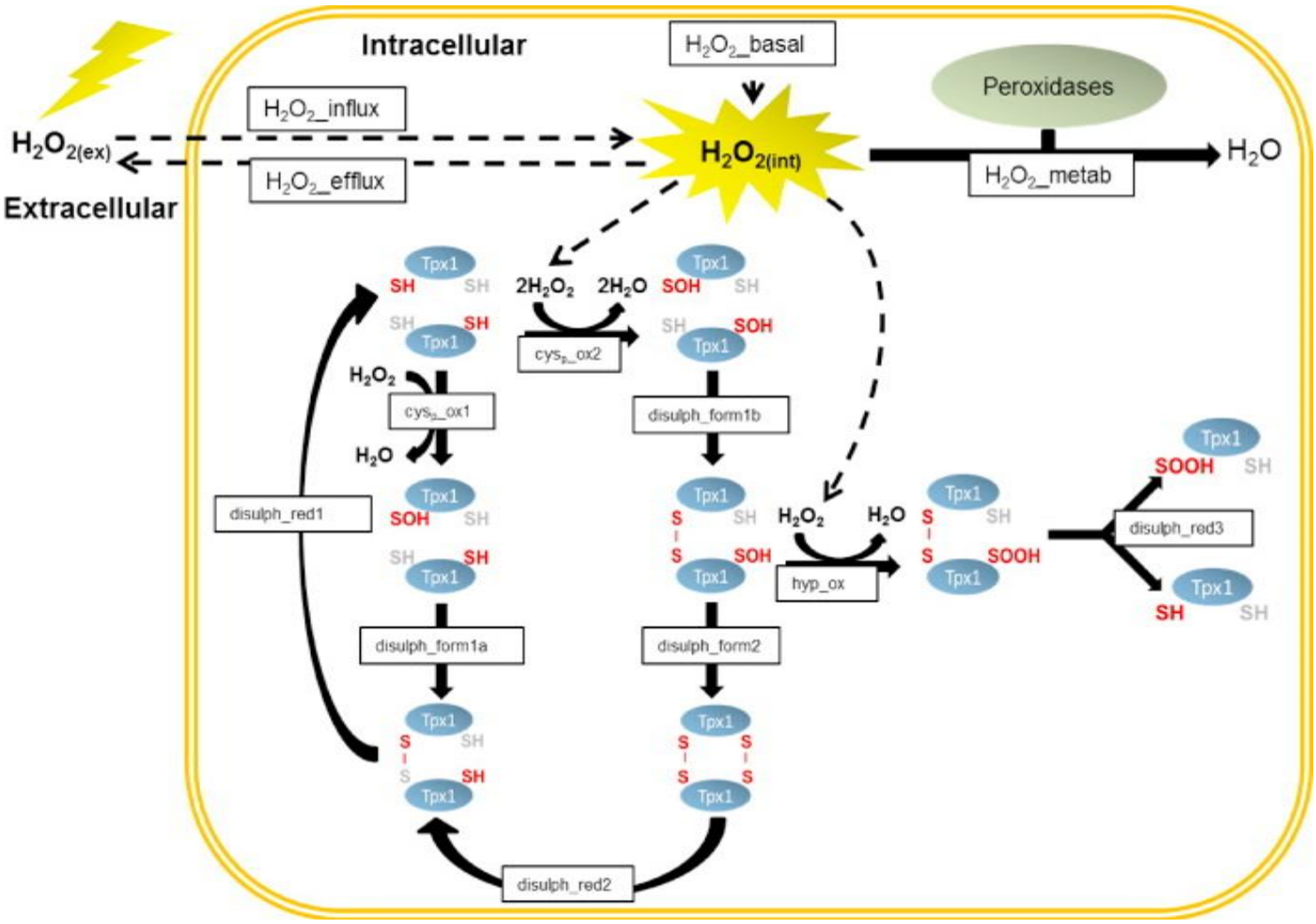


**Figure 4.2: Schematic diagram for hydrogen peroxide degradation by the 2-Cysteine peroxiredoxin, Tpx1 in *S. pombe* (Tomalin *et al*, 2016)**. This model consists of 9 different isoforms of Tpx1 and their relevant oxidation, disulphide bridge formation, reduction and hyperoxidation reactions. Hydrogen peroxide is first transported across the membrane ($H_2O_2$_influx) and reacts with one peroxidatic cysteine residue (cys$_p$_ox1) on reduced Tpx1 or two hydrogen peroxide molecules react with both peroxidatic cysteines (cys$_p$_ox2). These oxidized forms of Tpx1 then condense to form disulphide bridges represented by disulph_form1a, disulph_form1b and disulph_form2. These disulphide bridges are then reduced by the thioredoxin system represented by reactions disulph_red1 and disulph_red2. Additionally, hydrogen peroxide can further react with the disulphide sulfenic Tpx1 form resulting in hyperoxidized Tpx1 dimer which then dissociates (disulph_red3) into Tpx1 hyperoxidized monomer and a reduced Tpx1 monomer. Permission to reproduce this image was obtained from Elsevier.

## 4.2 Methods

The computational model developed by Tomalin *et al* (2016) was previously converted from COPASI to Python Simulator for Cellular Systems (PySCeS) format (Olivier *et al*, 2005, http://pysces.sourceforge.net) and all further kinetic modelling was carried out in PySCeS. Modelling files were developed in the Sublime Text editor (https://www.sublimetext.com) and were simulated in the Jupyter notebook (https://jupyter.org/install).

## 4.3 Results

### 4.3.1 Addition of Pap1 reaction to Tpx1 model generated for *S. pombe*

The computational model of hydrogen peroxide metabolism in fission yeast (Tomalin *et al*, 2016) developed in COPASI was converted to PySCeS format and the PySCeS model was able to accurately simulate the published Tpx1 isoforms (data not shown) (File 1, supplementary data). For example, the PySCeS model was able to accurately predict how most of Tpx1 species changed over a 10 minute time-course at 100 and 200 µM hydrogen peroxide (Figure 4.3 A-H).

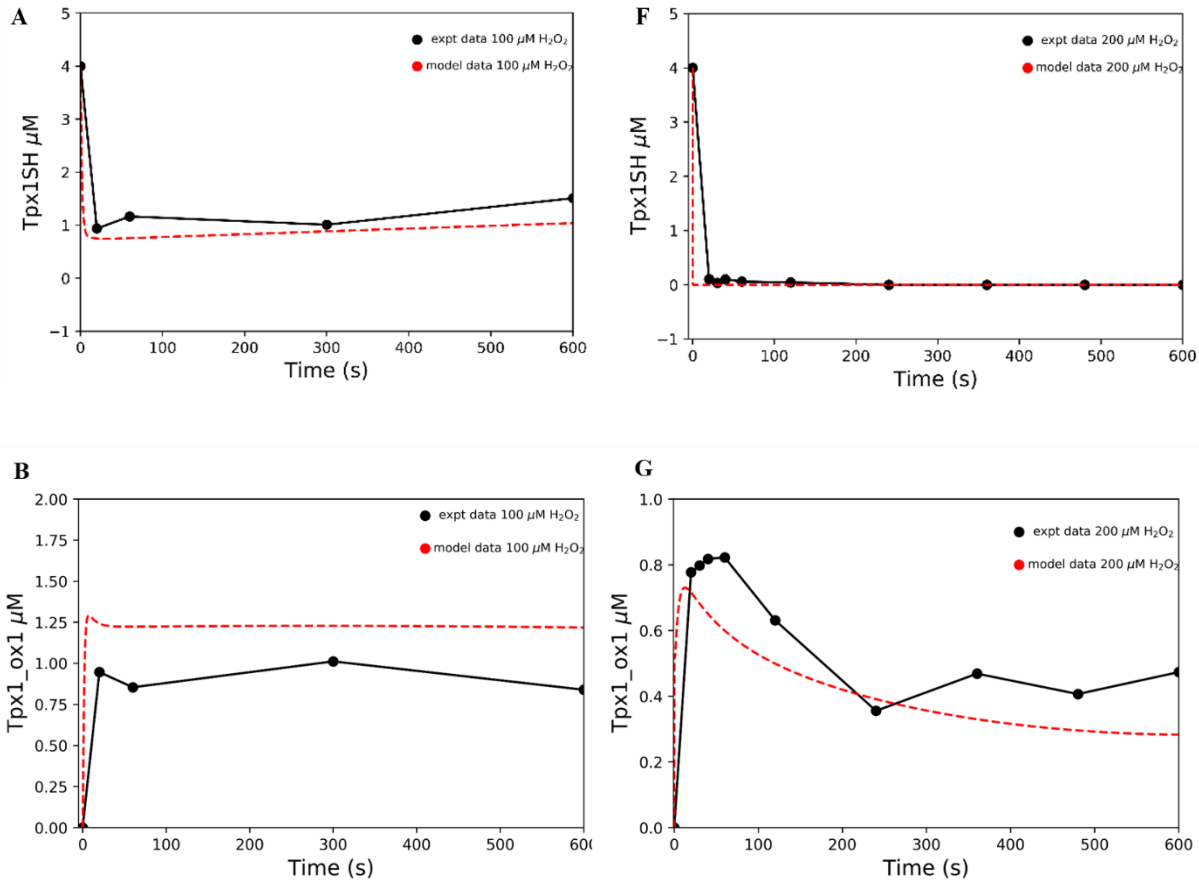

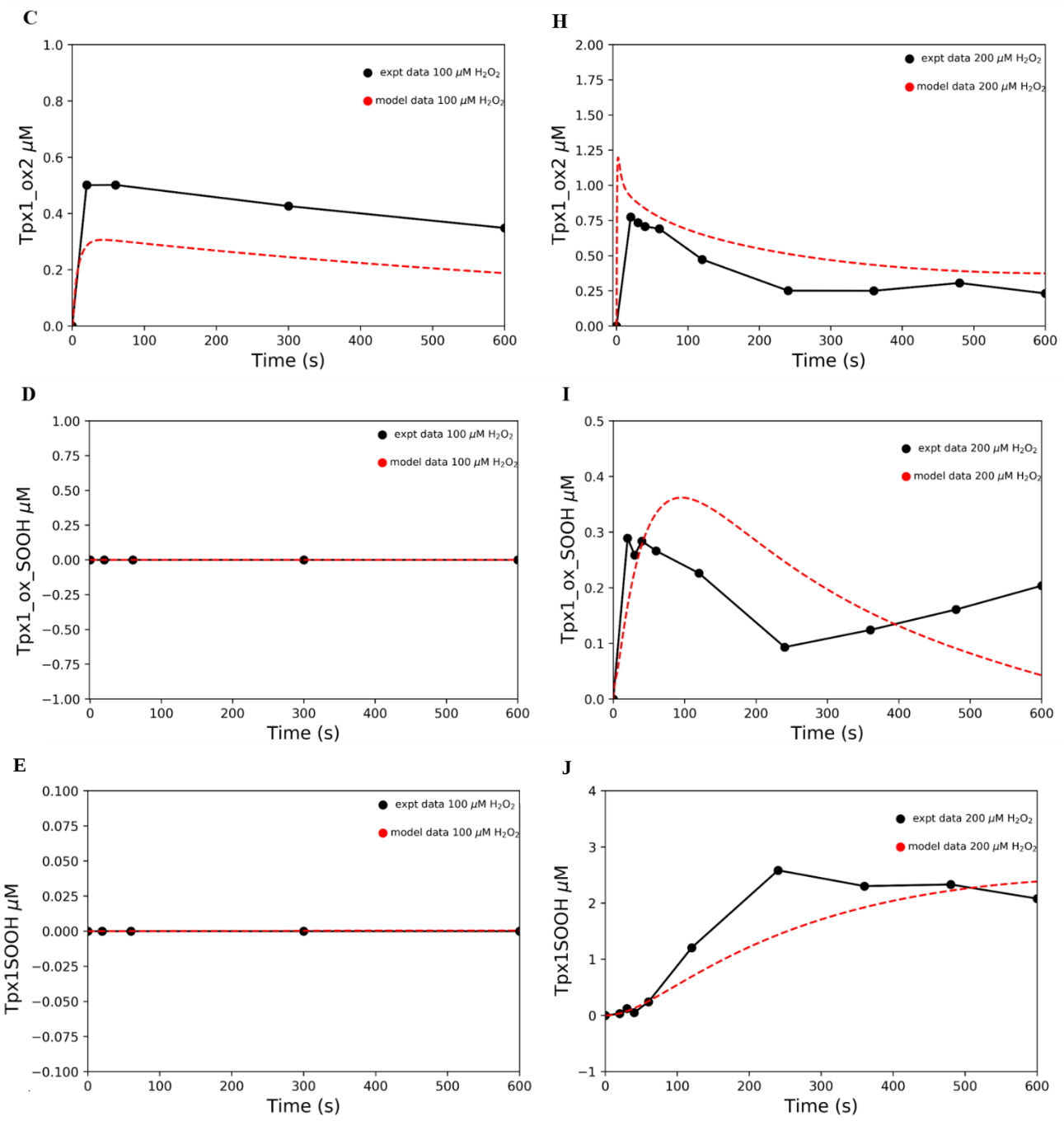


**Figure 4.3: Published Tpx1 computational model converted to PySCeS format fits experimental *in vivo* Tpx1 oxidation data.** *S. pombe* 972 cells were cultured to OD~0.5 and challenged with 100 µM hydrogen peroxide (A-E) or 200 µM hydrogen peroxide (F-J) for 10 minutes. Protein samples were extracted and alkylated with AMS or NEM to separate oxidized Tpx1 forms as revealed by western blot analysis with α-Tpx1 antibodies. Published western blotting data (black ● ) were obtained from Tomalin *et al* (2016) and plotted against computational simulations of Tpx1 oxidation (red --).

Pap1 oxidation was incorporated into this model with the kinetic parameters obtained from BRENDA (Table 4.1). Unfortunately, the oxidation state of Pap1 was unchanged in the presence of 100 µM hydrogen peroxide and therefore the model was not able to simulate Pap1 oxidation data (Figure 4.4A). Additionally, the thioredoxin oxidation state was also tested and showed no change when simulated with 100 µM hydrogen peroxide. Furthermore, even when the model was changed by increasing the hydrogen peroxide concentrations, no oxidation was observed for Pap1 or Trx1. These computational results did not correspond with published data (Bozonet *et al*, 2005; Day *et al*, 2012) or data obtained in Chapter 3 for Pap1 oxidation and therefore, the model was critically examined to highlight potential errors that contributed to the lack of Pap1 and Trx1 oxidation.

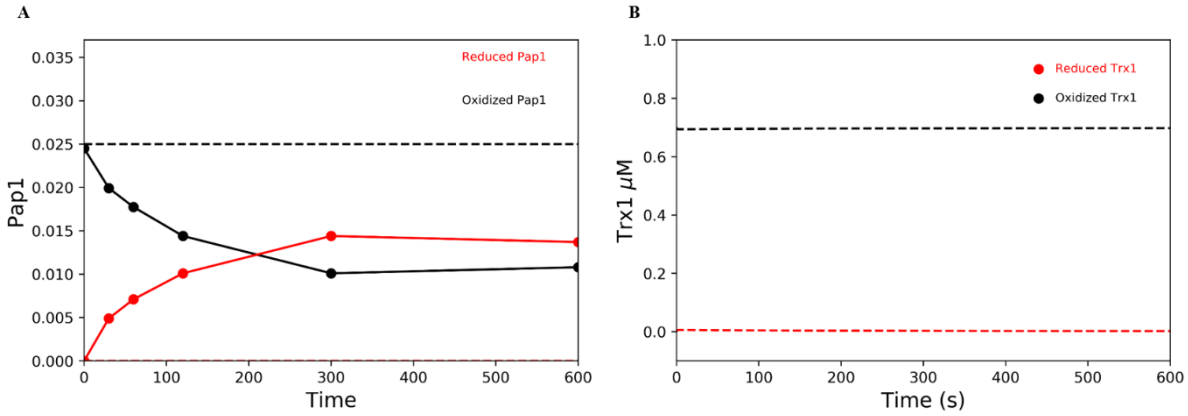


**Figure 4.4: Pap1 and Trx1 redox states in a computational model of hydrogen peroxide metabolism in fission yeast.** Experimental Pap1 oxidation data (solid, Chapter 3) was compared to model simulations (dashed) (A) for cells treated with 100 µM hydrogen peroxide for 10 minutes. The oxidation state of the thioredoxin redox couple in the model was also determined (B).

### 4.3.2 Developing a revised Tpx1 model for *S. pombe*

Upon examining the computational model of Tomalin *et al* (2016), a number of issues were found that could potentially influence the oxidation states of Tpx1, Trx1 and Pap1. First, in this model, Tpx1 was modelled as a monomer which becomes oxidized and then forms a disulphide bridge with another Tpx1 monomer (Tomalin *et al*, 2016). While there is some experimental evidence for Tpx1 being in a monomeric form, most studies agree that 2-Cys peroxiredoxins are dimeric (Figure 4.1) (Pace *et al*, 2013). Second, reduced Tpx1 was modelled to react with two hydrogen peroxide molecules oxidizing both cysteine residues simultaneously. We hypothesized that this reaction would occur in two separate reactions as only one cysteine residue would react at a time and therefore an additional reaction with hydrogen peroxide was added (Figure 4.5 R2, 3). Third, the hyperoxidized form of Tpx1 can be reduced by sulphiredoxin to be recycled back into the system reactivating Tpx1 for hydrogen peroxide degradation (Day *et al*, 2012). This reaction was not included in the published Tpx1 oxidation model as the simulations were only carried out for 10 minutes and Srx1 would not have been synthesized yet to reduce hyperoxidized Tpx1 (Vivancos *et al*, 2005). However, we intended to carry out simulations to match experimental data and therefore included this reaction into the revised Tpx1 oxidation model (Figure 4.5 R9, 14, 16, 21). Fourth, when the sulphenic acid reacts with another hydrogen peroxide to become hyperoxidized, it was shown that the molecule then dissociated into a monomeric form (Figure 4.2, disulph_red3). In the revised model, an additional six routes to hyperoxidation were included with another five species of hyperoxidized Tpx1 (Figure 4.5 R8, 13, 15, 17, 20). Fifth, in the original model the only parameters that were obtained from experimental data were the initial Tpx1 reaction with hydrogen peroxide, the hyperoxidation reaction and the reduction of oxidized Tpx1 by thioredoxin. All other parameters values were obtained through parameter estimation by Tomalin *et al* (2016) and therefore the validity of these parameters had not been tested. Additional parameters and changed kinetics are indicated by an asterisk (Table 4.1 and 4.2).

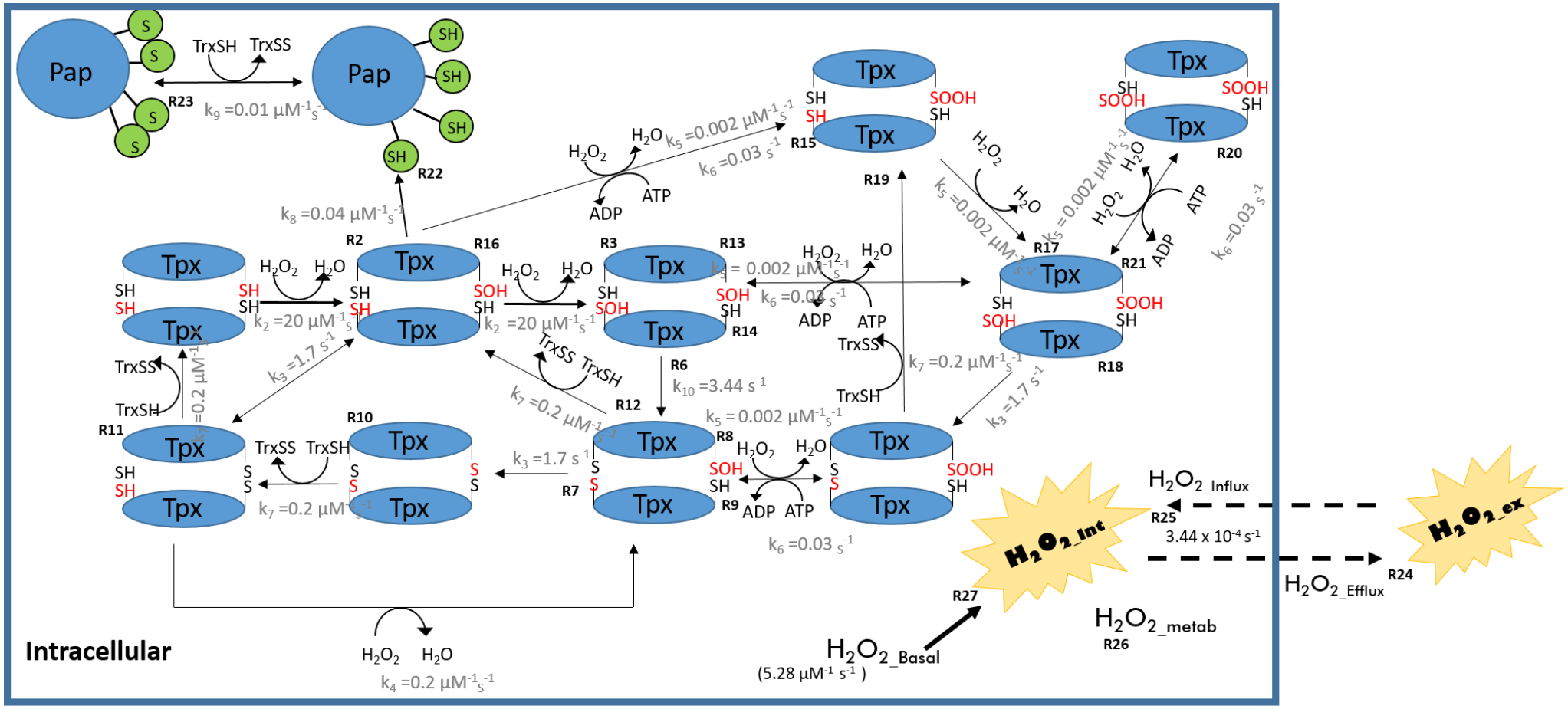


**Figure 4. 5: Revised schematic diagram for the degradation of hydrogen peroxide by Tpx1 in *S. pombe*.** Reduced Tpx1 oxidation with hydrogen peroxide was represented in reactions 2, 3 and 5. Disulphide bond formation was represented by reactions 4, 6, 7 and 18. The reduction of disulphide bridges are captured in reactions 10, 11, 12, and 19. Further hyperoxidation reactions are 8, 13, 15, 17 and 20 and the subsequent reduction reactions are 9, 14, 16 and 21. The oxidation of Pap1 by oxidized Tpx1 was captured in reaction 22 and Pap1 reduction in reaction 23. Lastly, hydrogen peroxide transport across the cell membrane and metabolism was represented in reactions 24-27.

**Table 4. 1: Reactions used to develop Tpx1 oxidation pathway in Figure 4.5. Asterisks indicate reactions in common with Tomalin *et al* (2016).**

| Reaction | Parameter | Value | Unit |
|---|---|---|---|
| **Thioredoxin Reduction** | | | |
| R1: NADPH + TrxSS = NADP + TrxSH | $K_{cat1}$ | 66 | $s^{-1}$ |
| **Peroxiredoxin oxidation** | | | |
| R2: H2O2_int + TpxSH_TpxSH = TpxSOH_TpxSH + H2O | $k_2$ | 20 | $\mu M^{-1}.s^{-1}$ |
| R3: H2O2_int + TpxSOH_TpxSH = TpxSOH_TpxSOH + H2O | $k_2$ | 20 | $\mu M^{-1}.s^{-1}$ |
| R5: TpxSS_TpxSH + H2O2_int = TpxSS_TpxSOH + H2O | $k_5$ | 0.2 | $\mu M^{-1}.s^{-1}$ |
| **Disulphide bond formation** | | | |
| R4: TpxSOH_TpxSH = TpxSS_TpxSH | $k_3$ | 1.7 | $s^{-1}$ |
| R6: TpxSOH_TpxSOH = TpxSS_TpxSOH | $k_3$ | 1.7 | $s^{-1}$ |
| *R7: TpxSS_TpxSOH = TpxSS_TpxSS | $k_{10}$ | 3.44 | $s^{-1}$ |
| R18:TpxSOH_TpxSOOH = TpxSS_TpxSOOH | $k_3$ | 1.7 | $s^{-1}$ |
| **Disulphide bridge reduction by thioredoxin** | | | |
| *R10: TpxSS_TpxSS + TrxSH = TpxSS_TpxSH + TrxSS | $k_7$ | 0.2 | $\mu M^{-1}.s^{-1}$ |
| R11: TpxSS_TpxSH + TrxSH = TpxSH_TpxSH + TrxSS | $k_7$ | 0.2 | $\mu M^{-1}.s^{-1}$ |
| R12: TpxSS_TpxSOH + TrxSH = TpxSOH_TpxSH + TrxSS | $k_7$ | 0.2 | $\mu M^{-1}.s^{-1}$ |
| R19:TpxSS_TpxSOOH + TrxSH = TpxSH_TpxSOOH + TrxSS | $k_7$ | 0.2 | $\mu M^{-1}.s^{-1}$ |

| | | | |
|---|---|---|---|
| **Peroxiredoxin hyperoxidation** | | | |
| *R8: TpxSS_TpxSOH + H2O2_int = TpxSS_TpxSOOH | $k_5$ | 0.002 | $\mu M^{-1}.s^{-1}$ |
| R13:TpxSOH_TpxSOH + H2O2_int = TpxSOH_TpxSOOH + H2O | $k_5$ | 0.002 | $\mu M^{-1}.s^{-1}$ |
| R15:TpxSOH_TpxSH + H2O2_int = TpxSH_TpxSOOH + H2O | $k_5$ | 0.002 | $\mu M^{-1}.s^{-1}$ |
| R17:TpxSH_TpxSOOH + H2O2_int = TpxSOH_TpxSOOH + H2O | $k_5$ | 0.002 | $\mu M^{-1}.s^{-1}$ |
| R20:TpxSOH_TpxSOOH + H2O2_int = TpxSOOH_TpxSOOH | $k_5$ | 0.002 | $\mu M^{-1}.s^{-1}$ |
| **Hyperoxidized Peroxiredoxin reduction by sulphiredoxin** | | | |
| R9: TpxSS_TpxSOOH + ATP = TpxSS_TpxSOH + ADP | $k_6$ | 0.03 | $\mu M^{-1}.s^{-1}$ |
| R14:TpxSOH_TpxSOOH + ATP = TpxSOH_TpxSOH + ADP | $k_6$ | 0.03 | $\mu M^{-1}.s^{-1}$ |
| R16:TpxSH_TpxSOOH + ATP = TpxSOH_TpxSH + ADP | $k_6$ | 0.03 | $\mu M^{-1}.s^{-1}$ |
| R21:TpxSOOH_TpxSOOH + ATP = TpxSOH_TpxSOOH + ADP | $k_6$ | 0.03 | $\mu M^{-1}.s^{-1}$ |
| **Pap1 oxidation and reduction** | | | |
| R22: Pap1_RED + TpxSOH_TpxSH = Pap1_OX + TpxSH_TpxSH | $k_8$ | 0.04 | $\mu M^{-1}.s^{-1}$ |
| R23: Pap1_OX + TrxSH = Pap1_RED + TrxSS | $k_9$ | 0.01 | $\mu M^{-1}.s^{-1}$ |
| **Hydrogen peroxide transport across cell membrane** | | | |
| *R24: H2O2_efflux -H2O2_int>H2O2_ex | k_H2O2_perm | 0.000344 | $s^{-1}$ |
| *R25: H2O2_influx -H2O2_ex>H2O2_int | k_H2O2_perm | 0.000344 | $s^{-1}$ |
| *R26: H2O2_metab -H2O2_int>$pool | $V_{max}$_H2O2_metab | 59.11 | $\mu M^{-1}.s^{-1}$ |
| *R27: H2O2_basal -$pool>H2O2_int | V-Basal | 5.2787 | $\mu M^{-1}.s^{-1}$ |

1019

**Table 4.2: List of protein species and relevant initial concentrations *in vivo* used for modelling experiments.**

| Species | Concentration (μm) | References |
|---|---|---|
| TpxSH_TpxSH | 4 | (Marguerat *et al*, 2012) |
| TpxSOH_TpxSH | 0 | N/A |
| TpxSS_TpxSH | 0 | N/A |
| TpxSS_TpxSOH | 0 | N/A |
| TpxSS_TpxSS | 0 | N/A |
| TpxSS_TpxSOOH | 0 | N/A |
| TpxSOH_TpxSOH | 0 | N/A |
| TpxSH_TpxSOOH | 0 | N/A |
| TpxSOH_TpxSOOH | 0 | N/A |
| TpxSOOH_TpxSOOH | 0 | N/A |
| TrxSH | 0.7 | (Marguerat *et al*, 2012) |
| TrxSS | 0.01 | N/A |
| Pap1_RED | 0.0245 | (Marguerat *et al*, 2012) |
| Pap1_OX | 0 | N/A |
| NADPH | 150 | (Lee *et al*, 1995) |
| NADP | 1 | N/A |
| H2O | 1 | N/A |
| ATP | 7 | (Lee *et al*, 1995) |
| ADP | 0 | N/A |
| H2O2 | 100 | |

The revised Tpx1/Pap1 model described above was simulated and the oxidation states of Trx1 and Pap1 were re-evaluated (Script 2, supplementary data). The oxidation states of Tpx1 at 100 and 200 µM hydrogen peroxide were plotted, but, this model still did not accurately simulate all the experimental data (Figure 4.6 A-J). Therefore, the reactions or kinetic parameters used need to be estimated by data fitting.

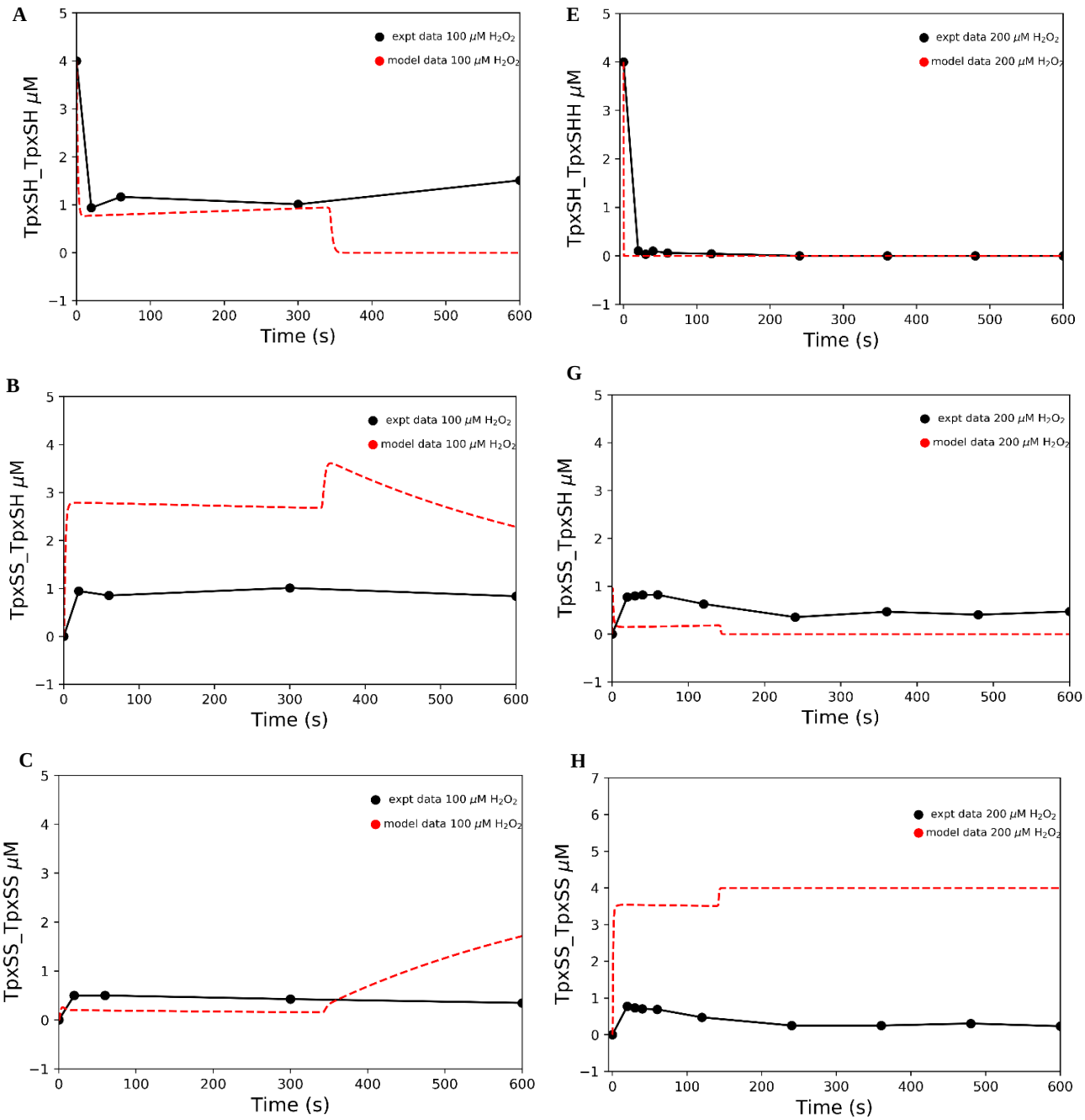

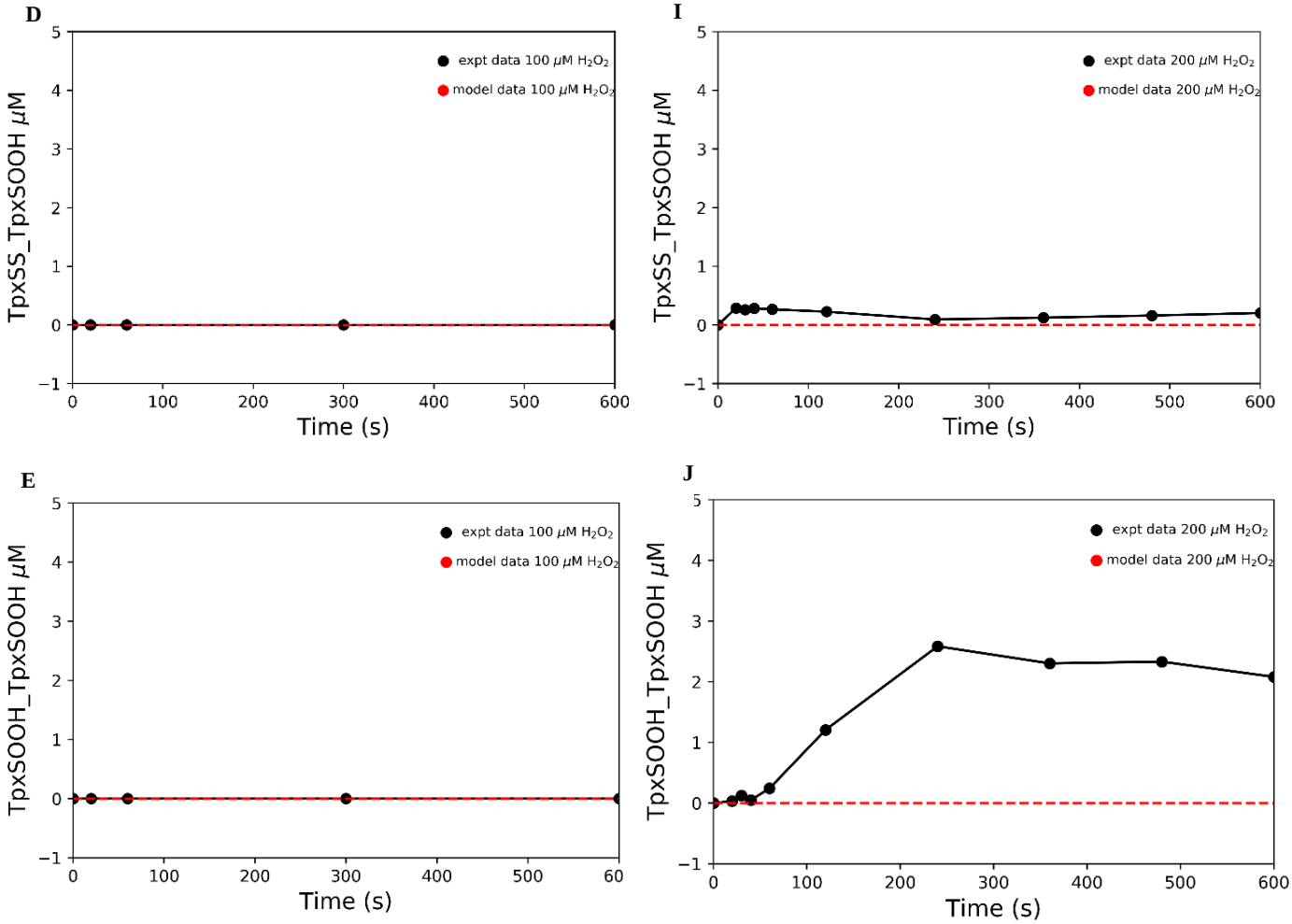


**Figure 4.6: A Revised Tpx1/Pap1 model could not accurately simulate *in vivo* oxidation of Tpx1 at 100 or 200 µM hydrogen peroxide aside from the hyperoxidized Tpx1 isoforms.** Experimental oxidation data (solid) for Tpx1 were obtained from Tomalin *et al* (2016) and compared to computer simulations (dashed).

Interestingly, at 100 µM hydrogen peroxide the model was able to accurately simulate Pap1 experimental data and Trx1 showed oxidation, but this will still need to be compared to experimental data (Figure 4.7). However, when the computational model was changed to a higher concentration of hydrogen peroxide of 200 µM, the Pap1 oxidation results did not match experimental data. The errors for simulating the experimental data for Pap1 could be due to the model and/or kinetic parameters chosen. In order to build a more accurate model Tpx1, Trr1, Trx1 from *S. pombe* would need to be cloned expressed and purified to obtain the kinetic parameters for the relevant reactions.

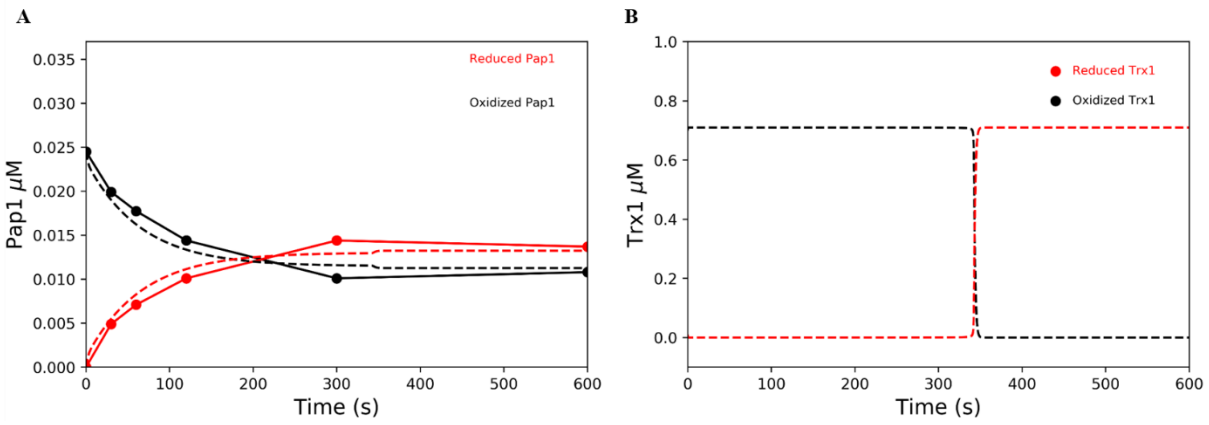


**Figure 4.7: Revised model was able to simulate experimental data for Pap1 oxidation at 100 µM hydrogen peroxide (A) and Trx1 oxidation was also present (B).** Western blot data was obtained as previously described in Figure 3.6.

## 4.4 Discussion

To understand which components of the Tpx1/Pap1 pathway controlled the Pap1 signal time, duration and amplitude, computational modelling of the system was attempted to resolve this question. A published model for Tpx1 oxidation was modified to include Pap1 oxidation and reduction, but, the model was not able to simulate experimental data for Pap1 oxidation obtained at 100 µM hydrogen peroxide in Chapter 3. Therefore, a number of revisions were made to the Tpx1 oxidation model in an attempt to simulate Pap1 oxidation *in silico* (Figure 4.5). However, this model was not able to accurately predict the Tpx1 oxidation data (Figure 4.6 A-J). Interestingly, the model was able to simulate the oxidation of Pap1 at 100 µM hydrogen peroxide, but not at higher hydrogen peroxide concentrations (Figure 4.7). Therefore, while the revised model showed promising results, further revisions are required to accurately simulate Tpx1 oxidation.

A number of recommendations can be made to improve this model, but due to time-constraints of this project, these revisions will have to be carried out in future work. Notably, the kinetic parameters used were mainly obtained from the model of Tomalin *et al* (2016) which did not include the Pap1 reaction. The main parameters that must be explored are the reaction rates for Tpx1 disulphide bridge forms with hydrogen peroxide and the rate at which hyperoxidation reactions occur. Nuclear thioredoxin-like protein (Txl1) is believed to effect reduction of Pap1 *in vivo*, however, these kinetic parameters are not available (Castillo *et al*, 2002; Day *et al*, 2012).

In conclusion, the computational model proposed by Tomalin *et al* (2016) has components that are able to accurately simulate Tpx1 oxidation, but not Pap1 or Trx1. In contrast, a revised model was able to simulate Pap1 oxidation and Trx1 oxidation (still to be validated) but Tpx1 oxidation was not accurate. Therefore, re-evaluation of the kinetic parameters must be done by *in vitro* analysis and data fitting experiments.

# Chapter 5: General Discussion

Increased levels of reactive oxygen species (ROS) have been strongly associated with a plethora of diseases including cancer, neurological disorders and atherosclerosis (Sultana *et al*, 2006; Reuter *et al*, 2010; Chroni *et al*, 2011; Liu *et al*, 2017; Chikara *et al*, 2018). On the other hand, ROS are also involved in normal signalling processes like insulin signalling and immune response activation (Tiganis, 2011; Piwkowska *et al*, 2013). Therefore, resolving the paradoxical role of ROS in health and disease remains a central question in the redox biology field. A contributing factor to this paradox is lack of quantitative tools to assess redox signals. Based on previous studies (Hornberg *et al*, 2005) it was proposed that measuring the signalling time, duration and amplitude of a redox signalling process may yield insights that could resolve this paradox.

In Chapter 3, the utility of this method was explored and it was found that the effects of increasing hydrogen peroxide concentrations on the Tpx1/Pap1 pathway in *S. pombe* could be quantified. Additionally, the effect of Pk-tagged proteins and changes in the culture media also affected signalling parameters. How other oxidants, like tBOOH, impacted Pap1signalling was also assessed. Furthermore, different transcription factors could be comparatively evaluated using this method and lastly, the effect of gene knockin technologies on the Tpx1/Pap1 signalling pathway could be determined. These results led to the question of which components of the Pap1 signalling pathway influenced signalling time, duration or amplitude. Computational modelling provided an efficient way to test this using a published model of Tpx1 oxidation by hydrogen peroxide that was available and had been experimentally verified (Tomalin *et al*, 2016). The Pap1 reaction was added to the model, but no change in reduced or oxidized Pap1 was observed. Therefore, a number of modifications to this model were made in an attempt to predict Pap1 oxidation *in silico*. However, the modified model could not predict Tpx1 oxidation, but did show promising results for describing Pap1 oxidation dynamics at 100 μM hydrogen peroxide.

In future work, it would be interesting to relate how gene expression data correlates to signalling parameters under different experimental conditions. For example, in a gene expression study by Chen *et al* (2008), *S. pombe* cells were exposed to low (0.07 μM) and medium (500 μM) hydrogen peroxide concentrations, and gene expression was observed 15 and 60 minutes after exposure. It was found that the Pap1 pathway was responsible for the activation of 127 core stress response genes whose mRNA transcripts were strongly induced after 15 minutes of

hydrogen peroxide exposure (Chen *et al*, 2008). In comparison, at medium hydrogen peroxide concentrations the Pap1 pathway did not solely activate the stress response as the Atf1 and Sty1 pathways began to regulate transcription at these hydrogen peroxide concentrations (Chen *et al*, 2008). In this study, hydrogen peroxide concentrations of 500 and 1000 μM showed a unique signalling profile with two oxidation peaks. Could the presence of two oxidation peaks be linked to changes in gene expression regulation where Pap1 is deactivated and where the Aft1 and Sty1 pathways are activated to transcribe Srx1 for Pap1 to be reactivated? If gene expression data could be obtained for the hydrogen peroxide concentrations used in this thesis, we would be able to determine if there is indeed a correlation between the signalling parameters outlined and stress response gene regulation. This then leads to the question of whether hydrogen peroxide signalling could be distinguished from oxidative stress response using time-dependent quantification. Additionally, if gene expression could be correlated to the quantified signalling parameters, it would be interesting to consider how much cellular information is captured by this quantification method. Lastly, the precise role of Tpx1 hyperoxidation is an unanswered question in the redox biology field although it is known that the Pap1 pathway is deactivated upon Tpx1 hyperoxidation (Veal *et al*, 2018). Here, quantification may provide insights into the role of hyperoxidation in redox signalling. One of the most pressing questions facing this field is that there are no effective redox-based therapies (Steinhubl, 2008). Comparing the signalling parameters for diseased or chemically stressed cells could provide insight into potential drug targets using computational modelling.

To conclude, a major limitation in redox biology has been the lack of the ability to quantify the stress response signal in cell types. In this study, time-dependent quantification of redox signalling was proposed and the utility of this method to graphically visualize and compare signalling regimes was established. This method now provides us with another tool to explore the paradox nature of ROS in health and disease.

# References


Aslund, F., Zheng, M., Beckwith, J., and Storz, G. (1999). Regulation of the OxyR transcription factor by hydrogen peroxide and the cellular thiol--disulfide status. Proc. Natl. Acad. Sci. *96*, 6161–6165.

Birben, E., Sahiner, U.M., Sackesen, C., Erzurum, S., and Kalayci, O. (2012). Oxidative Stress and Antioxidant Defense- review article. World Allergy Organ. J. *5*, 9–19.

Boronat, S., Domènech, A., Paulo, E., Calvo, I.A., García-santamarina, S., García, P., Encinar, J., Barcons, A., Serrano, E., and Carmona, M. (2014). Redox Biology Thiol-based H 2 O 2 signalling in microbial systems. Redox Biol. *2*, 395–399.

Bozonet, S.M., Findlay, V.J., Day, A.M., Cameron, J., Veal, E.A., and Morgan, B.A. (2005). Oxidation of a Eukaryotic 2-Cys Peroxiredoxin Is a Molecular Switch Controlling the Transcriptional Response to Increasing Levels of Hydrogen Peroxide *. *280*, 23319–23327.

Brown, J.D., Day, A.M., Taylor, S.R., Tomalin, L.E., Morgan, B.A., and Veal, E.A. (2013). Article A Peroxiredoxin Promotes H 2 O 2 Signaling and Oxidative Stress Resistance by Oxidizing a Thioredoxin Family Protein. Cell Rep. *5*, 1425–1435.

Buettner, G. R., Wagner, B. A., & Rodgers, V.G.J. (2013). Quantitative Redox Biology: An approach to understanding the role of reactive species in defining the cellular redox environment. Cell Biochem. Biophys. *67*, 1–13.

Calvo, I., Boronat, S., Domènech, A., García-Santamarina, S., Ayté, J., and Hidalgo, E. (2013a). Dissection of a redox relay: H2O2-dependent activation of the transcription factor pap1 through the peroxidatic Tpx1-Thioredoxin Cycle. Cell Rep. *5*, 1413–1424.

Calvo, I.A., Garcı, P., Hidalgo, E., and Jose, A. (2012). The transcription factors Pap1 and Prr1 collaborate to activate antioxidant , but not drug tolerance , genes in response to H 2 O 2. Nucleic Acids Res. *40*, 4816–4824.

Calvo, I.A., Ayte, J., and Hidalgo, E. (2013b). Reversible thiol oxidation in the H2O2-dependent activation of the transcription factor Pap1. J. Cell Sci. *126*, 2279–2284.

Cao, Z., Tavender, T.J., Roszak, A.W., Cogdell, R.J., and Bulleid, N.J. (2011). Crystal Structure of Reduced and of Oxidized Peroxiredoxin IV Enzyme Reveals a Stable Oxidized Decamer and a Non-disulfide-bonded Intermediate in the Catalytic Cycle *. J. Biol. Chem. *286*, 42257–42266.

Castillo, E.A., Ayté, J., Chiva, C., Moldón, A., Carrascal, M., Abián, J., Jones, N., and Hidalgo, E. (2002). Diethylmaleate activates the transcription factor Pap1 by covalent modification of critical cysteine residues. Mol. Microbiol. *45*, 243–254.

Chen, D., Wilkinson, C.R.M., Watt, S., Penkett, C.J., Toone, W.M., and Jones, N. (2008). Multiple Pathways Differentially Regulate Global Oxidative Stress Responses in Fission Yeast. Mol. Biol. Cell *19*, 308–317.

Chen, X., Song, M., Zhang, B., and Zhang, Y. (2016). Reactive Oxygen Species Regulate T Cell Immune Response in the Tumor Microenvironment. Oxid. Med. Cell. Longev. *1*, 11–16.

Chikara, S., Dalasanur, L., Singhal, J., Horne, D., Awasthi, S., and Singhal, S.S. (2018). Oxidative stress and dietary phytochemicals : Role in cancer chemoprevention and treatment. Cancer Lett. *413*, 122–134.

Choi, H., Kim, S., Mukhopadhyay, P., Cho, S., Woo, J., Storz, G., and Ryu, S. (2001). Structural Basis of the Redox Switch in the OxyR Transcription Factor. *105*, 103–113.

Chroni, A., Leondaritis, G., and Karlsson, H. (2011). Lipids and Lipoproteins in Atherosclerosis. J. Lipids *1*, 2–4.

Circu, M. L; Aw, T.Y. (2010). REACTIVE OXYGEN SPECIES, CELLULAR REDOX SYSTEMS AND APOPTOSIS. Free Radic. Biol. Med. *48*, 749–762.

Cokus, S., Rose, S., Haynor, D., Grønbech-jensen, N., and Pellegrini, M. (2006). Modelling the network of cell cycle transcription factors in the yeast Saccharomyces cerevisiae. BMC Bioinformatics *12*, 1–12.

Day, A.M., Brown, J.D., Taylor, S.R., Rand, J.D., Morgan, B.A., and Veal, E.A. (2012). Inactivation of a Peroxiredoxin by Hydrogen Peroxide Is Critical for Thioredoxin-Mediated Repair of Oxidized Proteins and Cell Survival. Mol. Cell *45*, 398–408.

Dayer, R., Fischer, B.B., Eggen, R.I.L., and Lemaire, S.D. (2008). The peroxiredoxin and glutathione peroxidase families in Chlamydomonas reinhardtii. Genetics *179*, 41–57.

Delaunay, Á., and Isnard, Anne-dominique; Toledano, M.B. (2000). H2O2 sensing through oxidation of the Yap1 transcription factor AgneÁ. EMBO *19*, 5157–5166.

Dietz, K. (2016). Thiol-Based Peroxidases and Ascorbate Peroxidases: Why Plants Rely on Multiple Peroxidase Systems in the Photosynthesizing Chloroplast? Mol. Cells *39*, 20–25.

Domènech, A., Ayté, J., Antunes, F., and Hidalgo, E. (2018). Using in vivo oxidation status of one- and two-component redox relays to determine H2O2levels linked to signaling and toxicity. BMC Biol. *16*, 1–15.

Du, Y., Zhang, H., Lu, J., and Holmgren, A. (2012). Glutathione and glutaredoxin act as a backup of human thioredoxin reductase 1 to reduce thioredoxin 1 preventing cell death by aurothioglucose. J. Biol. Chem. *287*, 38210–38219.

Dubbs, J.M., and Mongkolsuk, S. (2016). Peroxide-Sensing Transcriptional Regulators in Bacteria. J. Bacteriol. *194*, 5495–5503.

Fan, Y., Makar, M., Wang, M.X., and Ai, H. (2017). Monitoring thioredoxin redox with a genetically encoded red fluorescent biosensor. Nat. Publ. Gr. *1*, 1–7.

Fernandes, A. P; Holmgren, A. (2004). Glutaredoxins: Glutathione-Dependent Redox Enzymes with Functions Far Beyond a Simple Thioredoxin Backup System. Antioxid. Redox Signal. *6*, 63–74.

Finkel, T. (2011). Signal transduction by reactive oxygen species. J. Cell Biol. *194*, 7–15.

Fomenko, D.E., Koc, A., Agisheva, N., Jacobsen, M., Kaya, A., and Malinouski, M. (2011). Thiol peroxidases mediate specific genome-wide regulation of gene expression in response to hydrogen peroxide. PNAS *108*, 2729–2734.

Fujino, G., Noguchi, T., Matsuzawa, A., Yamauchi, S., Saitoh, M., Takeda, K., and Ichijo, H. (2007). Thioredoxin and TRAF Family Proteins Regulate Reactive Oxygen Species-Dependent Activation of ASK1 through Reciprocal Modulation of the N-Terminal Homophilic Interaction. Mol. Cell. Biol. *27*, 8152–8163.

Gadaleta, M.C., Iwasaki, O., Noguchi, C., Noma, K., and Noguchi, E. (2014). New vectors for epitope tagging and gene disruption in Schizosaccharomyces pombe. Biotechniques *55*, 1–10.

Gough, D.R., and Cotter, T.G. (2011). Hydrogen peroxide: A Jekyll and Hyde signalling molecule. Cell Death Dis. *2*, e213-8.

Grainge, C. (2004). Breath of life: The evolution of oxygen therapy. J. R. Soc. Med. *97*, 489–493.

Gregory, A., Ewer, A.K., and Singh, A. (2018). Is high-concentration oxygen therapy more effective than targeted oxygen therapy in neonatal non-tension pneumothorax ? Arch. Dis. Child.

*0*, 1–2.

Halliwell, B. A; Gutteridge, J.M.C. (2015). Free radicals in biology and medicine (Oxford: Oxford University Press).

Hampton, M.B., and Connor, K.M.O. (2016). Peroxiredoxins and the Regulation of Cell Death. Mol. Cells *39*, 72–76.

Hanschmann, E.-M., Godoy, J.R., Berndt, C., Hudemann, C., and Lillig, C.H. (2013). Thioredoxins, Glutaredoxins, and Peroxiredoxins—Molecular Mechanisms and Health Significance: from Cofactors to Antioxidants to Redox Signaling. Antioxid. Redox Signal. *19*, 1539–1605.

Heinrich, R., Neel, B.G., and Rapoport, T.A. (2002). Mathematical models of protein kinase signal transduction. Mol. Cell *9*, 957–970.

Henkel, R., Singh, I., and Ashok, S. (2018). The excessive use of antioxidant therapy : A possible cause of male infertility ? Andrologia *10*, 1–8.

Heyboer, M., Sharma, D., Santiago, W., and Mcculloch, N. (2017). Hyperbaric Oxygen Therapy : Side Effects Defined and Quantified. Wound Heal. Soc. *00*, 1–15.

Hildebrandt, G and Roots, I. (1975). Reduced Nicotinamide Adenine Dinucleotide Phosphate ( NADPH ) - Dependent Formation and Breakdown of Hydrogen Peroxide during Mixed Function Oxidation Reactions in Liver Microsomes. Arch. Biochem. Biophys. *171*, 385–397.

Hornberg, J.J., Bruggeman, F.J., Binder, B., Geest, C.R., Bij De Vaate, A.J.M., Lankelma, J., Heinrich, R., and Westerhoff, H. V. (2005). Principles behind the multifarious control of signal transduction: ERK phosphorylation and kinase/phosphatase control. FEBS J. *272*, 244–258.

Hyun, A.W., Jeong, W., Chang, T.S., Kwang, J.P., Sung, J.P., Jeong, S.Y., and Sue, G.R. (2005). Reduction of cysteine sulfinic acid by sulfiredoxin is specific to 2-Cys peroxiredoxins. J. Biol. Chem. *280*, 3125–3128.

Imber, M., Hillion, M., Tha, L., Hamilton, C.J., Adrian, L., and Wahl, M.C. (2017). Protein S -Bacillithiolation Functions in Thiol Protection and Redox Regulation of the Glyceraldehyde-3-Phosphate Dehydrogenase Gap in Staphylococcus aureus. Antioxid. Redox Signal. *00*, 1–21.

Kang, H.W., Cho, Yong, G., Yoon, U.H., and Eun, M.Y. (1998). A Rapid DNA Extraction Method for RFLP and PCR Analysis from a Single Dry Seed. Plant Mol. Biol. Report. *16*, 23–

30.

Karplus, P.A., and Poole, L.B. (2012). Peroxiredoxins as Molecular Triage Agents, Sacrificing Themselves to Enhance Cell Survival During a Peroxide Attack. Mol. Cell *45*, 275–278.

Kawagishi, H., and Finkel, T. (2014). ROS and disease: Finding the right balance. Nat. Med. *20*, 711–713.

Kelly, C. (2014). Oxygen therapy: Time to move on? Ther. Adv. Respir. Dis. *8*, 191–199.

Kim, S.O., Merchant, K., Nudelman, R., Beyer, W.F., Keng, T., Deangelo, J., Hausladen, A., Stamler, J.S., Carolina, N., and Carolina, N. (2002). OxyR : A Molecular Code for Redox-Related Signaling. Cell *109*, 383–396.

Klomsiri, C., Karplus, P.A., and Poole, L.B. (2011). Cysteine-Based Redox Switches in Enzymes 1. Antioxid. Redox Signal. *14*, 1065–1077.

Knight, J.A. (1998). Free Radicals: Their History and Current Status in Aging and Disease. Ann. Clin. Lab. Sci. *28*, 331–346.

Kullik, I., Toledano, M.B., Tartaglia, L.A., and Storz, G. (1995). Mutational Analysis of the Redox-Sensitive Transcriptional Regulator OxyR : Regions Important for Oxidation and Transcriptional Activation. J. Bacteriol. *177*, 1275–1284.

Lee, B., Oh, S.W., and Myung, S.K. (2015). Efficacy of vitamin C supplements in prevention of cancer: A meta-analysis of randomized controlled trials. Korean J. Fam. Med. *36*, 278–285.

Lee, J., Dawes, I.W., and Roe, J. (1995). Adaptive response of Schizosaccharomyces pombe to hydrogen peroxide and menadione. Microbiol. (United Kingdom) *141*, 0–5.

Leopold, J.A. (2015). Antioxidants and coronary artery disease: From pathophysiology to preventive therapy. Coron. Artery Dis. *26*, 176–183.

Liu, Z., Zhou, T., Ziegler, A.C., Dimitrion, P., and Zuo, L. (2017). Review Article Oxidative Stress in Neurodegenerative Diseases : From Molecular Mechanisms to Clinical Applications. Oxid. Med. Cell. Longev. *1*, 1–11.

Lukyanov, K.A., and Belousov, V. V (2014). Genetically encoded fluorescent redox sensors. BBA - Gen. Subj. *1840*, 745–756.

Maeta, K., Izawa, S., Okazaki, S., Kuge, S., and Inoue, Y. (2004). Activity of the Yap1 Transcription Factor in Saccharomyces cerevisiae Is Modulated by Methylglyoxal, a Metabolite

Derived from Glycolysis. Mol. Cell Biol. *24*, 8753–8764.

Mailloux, R.J. (2015). Redox Biology Teaching the fundamentals of electron transfer reactions in mitochondria and the production and detection of reactive oxygen species. Redox Biol. *4*, 381–398.

Marguerat, S., Schmidt, A., Codlin, S., Chen, W., and Aebersold, R. (2012). Resource Quantitative Analysis of Fission Yeast Transcriptomes and Proteomes in Proliferating and Quiescent Cells. Cell *151*, 671–683.

Marinho, H.S., Real, C., Cyrne, L., Soares, H., and Antunes, F. (2014). Hydrogen peroxide sensing, signaling and regulation of transcription factors. Redox Biol. *2*, 535–562.

McCord, J. M; Fridovich, I. (1969). An enzymic function for erythrocuprein (hemocuprein). J. Biol. Chem. *244*, 6049–6055.

Meister, A. (1992). COMMENTARY ON THE ANTIOXIDANT EFFECTS OF ASCORBIC ACID AND. Biochem. Pharmacol. *44*, 1905–1915.

Moskovitz, J. (2005). Methionine sulfoxide reductases: Ubiquitous enzymes involved in antioxidant defense, protein regulation, and prevention of aging-associated diseases. Biochim. Biophys. Acta - Proteins Proteomics *1703*, 213–219.

Nash, G. (1967). Pulmonary lesions associated with oxygen therpay and artifical ventilations. N. Engl. J. Med. *276*, 368–373.

Netto, L.E.S., and Antunes, F. (2016). The Roles of Peroxiredoxin and Thioredoxin in Hydrogen Peroxide Sensing and in Signal Transduction. Mol. Cells *39*, 65–71.

Okazaki, S., Tachibana, T., Naganuma, A., Mano, N., and Kuge, S. (2007). Article Multistep Disulfide Bond Formation in Yap1 Is Required for Sensing and Transduction of H 2 O 2 Stress Signal. Mol. Cell *1*, 675–688.

Olivier, B.G., Rohwer, J.M., and Hofmeyr, J.S. (2005). Modelling cellular systems with PySCeS. Bioinformatics *21*, 560–561.

Pace, P.E., Peskin, A. V, Han, M., Hampton, M.B., and Winterbourn, C.C. (2013). Hyperoxidized peroxiredoxin 2 interacts with the protein disulfide- isomerase ERp46. Biochem. Soc. *485*, 475–485.

Peskin, A. V., Dickerhof, N., Poynton, R.A., Paton, L.N., Pace, P.E., Hampton, M.B., and

Winterbourn, C.C. (2013). Hyperoxidation of peroxiredoxins 2 and 3: Rate constants for the reactions of the sulfenic acid of the peroxidatic cysteine. J. Biol. Chem. *288*, 14170–14177.

Pillay, C.S., Eagling, B.D., Driscoll, S.R.E., and Rohwer, J.M. (2016). Quantitative measures for redox signaling. Free Radic. Biol. Med. *96*, 290–303.

Pingitore, A., Lima, G.P.P., Mastorci, F., Quinones, A., Iervasi, G., and Vassalle, C. (2015). Exercise and Oxidative Stress: Potential Effects of Antioxidant Dietary Strategies in Sports. Nutrition *31*, 916–922.

Piwkowska, A., Rogacka, D., Angielski, S., and Jankowski, M. (2013). Biochimica et Biophysica Acta Insulin increases glomerular fi ltration barrier permeability through dimerization of protein kinase G type I α subunits. Biochim. Biophys. Acta *1832*, 791–804.

Poole, L.B., Hall, A., and Nelson, K.J. (2011). Overview of Peroxiredoxins in oxidant defense and redox regulation. Curr. Protoc. Toxicol. *7*, 1–20.

Postovit, L., Widmann, C., Huang, P., and Gibson, S.B. (2018). Editorial Harnessing Oxidative Stress as an Innovative Target for Cancer Therapy. Oxid. Med. Cell. Longev. *2018*, 10–12.

Priestley, J. (1775). Royal Society.

Quinn, J., Findlay, V.J., Dawson, K., Millar, J.B.A., Jones, N., Morgan, B.A., and Toone, W.M. (2002). Distinct Regulatory Proteins Control the Graded Transcriptional Response to Increasing H 2 O 2 Levels in Fission Yeast Schizosaccharomyces pombe. Mol. Biol. Cell *13*, 805–816.

Ray, P. D; Haung, B; Tsuji, Y. (2012). Reactive oxygen species (ROS) homeostasis and redox regulation in cellular signaling. Cell Signal. *24*, 981–990.

Reuter, S; Gupta, S. C; Madan, M. M; Bharat, A.B. (2010). Oxidative stress, inflammation, and cancer: How are they linked? FEBS J. *49*, 1603–1616.

Rhee, S.G. (2016). Overview on Peroxiredoxin. Mol. Cells *39*, 1–5.

Rhee, S.G., Kang, S.W., Chang, T.S., Jeong, W., and Kim, K. (2001). Peroxiredoxin, a novel family of peroxidases. IUBMB Life *52*, 35–41.

Rhee, S.G., Chae, H.Z., and Kim, K. (2005). Peroxiredoxins: A historical overview and speculative preview of novel mechanisms and emerging concepts in cell signaling. Free Radic.

Biol. Med. *38*, 1543–1552.

Robinson, C., Woo, S., Walsh, A., Nowak, A.K., and Lake, R.A. (2012). The antioxidants vitamins A and E and selenium do not reduce the incidence of asbestos-induced disease in a mouse model of mesothelioma. Nutr. Cancer *64*, 315–322.

Rocha, E.R., Owens, G., Smith, C.J., and Carolina, N. (2000). The Redox-Sensitive Transcriptional Activator OxyR Regulates the Peroxide Response Regulon in the Obligate Anaerobe Bacteroides fragilis. J. Bacteriol. *182*, 5059–5069.

Santos, M.C., Breyer, C.A., Schultz, L., Romanello, K.S., Cunha, A.F., Jr, C.A.T., and Oliveira, M.A. de (2017). Saccharomyces cerevisiae Peroxiredoxins in Biological Processes: Antioxidant Defense, Signal Transduction, Circadian Rhythm, and More. In Old Yeasts - New Questions, p.

Sies, H. (2017). Hydrogen peroxide as a central redox signaling molecule in physiological oxidative stress: Oxidative eustress. Redox Biol. *11*, 613–619.

Sies, H., Berndt, C., and Jones, D.P. (2017). Oxidative Stress. Annu. Rev. Biochem. *86*, 15–48.

Sorriento, D., Luca, N. De, Trimarco, B., and Iaccarino, G. (2018). The Antioxidant Therapy : New Insights in the Treatment of Hypertension. Front. Physiol. *9*, 1–11.

Steinhubl, S.R. (2008). Why Have Antioxidants Failed in Clinical Trials? Am. J. Cardiol. *101*, 14–19.

Stöcker, S., Van Laer, K., Mijuskovic, A., and Dick, T.P. (2018). The Conundrum of Hydrogen Peroxide Signaling and the Emerging Role of Peroxiredoxins as Redox Relay Hubs. Antioxid. Redox Signal. *28*, 558–573.

Stone, J. R; Yang, S. (2006). Hydrogen peroxide: A signaling messenger. Antioxid. Redox Signal. *8*, 1907–1939.

Storz, G; Imlay, J.A. (1999). Oxidative Stress. Curr. Opin. Microbiol. *2*, 188–194.

Study, H.P. (2002). MRC / BHF Heart Protection Study of antioxidant vitamin supplementation in 20 536 high-risk individuals : a randomised.

Sultana, R., Perluigi, M., and Butterfield, D.A. (2006). Protein Oxidation and Lipid Peroxidation in Brain of Subjects Neurodegeneration from Redox Proteomics. Antioxid. Redox

Signal. *8*, 2021–2037.

Tiganis, T. (2011). Reactive oxygen species and insulin resistance : the good , the bad and the ugly. Trends Pharmacol. Sci. *32*, 82–89.

Toledano, M.B., and Huang, B. (2016). Microbial 2-Cys Peroxiredoxins: Insights into Their Complex Physiological Roles. Mol. Cells *39*, 31–39.

Tomalin, L.E., Day, A.M., Underwood, Z.E., Smith, Graham, R., Pezze, P.D., Rallis, C., Patel, W., Dickinson, B.C., Bahler, J., Brewer, Thomas, F., et al. (2016). Increasing extracellular H2O2 produces a bi-phasic response in intracellular H2O2, with peroxiredoxin hyperoxidation only triggered once the cellular H2O2-buffering capacity is overwhelmed. Free Radic. Biol. Med. *95*, 333–348.

Toone, W.M., Kuge, S., Samuels, M., Morgan, B.A., Toda, T., and Jones, N. (1998). Regulation of the fission yeast transcription factor Pap1 by oxidative stress: Requirement for the nuclear export factor Crm1 (Exportin) and the stress-activated MAP kinase Sty1/Spc1. Genes Dev. *12*, 1453–1463.

Veal, E. A., Underwood, Z. E., Tomalin, L. E., Morgan, B. A., & Pillay, C.S. (2018). Hyperoxidation of Peroxiredoxins : Gain or Loss of Function ? Antioxid. Redox Signal. *28*, 574–590.

Veal, E.A., Tomalin, L.E., Morgan, B.A., and Day, A.M. (2014). The fission yeast *Schizosaccharomyces pombe* as a model to understand how peroxiredoxins influence cell responses to hydrogen peroxide. Biochem. Soc. Trans. *42*, 909–916.

Vivancos, A.P., Castillo, E.A., Biteau, B., Nicot, C., Ayte, J., Toledano, M.B., and Hidalgo, E. (2005). A cysteine-sulfinic acid in peroxiredoxin regulates H2O2-sensing by the antioxidant Pap1 pathway. Proc. Natl. Acad. Sci. *102*, 8875–8880.

Wei, Q., Minh, P.N.L., Dotsch, A., Hildebrand, F., Panmanee, W., Elfarash, A., Schulz, S., Plaisance, S., Charlier, D., Hassett, D., et al. (2012). Global regulation of gene expression by OxyR in an important human opportunistic pathogen. Nucleic Acids Res. *40*, 4320–4333.

West, J.B. (2014). Carl Wilhelm Scheele , the discoverer of oxygen , and a very productive chemist. Am J Physiol Lung Cell Mol Physiol *307*, 811–816.

Winterbourn, C.C. (2018). Biological Production , Detection and Fate of Hydrogen Peroxide. Antioxid. Redox Signal. *26*, 1–32.

Wood, Z.A., Poole, L.B., and Karplus, P.A. (2003). Peroxiredoxin evolution and the regulation of hydrogen peroxide signaling. Science (80-. ). *300*, 650–653.

Wu, A., and Moye-rowleyl, W.S. (1994). GSH1 , Which Encodes y-Glutamylcysteine Synthetase , Is a Target Gene for yAP-i Transcriptional Regulation. Mol. Cell. Biol. *14*, 5832–5839.

Zheng, M; Aslund, F; Storz, G. (1998). Activation of the OxyR Transcription Factor by Reversible Disulfide Bond Formation. Science (80-. ). *279*, 11–14.

Zheng, M., Wang, X., Doan, B., Lewis, K.A., Schneider, T.D., and Storz, G. (2001). Computation-Directed Identification of OxyR DNA Binding Sites in Escherichia coli. J. Bacteriol. *183*, 4571–4579.

# Appendix

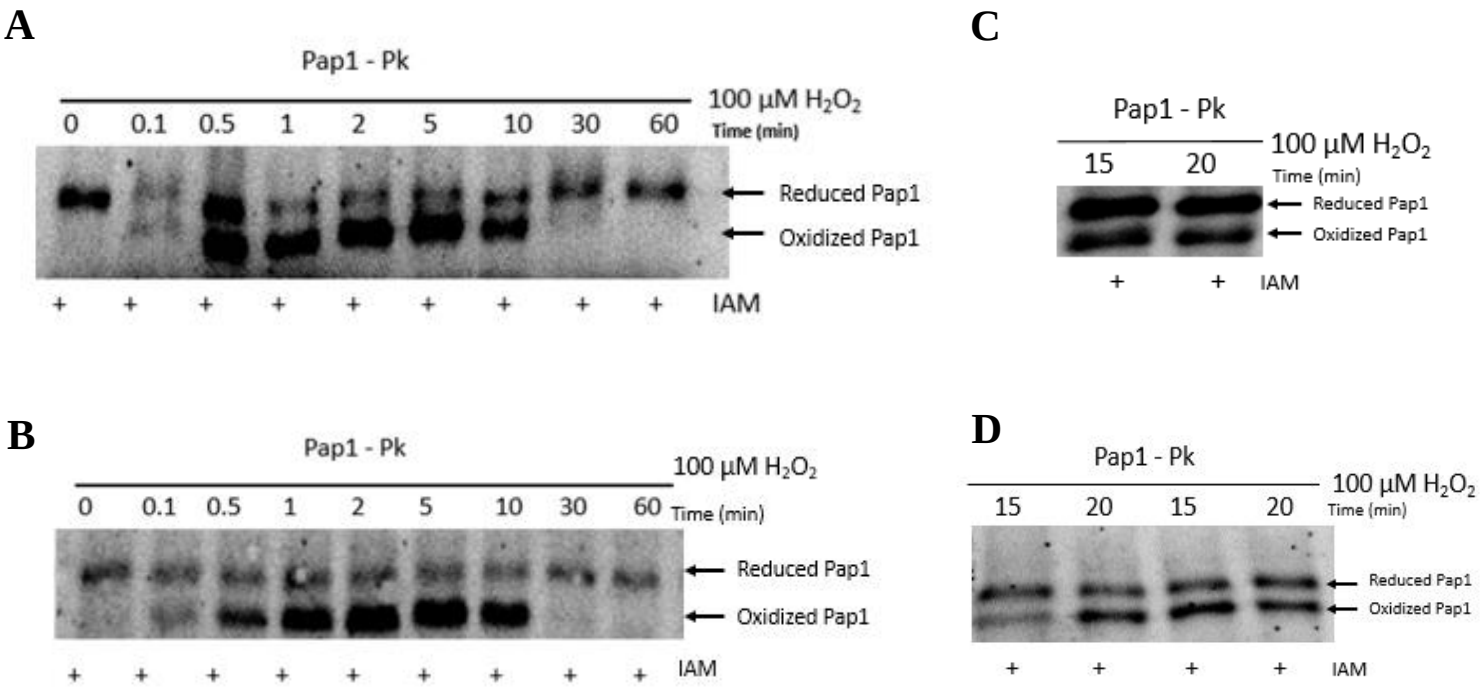


**Figure S1: Additional western blot replicates for 100 µM hydrogen peroxide challenge of SB3 S. pombe cells for 60 minutes A and B and further time points at 15 and 20 minutes.** *S. pombe* SB3 cells were exposed to 100 µM hydrogen peroxide and samples harvested over a 60 minute time-course. Protein was extracted and subjected to western blot analysis. Pap1 oxidation was identified using α-Pk antibodies (A, B). Additional time points at 15 and 20 minutes were also taken (C, D).

**Table S1: Western blots from *S. pombe* cells exposed to 100 µM hydrogen peroxide were analysed using Image J to obtain $Pap1_{ox}/Pap1_{total}$.** The average from the three independent experiments were plotted against time with standard errors indicated. Blank space indicates outlying points that were excluded. Signal parameters were calculated from these values.

| Time | Exp 1 | Exp 2 | Exp 3 | AVERAGE | STD ERROF |
|---|---|---|---|---|---|
| 0 | 0 | 0 | 0 | 0 | 0 |
| 0,1 | 0,49984 | 0,696565 | 0,489021 | 0,561809 | 0,067451 |
| 0,3 | 0,566829 | 0,535018 | 0,597541 | 0,566463 | 0,01805 |
| 1 | 0,597191 | 0,769791 | 0,629502 | 0,665495 | 0,052976 |
| 2 | 0,614055 | 0,702042 | 0,631507 | 0,649201 | 0,026896 |
| 5 | 0,623274 | 0,63646 | 0,617319 | 0,625684 | 0,005655 |
| 10 | 0,564542 | 0,608388 | 0,653776 | 0,608902 | 0,025761 |
| 15 | 0,480289 | | 0,543072 | 0,511681 | 0,031392 |
| 20 | 0,473609 | 0,53064 | 0,41996 | 0,474737 | 0,031956 |

| Time | Exp 1 | Exp 2 | Exp 3 | AVERAGE | STD ERROR |
|---|---|---|---|---|---|
| 30 | 0,260476 | 0,083752 | 0,02658 | 0,123603 | 0,070398 |
| 60 | 0 | 0 | 0 | 0 | 0 |

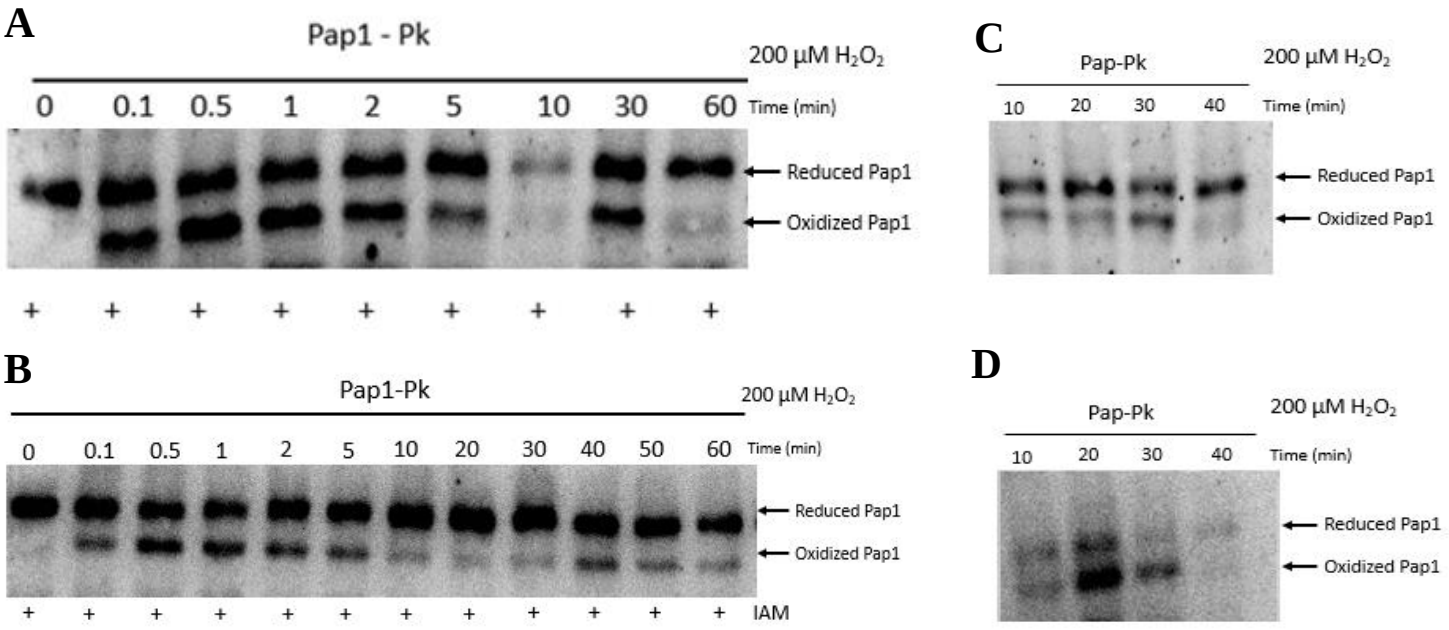


1413

**Figure S2: Western blot replicates for SB3 strain exposed to 200 µM hydrogen peroxide for 60 minutes (A, B) and additional time points at 10 to 40 minutes were also included (C, D).** *S. pombe* cells were exposed to 200 µM hydrogen peroxide for 60 minutes and proteins samples extracted at time-points indicated. Protein was subjected to western blot analysis and Pap1 reduced and oxidized bands detected using α-Pk antibodies (A-D).

**Table S2: Western blots of *S. pombe* SB3 strain exposed to 200 µM hydrogen peroxide was analysed using Image J for the intensity of $Pap1_{ox}/Pap1_{total}$.** The average Pap1 oxidation was plotted against time with standard errors across the replicates. Blank spaces indicate outliers that were not included. Signal quantification of time-dependent signalling was carried out using these values.

| Time | Exp1 | Exp2 | Exp3 | Average | STD ERROR |
|---|---|---|---|---|---|
| 0 | 0 | 0 | 0 | 0 | 0 |
| 0,1 | 0,429463 | 0,500635 | 0,20133 | 0,377143 | 0,0902752 |
| 0,5 | 0,578553 | 0,618337 | 0,470654 | 0,555848 | 0,04411795 |
| 1 | 0,568407 | 0,470898 | 0,574345 | 0,537883 | 0,03353652 |
| 2 | 0,519473 | 0,360018 | 0,617432 | 0,498974 | 0,07501264 |
| 5 | 0,499185 | 0,312484 | 0,468401 | 0,42669 | 0,05779037 |
| 10 | 0,354764 | 0,259236 | 0,296131 | 0,374252 | 0,05174674 |
| 20 | 0,277652 | 0,388467 | 0,481287 | 0,382469 | 0,05886083 |
| 30 | 0,299708 | 0,355048 | | 0,327378 | 0,02767027 |
| 40 | 0,509695 | 0,310926 | 0,215142 | 0,345254 | 0,08674522 |
| 60 | 0,147625 | 0,133243 | | 0,140434 | 0,0071908 |

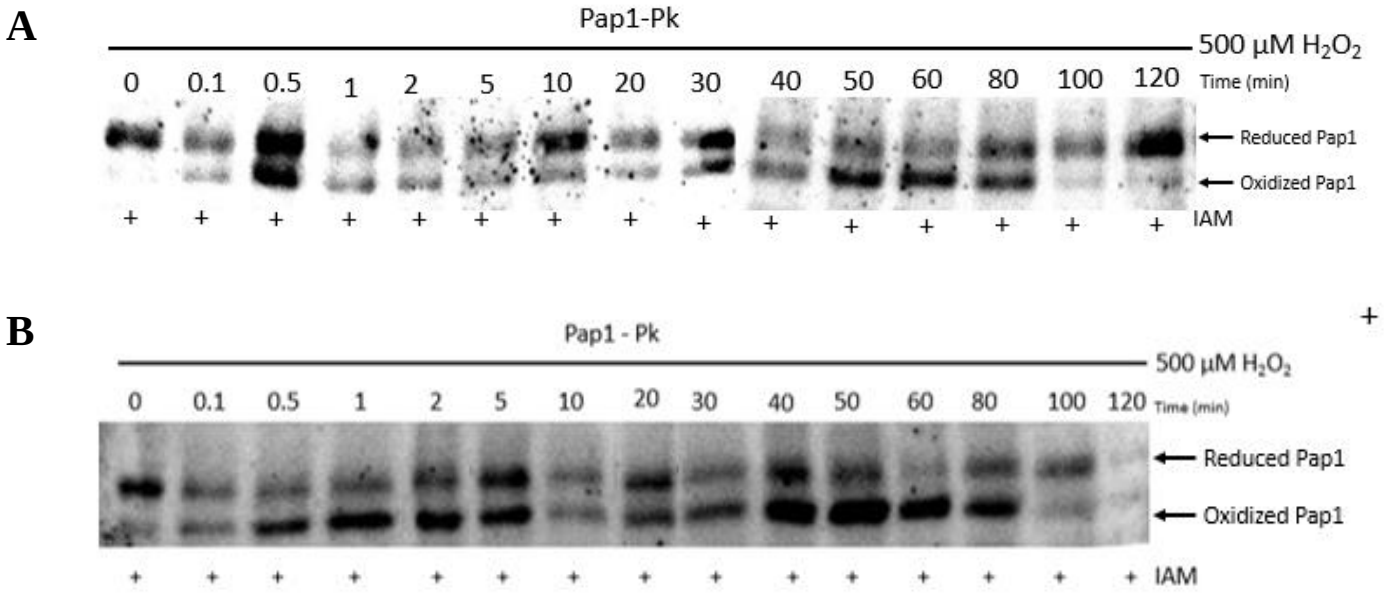


**Figure S3: Western blot replicates for *S. pombe* SB3 strain exposed to 500 µM hydrogen peroxide challenge (A, B).** *S. pombe* cells were exposed to 500 µM hydrogen peroxide and samples were harvested over the 120 minute time-course. Protein was then extracted and subjected to western blot analysis. Pap1 oxidation bands were detected using an α-Pk antibody (A, B).

**Table S4: Image J analysis of Pap1 oxidation from western blotting data after exposure to 500 µM hydrogen peroxide.** Average values against time were used to generate signalling profile for Pap1 oxidation at 500 µM hydrogen peroxide. Signalling parameters were calculated using these values.

| Time | Exp 1 | Exp 2 | Exp 3 | Average | STD Error |
|---|---|---|---|---|---|
| 0 | 0 | 0 | 0 | 0 | 0 |
| 0,1 | 0,41251 | 0,29007 | 0,54437 | 0,41565 | 0,07343 |
| 0,5 | 0,45349 | 0,52399 | 0,68258 | 0,55335 | 0,06774 |
| 1 | 0,50635 | 0,54409 | 0,69454 | 0,58166 | 0,05748 |
| 2 | 0,45509 | 0,47236 | 0,65994 | 0,52913 | 0,06559 |
| 5 | 0,42047 | 0,53563 | 0,59919 | 0,51843 | 0,05230 |
| 10 | 0,37029 | 0,37431 | 0,44639 | 0,39700 | 0,02472 |
| 20 | 0,40963 | 0,34301 | 0,49563 | 0,41609 | 0,04417 |
| 30 | 0,47805 | 0,40867 | | 0,44336 | 0,03469 |
| 40 | 0,52386 | 0,45885 | 0,45077 | 0,47783 | 0,02313 |
| 50 | 0,54965 | 0,59147 | 0,48194 | 0,54102 | 0,03191 |
| 60 | 0,53664 | 0,63578 | 0,61614 | 0,59618 | 0,03031 |
| 80 | 0,34619 | 0,53637 | 0,46150 | 0,44802 | 0,05531 |
| 100 | 0,26235 | 0,29464 | 0,19455 | 0,25051 | 0,02949 |
| 120 | 0 | 0,12009 | 0 | 0,04003 | 0,04003 |

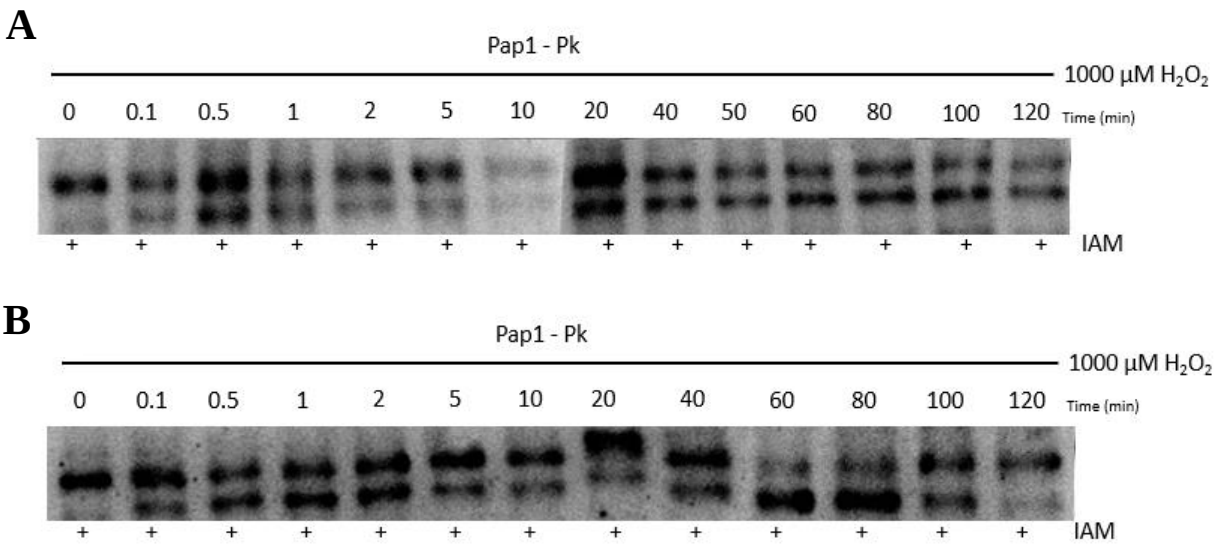

**Figure S4: Western blot analysis of *S. pombe* SB3 cells exposed to 1000 μM hydrogen peroxide for 120 minutes.** *S. pombe* cells were exposed to 1000 μM hydrogen peroxide and samples harvested over the 120 minute time-course. Protein samples were extracted and subjected to western blot analysis. Pap1 oxidized and reduced bands were detected using α-Pk antibodies (A, B).

**Table S5: Western blots of *S. pombe* SB3 strain exposed to 1000 μM hydrogen peroxide were analysed using Image J for the intensity of $Pap1_{ox}/Pap1_{total}$.** Values obtained were used to plot signalling profiles Pap1 oxidation at 1000 μM hydrogen peroxide. Signal quantification was determined using these values.

| Time | Exp 1 | Exp 2 | Exp 3 | Average | STD ERR |
|---|---|---|---|---|---|
| 0 | 0 | 0 | 0 | 0 | 0 |
| 0,1 | 0,46873 | 0,42018 | 0,52986 | 0,47292 | 0,03173 |
| 0,5 | 0,49770 | 0,47230 | 0,49782 | 0,48927 | 0,00849 |
| 1 | 0,48581 | 0,49183 | 0,41343 | 0,46369 | 0,02519 |
| 2 | 0,43033 | 0,34817 | 0,51387 | 0,43079 | 0,04783 |
| 5 | 0,37303 | 0,45740 | 0,37826 | 0,40290 | 0,02730 |
| 10 | 0,37665 | 0,43279 | 0,39264 | 0,40069 | 0,01670 |
| 20 | 0,15045 | 0,43411 | 0,46932 | 0,45171 | 0,01761 |
| 30 | 0,51939 | | | 0,51939 | |
| 40 | 0,46882 | 0,41529 | 0,54241 | 0,47551 | 0,03685 |
| 50 | 0,57367 | 0,39789 | | 0,48578 | 0,08789 |
| 60 | 0,57794 | 0,43907 | 0,79017 | 0,60240 | 0,10209 |
| 80 | 0,51703 | 0,38703 | 0,72640 | 0,54349 | 0,09886 |
| 100 | 0,28281 | 0,45444 | 0,57655 | 0,43793 | 0,08519 |
| 120 | 0 | 0 | 0,25803 | 0,08601 | 0,08601 |

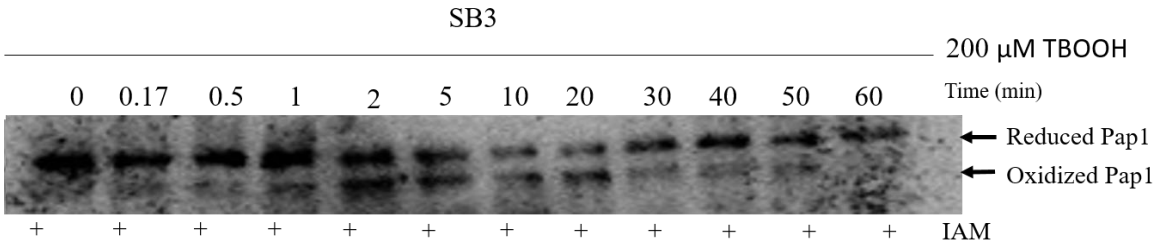


**Figure S5: Replicate blot of** *S. pombe* SB3 cells exposed to 200 µM tBOOH for 60 minutes. *S. pombe* cells were cultured to ~OD-0.5 and exposed to 200 µM tBOOH for 60 minutes. Proteins samples were extracted at various time-points and subjected to western blot analysis. The oxidation of Pap1 was detected using α-Pk antibodies.

**Table S5: Values obtained from ImageJ analysis for Pap1 oxidation after exposure to 200 µm tBOOH.** These values were used to generate the Pap1 oxidation signalling profile and signalling parameters were calculated from these values.

| Time | Exp1 | Exp2 | STERROR |
|---|---|---|---|
| 0 | 0 | 0 | 0 |
| 0,1 | 0 | 0 | 0 |
| 0,3 | 0 | 0 | 0 |
| 1 | 0,38414 | 0,01649 | 0,01649 |
| 2 | 0,53757 | 0,07835 | 0,07835 |
| 5 | 0,54417 | 0,00470 | 0,00470 |
| 10 | 0,62116 | 0,09257 | 0,09257 |
| 20 | 0,50573 | 0,10750 | 0,10750 |
| 30 | 0 | 0 | 0 |
| 40 | 0 | 0 | 0 |
| 50 | 0 | 0 | 0 |
| 60 | 0 | 0 | 0 |

**Table S6: ImageJ analysis of OxyR and Yap1 oxidation after exposure to 200 µM hydrogen peroxide for 30 and 60 minutes respectively.** These values were used to plot signalling profiles and to calculate the signalling parameters.

| Yap1 | | OxyR | |
|---|---|---|---|
| Time | Exp1 | Time | Exp1 |
| 0 | 0 | 0 | 0 |
| 2,5 | 0,953056 | 0,5 | 1 |
| 5 | 0,854655 | 2 | 1 |
| 15 | 0,815516 | 4 | 0,851669 |
| 30 | 0,760693 | 6 | 0,242958 |
| 45 | 0,455449 | 10 | 0,070767 |
| 60 | 0,2024 | 20 | 0,088527 |
| | | 30 | 0,083281 |

**Table S7: *S. pombe* AD29 strain exposed to 100 and 500 µM hydrogen peroxide for 50 minutes.** ImageJ analysis was done and Pap1 oxidation was plotted to generate signal profiles at these hydrogen peroxide concentrations. Signalling parameters were then calculated.

| | 100 um | | 500 um | |
|---|---|---|---|---|
| Time | Exp average | error | exp average | error |
| 0 | 0 | 0 | 0 | 0 |
| 0,1 | 0,6940 | 0 | 0,5163 | 0,0816 |
| 0,25 | 0,7451 | 0,0333 | 0,7307 | 0,0204 |
| 0,5 | 0,6902 | 0,2309 | 0,6620 | 0,0082 |
| 1 | 0,7880 | 0,1453 | 0,7120 | 0,0816 |
| 2 | 0,8571 | 0,0882 | 0,7041 | 0,0735 |
| 5 | 0,9326 | 0 | 0,5419 | 0,1511 |
| 10 | 0,9385 | 0,1333 | 0,4568 | 0,0939 |
| 20 | 0,4931 | 0,0667 | 0,0133 | 0 |
| 30 | 0,4046 | 0 | 0,0137 | 0,0653 |
| 40 | 0,3730 | 0 | 0,0565 | 0,1061 |
| 50 | 0,1988 | 0 | 0,8128 | 0,1225 |

**Script 1: Converted COPASI Tpx1 oxidation to PySCeS format**

**# Tomalin model with Pap1**

**# Keywords**
Description: NoName
Modelname: NoName
Output_In_Conc: True
Species_In_Conc: True

**# GlobalUnitDefinitions**

UnitVolume: litre, 1.0, 0, 1
UnitLength: metre, 1.0, 0, 1
UnitSubstance: mole, 1.0, -6, 1
UnitArea: metre, 1.0, 0, 2
UnitTime: second, 1.0, 0, 1

**# Compartments**

Compartment: vol_int, 5.2e-05, 3
Compartment: vol_ex, 0.05, 3

**# Reactions**

**# Oxidation reactions**

Reaction 1: Prx_SH + H2O2_int > Prx_SOH
   vol_int*k_cys_ox*Prx_SH*H2O2_int

**# Over-oxidation reactions**

Reaction 2: Prx_SOH_SS + H2O2_int > Prx_SS_SOOH
   vol_int*k_hyp_ox*hyp_ox_param*Prx_SOH_SS*H2O2_int

**# Disulphide bridge formation**

Reaction 4: {2.0}Prx_SOH > Prx_SOH_SS
vol_int*k_disulph_form1*pow(Prx_SOH,2.0)

Reaction 5: Prx_SH + Prx_SOH > Prx_SH_SS
vol_int*k_disulph_form1*Prx_SH*Prx_SOH

Reaction 6: Prx_SOH_SS > Prx_SS_SS
vol_int*k_disulph_form2*Prx_SOH_SS

**# Disulphide bridge reduction via Thioredoxin**

Reaction 7: Trx_SH + Prx_SH_SS > Trx_SOH + {2.0}Prx_SH
vol_int*k_disulph_red1*Trx_SH*Prx_SH_SS

Reaction 8: Trx_SH + Prx_SS_SS > Trx_SOH + Prx_SH_SS
vol_int*k_disulph_red2*Trx_SH*Prx_SS_SS

Reaction 9: Trx_SH + Prx_SS_SOOH > Trx_SOH + Prx_SH + Prx_SOOH
vol_int*k_disulph_red3*Trx_SH*Prx_SS_SOOH

**# Trx_reduction**

Reaction 10: Trx_SOH > Trx_SH
vol_int*k_Trx_red*Trx_SOH

**#Reaction of Tpx1 with PAp1**

Reaction 10: Pap1_RED + Prx_SOH_SS > Pap1_OX + Prx_SS_SS
vol_int*k8*Prx_SOH_SS*Pap1_RED

Reaction 11: Pap1_OX + Trx_SH > Pap1_RED + Trx_SOH
vol_int*k9*Pap1_OX*Trx_SH

**# H2O2 reactions**

H2O2_efflux:
H2O2_int > H2O2_ex
k_H2O2_perm*(vol_ex/vol_int)*H2O2_int*vol_int

```
H2O2_influx:
    H2O2_ex > H2O2_int
    k_H2O2_perm*H2O2_ex*vol_ex


H2O2_metab:
    H2O2_int > $pool
    vol_int*Vmax_H2O2_metab*(H2O2_int/(Km_H2O2_metab + H2O2_int))

H2O2_basal:
    $pool > H2O2_int
    vol_int*V_basal
```

**# Fixed species**

**# Variable species**

```
Prx_SH@vol_int = 4.0        # uM
Prx_SOH@vol_int = 0.0       # uM
Prx_SOOH@vol_int = 0.0      # uM

Prx_SH_SS@vol_int = 0.0     # uM
Prx_SOH_SS@vol_int = 0.0    # uM
Prx_SS_SS@vol_int = 0.0     # uM
Prx_SS_SOOH@vol_int = 0.0   # uM
Pap1_RED@vol_int = 0.025
Pap1_OX@vol_int = 0


Trx_SH@vol_int = 0.7        # uM
Trx_SOH@vol_int = 0.0       # uM

H2O2_ex@vol_ex = 500.0      # uM
H2O2_int@vol_int = 0.0      # uM
```

**# Parameters**

```
k_cys_ox = 20.0                 # uM**-1 s**-1
k_hyp_ox = 0.012                # uM**-1 s**-1
hyp_ox_param = 1.0

k_sulfi_red = 0.000400197915422   # uM**-1 s**-1

k_disulph_form1 = 1.00755933105   # uM**-1 s**-1
k_disulph_form2 = 3.43491295032   # s**-1

k_disulph_red1 = 0.189972075394   # uM**-1 s**-1
k_disulph_red2 = 0.142827879843   # uM**-1 s**-1
```

k_disulph_red3 = 0.0659352854765  # uM**-1 s**-1
k8 = 0.04
k9 = 0.01

k_Trx_red = 33.6  # s**-1

k_H2O2_perm = 0.000344145752146  # l s**-1
Km_H2O2_metab = 0.00727013132059  # uM
Vmax_H2O2_metab = 59.1101286989  # uM s**-1
V_basal = 5.27874025944  # uM s**-1

**Script 2: Ammended Tpx1/Pap1 oxidation model**

Output_In_Conc: True
Species_In_Conc: True

**# GlobalUnitDefinitions**

UnitVolume: litre, 1.0, 0, 1
UnitLength: metre, 1.0, 0, 1
UnitSubstance: mole, 1.0, -6, 1
UnitArea: metre, 1.0, 0, 2
UnitTime: second, 1.0, 0, 1

**# Compartments**

Compartment: vol_int, 5.2e-05, 3
Compartment: vol_ex, 0.05, 3

Function: function_4, V_basal  {
V_basal
}
Function: function_3, substrate , Km , V  {
V*substrate/(Km+substrate)
}
Function: function_2, k_H2O2_perm , H2O2_ex , vol_ex  {
k_H2O2_perm*H2O2_ex*vol_ex
}
Function: function_1, k_H2O2_perm , vol_ex , vol_int , H2O2_int  {
k_H2O2_perm*(vol_ex/vol_int)*H2O2_int*vol_int
}

R1: NADPH + TrxSS = NADP + TrxSH
vol_int*kcat1*NADPH*TrxSS

#(kcat1*TR*(NADPH/Knadph)*(TrxSS/K1trxss))/((1+NADPH/Knadph)*(1+TrxSS/K1trxss)) # kcat1 = 66 TR = 0.5 Knadph 1.2 K1trxss = 4.4

R2: H2O2_int + TpxSH_TpxSH = TpxSOH_TpxSH + H2O
vol_int*2*k2*H2O2_int*TpxSH_TpxSH # Cysteine oxidation 20 for pombe

R3: H2O2_int + TpxSOH_TpxSH = TpxSOH_TpxSOH + H2O
vol_int*k2*H2O2_int*TpxSOH_TpxSH # Also 20

R4: TpxSOH_TpxSH = TpxSS_TpxSH
vol_int*k3*TpxSOH_TpxSH # Disulphide bond formation k3 = 1

R5: TpxSS_TpxSH + H2O2_int = TpxSS_TpxSOH + H2O
vol_int*k4*TpxSS_TpxSH*H2O2_int # Could have a slower oxidation k4 = 2/0.2

R6: TpxSOH_TpxSOH = TpxSS_TpxSOH
vol_int*2*k3*TpxSOH_TpxSOH # Also k3 = 1

R7: TpxSS_TpxSOH = TpxSS_TpxSS
vol_int*k10*TpxSS_TpxSOH # Also k3 = 1 but could be k10= 3.44

R8: TpxSS_TpxSOH + H2O2_int = TpxSS_TpxSOOH
vol_int*k5*TpxSS_TpxSOH*H2O2_int # Anticipate this could be even slower k5 = 0.2/0.002

R9: TpxSS_TpxSOOH + ATP = TpxSS_TpxSOH + ADP
vol_int*k6*TpxSS_TpxSOOH*ATP # Brenda 0.03 for S. cerevisiae

R10: TpxSS_TpxSS + TrxSH = TpxSS_TpxSH + TrxSS
#vol_int*2*k7*((TpxSS_TpxSS*TrxSH)-(TpxSS_TpxSH*TrxSS)/Keq) # Keq = 3.272e-7 # k7 = 10
vol_int*2*k7*TpxSS_TpxSS*TrxSH

R11: TpxSS_TpxSH + TrxSH = TpxSH_TpxSH + TrxSS
#vol_int*k7*((TpxSS_TpxSH*TrxSH)-(2*TpxSH_TpxSH*TrxSS)/Keq) # k7 = 10
vol_int*k7*TpxSS_TpxSH*TrxSH

R12: TpxSS_TpxSOH + TrxSH = TpxSOH_TpxSH + TrxSS
#vol_int*k7*((TpxSS_TpxSOH*TrxSH)-(TpxSOH_TpxSH*TrxSS)/Keq)# k7 = 10
vol_int*k7*TpxSS_TpxSOH*TrxSH

**#Additional routes to hyperoxidation**

R13:TpxSOH_TpxSOH + H2O2_int = TpxSOH_TpxSOOH + H2O
vol_int*2*k5*TpxSOH_TpxSOH*H2O2_int

R14:TpxSOH_TpxSOOH + ATP = TpxSOH_TpxSOH + ADP
vol_int*k6*TpxSOH_TpxSOOH*ATP

R15:TpxSOH_TpxSH + H2O2_int = TpxSH_TpxSOOH + H2O
vol_int*k5*TpxSOH_TpxSH*H2O2_int

R16:TpxSH_TpxSOOH + ATP = TpxSOH_TpxSH + ADP
vol_int*k6*TpxSH_TpxSOOH*ATP

R17:TpxSH_TpxSOOH + H2O2_int = TpxSOH_TpxSOOH + H2O
vol_int*k5*TpxSH_TpxSOOH*H2O2_int

R18:TpxSOH_TpxSOOH = TpxSS_TpxSOOH
vol_int*k3*TpxSOH_TpxSOOH

R19:TpxSS_TpxSOOH + TrxSH = TpxSH_TpxSOOH + TrxSS
#vol_int*k7*((TpxSS_TpxSOOH*TrxSH) - (TpxSH_TpxSOOH*TrxSS)/Keq)
vol_int*k7*TpxSS_TpxSOOH*TrxSH

R20:TpxSOH_TpxSOOH + H2O2_int = TpxSOOH_TpxSOOH
vol_int*k5*TpxSOH_TpxSOOH*H2O2_int

R21:TpxSOOH_TpxSOOH + ATP = TpxSOH_TpxSOOH + ADP
vol_int*k6*TpxSOOH_TpxSOOH*ATP

**# Pap1 activation by Tpx1 in fission yeast**

**# Pap1 is oxidised by TpxSOH_TpxSH (R14) and then reduced by thioredoxin**

R22: Pap1_RED + TpxSOH_TpxSH = Pap1_OX + TpxSH_TpxSH
vol_int*k8*Pap1_RED*TpxSOH_TpxSH #Pap1 oxidation rate k8 = 0.04

R23: Pap1_OX + TrxSH = Pap1_RED + TrxSS
#vol_int*k9*((Pap1_OX*TrxSH) - (Pap1_RED*TrxSS)/Keq) #k9 = 0.1
vol_int*k9*Pap1_OX*TrxSH

**# H2O2_efflux**

reaction_24:
H2O2_int > H2O2_ex
function_1(k_H2O2_perm,vol_ex,vol_int,H2O2_int)
1414

**# H2O2_influx**

reaction_25:
H2O2_ex > H2O2_int
function_2(k_H2O2_perm,H2O2_ex,vol_ex)

**# H2O2_metab**

reaction_26:
H2O2_int > $pool
vol_int*function_3(H2O2_int,Km_H2O2_metab,Vmax_H2O2_metab)

**# H2O2_basal**

reaction_27:
$pool > H2O2_int
vol_int*function_4(V_basal)

**#Kinetic Parameters = units in uM, s-1 and uM-1 s-1**

kcat1 = 66
#TR = 0.5
#Knadph = 1.3
#K1trxss = 4.4

k2 = 20
k3 = 1.7 #1
k4 = 0.2
k5 = 0.002
k6 = 0.03
k7 = 0.2 #10
k8 = 0.04
k9 = 0.01
k10 = 3.44
#Keq = 3.272e-7

**# NB. Units: per micromolar (uM)^-1**

**#Species concentrations**

NADPH@vol_int = 150
NADP@vol_int = 1
TrxSS@vol_int = 0.01
TrxSH@vol_int = 0.7
H2O2_int@vol_int = 0.0
H2O2_ex@vol_ex = 100.0
H2O@vol_int = 1
ATP@vol_int = 7000
ADP@vol_int = 0.0

k_H2O2_perm = 0.000344145752146  # l s**-1
Vmax_H2O2_metab = 59.1101286989  # uM s**-1
Km_H2O2_metab = 0.00727013132059  # uM
V_basal = 5.27874025944  # uM s**-1

TpxSH_TpxSH@vol_int = 4
TpxSOH_TpxSH@vol_int = 0.0
TpxSS_TpxSH@vol_int = 0.0
TpxSS_TpxSOH@vol_int = 0.0
TpxSS_TpxSS@vol_int = 0.0
TpxSS_TpxSOOH@vol_int = 0.0
TpxSOH_TpxSOH@vol_int = 0.0
Pap1_OX@vol_int = 0.0
Pap1_RED@vol_int = 0.0245
TpxSH_TpxSOOH@vol_int = 0.0
TpxSOH_TpxSOOH@vol_int = 0.0
TpxSOOH_TpxSOOH@vol_int = 0.